Operations Management

Creating a maintenance schedule for onshore wind turbines

MSc SET Thesis

Dhruv Vemuru

Operations Management

Creating a maintenance schedule for onshore wind turbines

by

Student Name	Student Number
Vemuru, Dhruv	5561108

to obtain the degree of Master of Science in Sustainable Energy Technology
at the Delft University of Technology,
to be defended publicly on Thursday 28th September, 2023 at 15:45 pm.

Project Duration:	February 2023 - September 2023,	
Supervisor:	Prof. Dr. Ir. Simon J. Watson	Wind Energy, Aerospace Engineering.
Supervisor:	Ir. Filippos Amoiralis	Asset Management, GTC
Committee member:	Dr. Stefan Pfenninger-Lee	Technology, Policy and Management.

An electronic version of this thesis is available at http://repository.tudelft.nl/.

Cover Photo by Author.

Acknowledgements

This master's thesis is submitted as part of the requirement for obtaining the degree of Master of Science in Sustainable Energy Engineering at the Delft University of Technology. The supervision from the Delft University of Technology was done by Prof. Dr. Ir. Simon J. Watson and Ir. Filippos Amoiralis was the supervisor from Green Trust Consultancy. I would like to thank them for their supervision and advice. They always steered me on the right path and never let me go on a tangent. Their strong feedback was the foundation of all the good that has come out of this project.

As an individual pursuing a career as a consultant in the onshore and offshore industry, this particular project offers an ideal platform to use the theoretical information acquired throughout my academic journey as a Wind Energy student. This project was completed through a collaborative effort with a reputable Energy consultancy organisation known as Green Trust Consultancy B.V. In addition to providing me with the necessary resources for my thesis, they have also offered valuable insights into the functioning of an energy consultancy organisation. This opportunity provides a platform to get insight into the diverse facets of wind turbines, encompassing licensing, construction/procurement, and asset management. Furthermore, I have acquired knowledge about alternative energy sources, including solar power, and have deepened my understanding of the storage mechanisms associated with renewable electricity.

This experience would not have been as enjoyable as it has been without the friends I have made over this 2-year period. To all those who have stuck by my side on this journey, I will always be grateful for having had this opportunity to share your friendship these past couple of years.

Finally, I would like to express my eternal gratitude to my family for always being there for me even though were are so far apart. Thank you for always believing in me.

Dhruv Vemuru
Delft, September 2023

Abstract

Routine maintenance is an essential requirement for the optimal functioning and longevity of any technical system that has been constructed. The issue occurs when the maintenance planning for such a structure becomes necessary. The adverse weather conditions prevalent in the Netherlands contribute to the heightened danger associated with the duty of a maintenance worker. Additionally, it is vital to comprehend the optimal time frame for minimising revenue losses when allocating time towards maintenance activities rather than operational tasks.

The objective of this project is to create a methodology for enhancing and improving the management of asset maintenance planning. This process is carried out by developing two statistical models. The primary objective of this study is to examine the feasibility of utilising API data from wind forecast sites to provide accurate production forecasts for individual wind turbines up to a 7-10 day period in advance. Furthermore, this study aims to forecast the electricity prices for the upcoming week by analysing historical data and recent day-ahead pricing. The outputs generated by these models are subsequently aggregated to yield a single outcome in terms of revenue.

The predictive model for electricity prices utilises data sourced from ENTSOE to generate an aggregate of electricity prices spanning the previous 7-8 years. This aggregate is subsequently adjusted by incorporating the electricity prices observed within the most recent three-week period. The model exhibits high accuracy in predicting day-ahead pricing during weekdays, but its performance is not consistently replicated on weekends.

The wind turbine output forecast model utilises operational archival data and high-resolution 10-day forecasts obtained from the European Centre for Medium-Range Weather Forecasts (ECMWF). A correlation has been established between the archival data and the historical turbine data provided by Green Trust Consultancy for the designated wind farm. The aforementioned correlation is subsequently employed to establish a connection between the output of a turbine and the real-time forecast data. The accuracy of the power generation forecast decreases from the initial day to the tenth day of the projection, resulting in inconsistent outcomes.

The combined outputs of these two models yield a solitary outcome that aids in predicting the potential revenue loss for the selected turbine during the period of maintenance-induced idleness. The limitations inherent in both models contribute to the generation of imprecise outcomes inside the revenue model pertaining to wind turbines. The model accurately predicts outcomes in two out of the four tested scenarios.

The model is additionally executed for an alternative wind farm situated at a distinct site to establish its independence from the selected wind farm or its specific geographical placement. The limitations of the three models are discussed, and potential strategies to address these limitations are explored to enhance the accuracy of the model's output.

The report is structured in the following manner. chapter 1 provides a comprehensive overview of the research problem. chapter 2 pertains to a thorough understanding of historical electricity prices, turbine data, and weather forecast data, and their use in calculating turbine-generated revenue. The prediction and forecasting models for the price of electricity and turbine power output are described in chapter 3 and chapter 4. The methodology and application are also included. In chapter 5, the combined results of both models are utilised to develop a unified output, which is subsequently employed to forecast the revenue generated by the turbines. Several case scenarios are offered for the turbines, and their performance is analysed for each situation. chapter 6 includes an alternative wind farm to assess the model's performance in a distinct geographical setting. Subsequently, chapter 7 provides an exposition of the limitations inherent in the model, accompanied by an examination of potential avenues for enhancement. The conclusion and future recommendations for the model can be observed in chapter 8.

Contents

List of Figures

List of Tables

Nomenclature

Abbreviations

Abbreviation	Definition
3T	3-Turbine
5T	5-Turbine
AI	Artificial Intelligence
API	Application Programming Interface
ASM	Asset Management
ATP	Averaged Turbine Power
BASH	Bourne-Again SHell
CSV	Comma-Separated Values
DAM	Day Ahead Market
DEP	Day-ahead Electricity Price
DWD	Deutscher Wetterdienst
DWIA	Danish Wind Industry Association
ECMWF	European Centre for Medium-Range Weather Forecast
ENS	Ensemble Weather Forecast
ENTSOE	European Network of Transmission System Operators for Electricity
FMWTP	Forecast Model for Wind Turbine Power
FTP	File Transfer Protocol
GRIB	Gridded Binary or General Regularly-distributed Information in Binary form
GTC	Green Trust Consultamcy
HRES	High-Resolution 10-Day Forecast
KNMI	Koninklijk Nederlands Meteorologisch Instituut
MARS	Meteorological Archival and Retrieval System.
NCEP	National Centers for Environmental Prediction
NOAA	National Oceanic and Atmospheric Administration
PMEP	Predictive Model for Electricity Prices
REQ	Request
RMSE	Root-Mean Square Error
RMWT	Revenue Model for Wind Turbines
S3	Simple Storage Solution
SOP	Standard Operating Procedure
TSA	Time-Based Series Availability
UTC	Coordinated Universal Time

Symbols

Symbol	Definition	Unit
V	Velocity	[m/s]
v	V- component of velocity	[m/s]
u	U- component of velocity	[m/s]
ϕ	Wind direction	[Â°]
t	Time	[s]
EUR	Money	[€]
c_f	Correction factor	[-]
P	Previous year average electricity price	[€/MWh]
R	Recent 3-week average electricity price	[€/MWh]
F	Predicted electricity price	[€/MWh]
h	Height	[m]
h_{ref}	Reference height	[m]
U	Wind speed	[m/s]

1 Introduction

By the end of 2020, the Netherlands had 2,606 wind turbines to generate electricity, of which 2,144 were located on land, and the rest were at sea (Central Bureau van Statistiek, 2022). In 2020, these turbines generated enough electricity to power 5.6 million households (15.3 billion kWh), with 36 % coming from offshore turbines and 64 % from onshore turbines. These ginormous structures are responsible for providing around 17% of the total electricity demand of the Netherlands. Wind turbines are complex systems that require proper maintenance and care to achieve high operational efficiency and long service life. The expected lifetime of a wind turbine is around 20–25 years, depending on the design, environmental conditions, and maintenance strategies. Therefore, it is essential for wind farm owners and operators to develop an optimal maintenance plan that ensures timely and regular inspection, repair, and replacement of the turbine components (Ding et al., 2013).

To ensure the continuous operation of wind turbines, a combination of preventative and corrective maintenance measures are implemented. Preventive maintenance can be categorised into two basic approaches: time-based and condition-based. Planning time-based maintenance is often considered to be more straightforward compared to condition-based maintenance. This is mostly due to the fact that condition-based maintenance relies on monitoring and responding to changes in the condition of the equipment, which are often difficult to foresee. Both forms of maintenance necessitate the need for preparatory measures and the subsequent wind turbine shutdown, leading to a reduction in production yield (Schouten et al., 2022).

Wind turbine maintenance comprises tasks like routine inspections, cleaning procedures, lubrication protocols, and corrective actions, which are undertaken to ensure the efficient and uninterrupted operation of wind turbines (Wang et al., 2019b). A couple of examples of these tasks being conducted are depicted in Figure 1.1. According to the Standard Operating Procedure (SOP), the frequency of maintenance is contingent upon various factors, including the specific wind turbine model, prevailing climatic conditions, and the maintenance approach embraced by the operator. However, it is generally advisable to do maintenance activities on an annual basis as depicted in research conducted by Besnard et al. (2011).

Figure 1.1: Technicians inspecting, cleaning and repairing the composite rotor blades.(Marsh, 2011)

In studies conducted by Costa et al. (2021) and Froger et al. (2018), state-of-the-art research was conducted on the topic of wind turbine maintenance, but, neither was able to provide the exact duration a maintenance task would need. After consulting with the technicians and the asset management team (ASM) at Green Trust Consultancy it was understood that, on average, completing the turbine maintenance task requires a time commitment of around 20 working hours. In many instances, this entails the technicians engaging in two separate 10-hour shifts whilst leaving the turbine inactive overnight.

The repair of rotor blades and gearboxes is a highly intricate process that necessitates a substantial amount of downtime (Lu et al., 2009). Blades are often made of carbon fibre-reinforced polymer composites. These materials are often plagued with a weak interface and a lack of toughness, which implies that the blades are prone to failure (Sayam et al., 2022). The safety concerns associated with certain blade designs encompass poor blade root and middle section dimensions, insufficient compliance with strength and stiffness criteria regarding section shape, and surpassing the expected load limit specified in the blade's design (Peng et al., 2023).

Furthermore, the blade's leading edge is susceptible to erosion caused by wind and rain (Sareen et al., 2014). Studies have shown that the performance of wind turbines decreases by up to 27% in power output due to the effects of rain (Bashir, 2022). Consequently, the turbines would experience a reduction in performance. The weather conditions prevalent in the Netherlands throughout the year, as depicted in the study conducted by Sabir et al. (2007), can pose a significant challenge for wind turbine blades.

Lightning strikes are infrequent occurrences that possess the potential to inflict substantial harm upon wind turbine blades, and, in certain cases, may even incite combustion, hence leading to considerable losses and associated hazards (Wang et al., 2019a). An example of the damage inflicted by lightning can be viewed in Figure 1.2.

Figure 1.2: Wind turbine catches fire due to lightning strike (Senn, 2022)

Wind turbines operate by harnessing the kinetic energy of wind and transforming it into mechanical energy, which is subsequently transformed into electrical energy through a gearbox. The rotational motion of the wind turbine facilitates the propulsion of the primary shaft, inducing the rotation of the generator via the gearbox (Zhang & Lu, 2019).

The gearbox comprises a significant quantity of gears, with gear failure responsible for around 60% of all gearbox failure instances. The primary cause of gear failure predominantly occurs within the teeth, encompassing issues such as tooth surface corrosion, tooth surface wear, tooth surface bonding, and tooth breakage. Gearboxes are typically engineered with an anticipated operational lifespan of approximately two decades. Frequently, the aforementioned failures result in the need for frequent replacement of gearboxes before their expected lifespan, hence causing increased turbine downtime and financial losses for the owner (Yan et al., 2021).

Additional turbine failures include the deterioration of the tower's foundation, flanges, and the structure itself. In a study by Reder et al. (2016), a downtime analysis was conducted for each of the failures associated with a wind turbine and its components. In Figure D.1 and Figure D.2 in Appendix D, the failure rates of and downtimes of typical geared and Direct drive turbines are plotted.

1.1. The problem with maintenance scheduling

During designated maintenance periods, the turbine is locked, the blades remain stationary and do not engage in rotational motion to harness energy from the incoming wind. Therefore, the production of power is not intended for the purpose of being delivered to the grid connection. In other words, the turbine does not generate any financial revenue. Investment funds often own wind farms, with the responsibility for operating and maintaining the turbines frequently delegated to a third-party entity (Froger et al., 2018). Consequently, additional financial resources must be committed in order to carry out the task of turbine maintenance successfully.

Frequently, turbine owners utilise consultancy services to manage the turbine's routine operations. The primary responsibility of the ”Operations Management” team is to engage technicians through subcontracting arrangements and provide them with particular dates and times for the execution of turbine maintenance tasks. Upon being notified of the scheduled maintenance, the technicians proceed to the wind farm location and establish their campsite. The technicians employ the utilisation of ropes as a means to descend onto the blades, as shown in Figure 1.4 and use self-hoisting cranes, which are depicted in Figure 1.3, to perform tasks like retrofitting, repair or replacement.

Figure 1.3: Gearbox repair/ replacement done by technicians using a self-hoisting crane (Enel, 2023)

Figure 1.4: Blade repair done by technicians using rope (Vivablast, 2023)

The safety of specialists engaged in turbine maintenance is crucial, as they consistently face life-threatening risks while carrying out their duties. Hence, it is of equal significance to take into account the operational aspects of the wind turbine farm location, including factors such as visibility and wind speed. The technicians shouldn't be expected to undertake these hazardous activities under conditions of limited sunlight or when wind speeds at hub height are significantly high. The study conducted by Liu et al. (2019), discusses the importance of safety and technical disclosures in wind turbine repair work. These disclosures directly affect the safety of maintenance work and the reliability of maintenance quality.

This academic research aims to tackle the difficulty faced by the Asset Management team (ASM) at Green Trust Consultancy in relation to wind turbine maintenance. Numerous scholarly investigations have been conducted to address the issue of scheduling maintenance for wind turbines. The study conducted by Froger et al. (2018) employed a distinct method that prioritised resource management, specifically the allocation of technicians, as opposed to a revenue-centric perspective when addressing the problem of turbine maintenance scheduling. In a study conducted by Schouten et al. (2022), the authors examined the issue of wind turbine maintenance planning, specifically focusing on a singular component with foreseeable time-dependent maintenance expenses. The emphasis was placed on age-based replacement plans for single components, as opposed to the various maintenance tasks discussed earlier in this chapter.

Returning to the issue encountered by the ASM team, typically, the technicians make contact on a Friday to indicate their intention of establishing their base for service work in the following week. There is a lack of definitive information regarding the optimal day for executing this task. The typical protocol entails a member of the Asset Management team at Green Trust making decisions based on the weather forecasts accessible on Windy (2023) to determine the suitable days for technicians to carry out their specified tasks in the forthcoming week. Regrettably, the available information provides no insight into the financial impact on the owner's earnings throughout the maintenance period. Consequently, choosing the optimal timing for undertaking this operation in the forthcoming week remains challenging.

1.2. Solving the problem of maintenance scheduling

The research objective of this report is to tackle the problem of wind turbine maintenance faced by the asset management team at Green Trust Consultancy. This is done by:

1. Creating a statistical model for the electricity price prediction for the coming seven days based on the historical and recent day-ahead prices.
2. Creating a statistical model for predicting the production forecast up to 7-10 days upfront on a wind turbine level using the API data from wind forecast sites.
3. Combining the outputs of the two models to generate the forecast revenue of the chosen wind turbine.

Turbine data from a specific wind farm site under the care of Green Trust Consultancy is used along with a 10-day weather forecast to predict the turbine output for the eventual calculation of the revenue generated by the turbines. In a research project performed by Hesselink (2018), a model that can translate day-ahead weather forecasts into power production forecasts for wind turbines was developed using regression models with historical turbine data. Whereas, the objective of this study was to utilise past turbine data and weather forecasts to develop a predictive model capable of estimating turbine output for a period of seven to ten days, as opposed to the existing approach of predicting output only one day in advance. Thus, the first step is to decide on a specific weather forecast model that will be implemented for the forecast model.

1.2.1. Choosing the right weather forecast model

The Windy website provides users with various choices for accessing weather forecasts (Windy, 2023). These options are illustrated in Figure A.1, Figure A.2 and Figure A.3 in Appendix A. The website also provides concise descriptions of each model, which can be viewed in Table 1.1, allowing users to understand why the ECMWF model is considered the optimal choice for weather forecasting. Moreover, in a study conducted by Iseh.A. and Woma.T. (2013), a survey on all the available weather forecast models is conducted. Previous research work on understanding the ECMWF data for weather forecast models was done by Yang et al. (2022). The aforementioned model is the sole model that effectively fulfils the requirement of serving as a high-resolution 10-day forecast model specifically tailored for the geographical area of the Netherlands.

Table 1.1: Windy forecast model comparison (Windy, 2023)

Model Name	Description
GFS 22km	The GFS is the most well-known free global weather model. It's updated every 6 hours and produced by the National Centers for Environmental Prediction (NCEP) of the United States National Oceanic and Atmospheric Administration (NOAA). It doesn't take topography and shapes of coastlines into account, so it isn't very accurate for places next to bodies of water.
ECMWF 9km	Very accurate global weather model created and operated by ECMWF. It is considered the best for precipitation and cloudiness.
METEOBLUE	Ensemble multiple global and local forecast models using AI. It beats other models in temperatures and wind. It is only a 7-day forecast.
ICON-D2 2.2 km	High resolution model developed and operated by German DWD. One of the most modern forecast models delivering very good results in central Europe. It produces only a 2-days forecast.
AROME 1.3km	AROME is a regional France and the surrounding territories weather model by the Meteo France (French National Meteorological Service). It is only a 7-day forecast.
UKV 2km	A post-processed regional downscaled configuration of the unified model, covering mainly the UK and Ireland, with hourly forecast data. With a resolution of approximately 0.018 degrees, hourly data is produced for the coming seven days at the surface level and at standard pressure levels.

ECMWF provides access to real-time data sets and archival datasets. The real-time datasets provide the user with two main kinds of forecasting data. The data required for this project was a medium-range forecast, i.e. up to 10 days ahead. First, HRES, a single high-resolution forecast (horizontal resolution around 9 km), provides a detailed description of future weather up to 10 days ahead. The other is ENS, which is an ensemble of 51 forecasts with a horizontal resolution of around 18km, whereas HRES is a deterministic model.

The archival datasets are of two main types. The first one is the operational archive, which is a collection of the deterministic forecast datasets from the previous 50 years. The second is the re-analyses dataset, which is essentially the same as the operational archive, but the main difference lies in the fact that the forecasted data is altered with the observed data, hence the term reanalysis. For uniformity in the real-time and archival datasets, the deterministic HRES and the operational archive model are chosen.

1.2.2. Previous work on electricity price prediction

The second statistical model in this research is the model to predict day-ahead electricity prices in the Netherlands for the coming seven days. Numerous attempts have been undertaken in the field of electricity price prediction. Each strategy employs a distinct facet of the electricity market. Several researchers have employed methodologies, such as machine learning, to assess various models in order to make predictions on electricity prices (Tschora et al., 2022). Others have used state-of-the-art algorithms to perform open-source forecasting models to predict electricity prices (Lago et al., 2021). For predicting the Day Ahead Market (DAM) in the Netherlands, a greedy algorithm was applied using candidate countries selected through an integrated analysis based on open-source European electricity market data or ENTSOE (Heijden et al., 2021). Another study focused on forecasting the day-ahead electricity spot prices in Germany (Johnsen, 2019)

However, these researches share two commonalities. Initially, the ML models under consideration exhibited a high level of complexity, mostly due to their limited explainability and interpretability. Consequently, reproducing these researches or incorporating their findings into a simplified multi-day predictive model posed significant challenges. Furthermore, it should be noted that the primary purpose of developing these models was to accurately anticipate the Day-ahead electricity price rather than to provide forecasts for prices several days in advance. The primary focus of the study discussed in the aforementioned publications is the accurate prediction of spot market prices through the utilisation of diverse regression models.

Nonetheless, there has been one research that created a Multi-Day-Ahead Electricity Price Forecasting while also considering the price spikes for up to four days ahead (Manfre Jaimes et al., 2023). A set of five models were developed with the purpose of facilitating a four-day weather forecast. These models specifically focused on analysing the output power of thermal units as a means to identify unanticipated outages or changes in the supply stack, hence addressing price spikes. The research was conducted in Canada, thus implying that reproducing the results within the context of the Canadian market may provide challenges.

This study adopted a simplified approach wherein historical data from previous years was utilised in conjunction with recent three-week data to develop a statistical model for forecasting electricity costs up to a seven-day horizon. This would not be possible with most existing complex models. Data was retrieved from ENTSOE (2023) regarding electricity price forecasting. The website provides data on the Load, Generation, Transmission, Balancing, etc., for the various member states of the European region. The historical day-ahead prices for electricity spanning a six-year period (2015-2023) in the Netherlands have been exported in order to facilitate comprehension of the fluctuations in electricity costs across daily, weekly, monthly, and annual timeframes. Figure C.1 in Appendix C presents an illustrative example of a website whereby the data obtained from ENTSOE is exported and saved as a CSV file for subsequent analysis.

1.2.3. Chosen wind farm

The selected subject for this model is a three-turbine wind farm located in the South-West region of the Netherlands. It comprises three Vestas V-90 3MW turbines *viz.* 3T-1, 3T-2 and

3T-3, with each turbine equipped with a hub height of 105m and a rotor diameter of 88m. These turbines' datasheet is available in Appendix B. Figure 1.5 displays the arrangement of the three turbines in terms of their alignment. Further details on the turbines are elaborated upon in section 2.2.

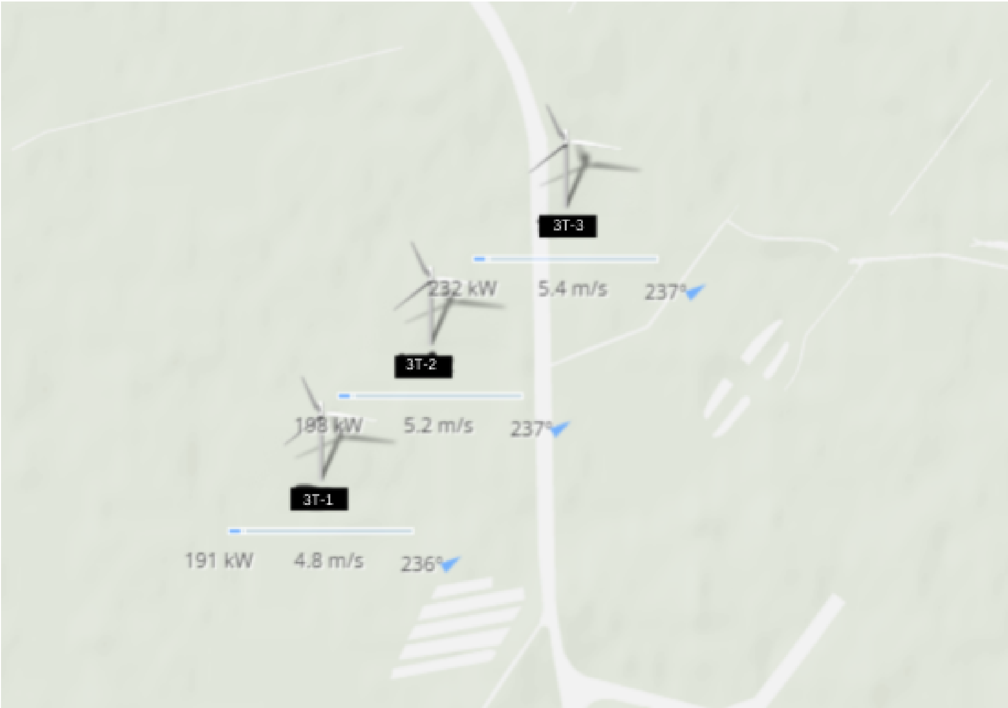

Figure 1.5: Terrain map of the 3-turbine wind farm

2 Data comprehension

This chapter provides a comprehensive analysis of both electricity costs and weather forecast data. The primary focus of the discussion in 2.1 pertains to the temporal volatility of electricity prices. Following that, the correlation between wind speed and turbine output is established in Section 2.2. Additionally, the subsequent sections, section 2.3 and section 2.4, delve into a detailed explanation of the data retrieval procedure from the European Centre for Medium-Range Weather Forecasts (ECMWF). Finally, the revenue generated by the turbines may be determined by utilising both the electricity pricing and weather forecast, as seen in 2.5.

2.1. Volatile nature of electricity prices

Before 2021, electricity prices in the Netherlands had only crossed the 100 €/MWh mark 129 times between the start of 2015 and the end of 2020. The year 2021 showed a massive spike in electricity prices, totaling up to 3026 times when the electricity prices crossed the 100 €/MWh mark. The average price of electricity went from a mere 40 €/MWh in 2015 to a massive 103 €/MWh in 2021. As the year 2021 progressed, there was a steady increase in electricity prices, which saw a further surge again in February 2022 following Russia's invasion of Ukraine, leading to an all-time high figure of 871 €/MWh in August 2022. The average day-ahead electricity price in the Netherlands in June 2023 was 91.98 €/MWh, one of the lowest month-average in the country since the summer of 2021 (In Statista, 2023). Figure 2.1 is plotted below, which depicts the variation in average monthly monthly prices from 2019 till the present.

Despite the inherent volatility of electrical prices, identifiable patterns and trends can nevertheless be observed in their diurnal, weekly, and annual fluctuations. Hence, it is necessary to undertake comprehensive efforts in order to have a clear understanding of the patterns exhibited by these prices. This section focuses on analysing the behavioural patterns exhibited by power prices.

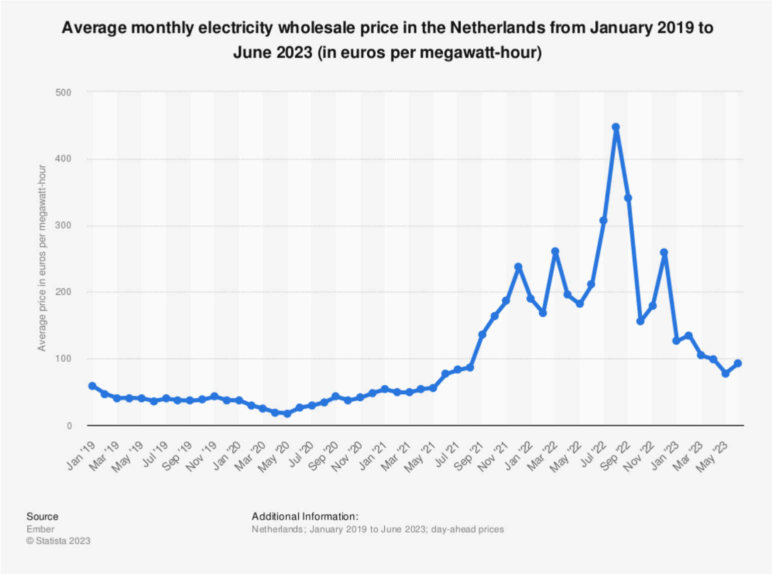

Figure 2.1: Netherlands; January 2019 to June 2023; day-ahead prices (In Statista, 2023)

2.1.1. 4 seasons

In Figure 2.2, how the season affects electricity prices can be easily observed. In the winter months (January, February, November and December), the electricity prices seem to be at the highest in 2019. A steady decrease in prices can be observed from January until June, where the average prices seem to be the lowest; at the end of the summer period or the beginning of fall (around the end of September), the average prices rise again, reaching a high point in November which is surprisingly more elevated than the average prices in December. This can be explained by the presence of the Christmas period. In the Netherlands, most people spend time with their families, and the major offices are often shut during this period. A comprehensive study is done in subsection 2.1.3.

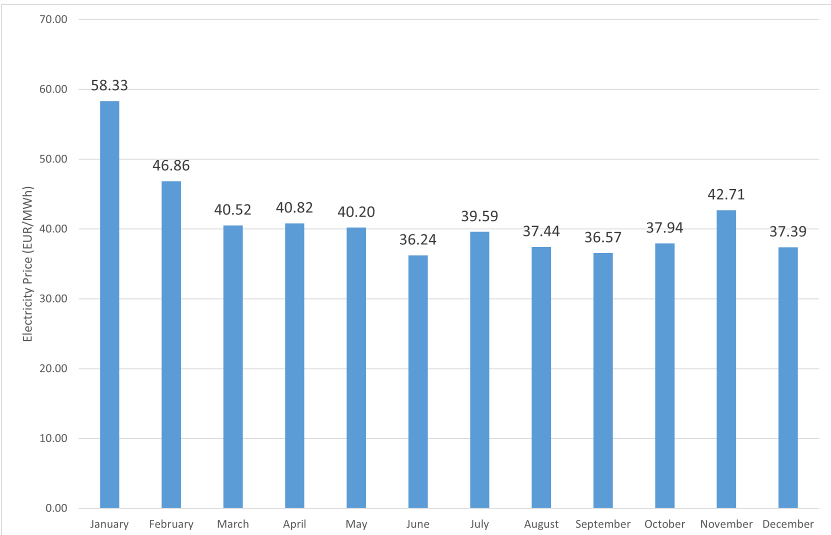

Figure 2.2: Average electricity prices throughout the year 2019.

Upon examination of Figure 2.3, it is evident that the average power prices exhibit a notable disparity between the colder months of January and February, as compared to the summer months of June and July. This discrepancy serves as a visual representation of the seasonal variations in electricity prices.

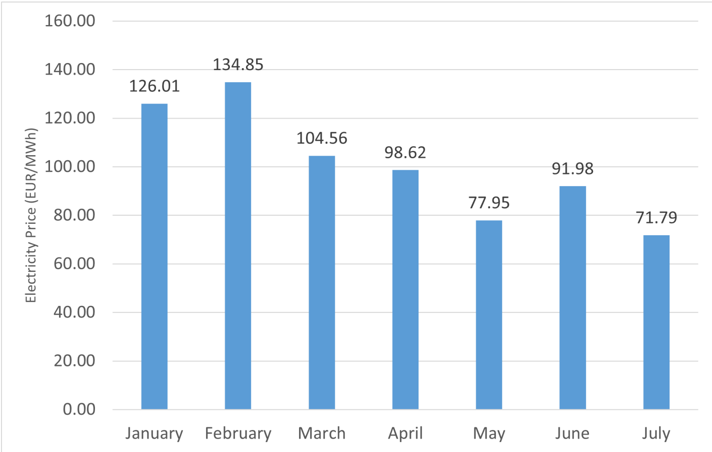

Figure 2.3: Average electricity prices throughout the year 2023.

2.1.2. Weekend vs. Weekday

Typically, on weekends, there is a notable decrease in electricity prices due to the closure of numerous industries, resulting in a reduction in the overall load on the grid system. In order to align with reduced demand, electricity is offered at a reduced price. In instances characterised by abundant sunlight and strong wind conditions, there is a possibility, albeit rare, for power prices to become negative due to continuous electricity generation without interruption. This is discussed in greater detail in subsection 2.1.4

A representative data set is extracted from the initial week of the year 2023 and is depicted in Figure 2.4. The electricity costs observed on Sunday and Saturday, representing the left and right ends of the graph, respectively, are lower than the prices observed during the weekdays from Monday through Friday, which are represented by the data sets in the middle of the graph.

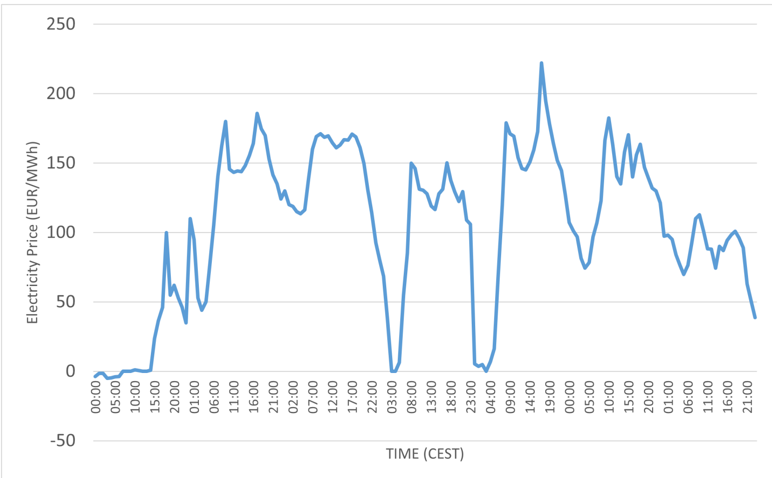

Figure 2.4: Electricity prices throughout the week 01/01/2023 till 07/01/2023.

2.1.3. Public holidays

Koningsdag, which falls on the 27th of April, is frequently celebrated by the general public in the Netherlands. This event signifies a period during which individuals gather in public spaces adorned in the hue of orange, engaging in wild festivities. The majority of offices are closed on this particular day. A preliminary examination is conducted on the day preceding, during, and following King's Day in order to understand the influence of this holiday on electricity pricing. The lack of apparent disparity in electricity prices on the day in question, as depicted in Figure 2.5, suggests that there is no noteworthy variation when compared to the preceding and subsequent days surrounding King's Day. The primary cause of pricing changes can be attributed to individuals' preferences for indoor or outdoor activities. As an illustration, the prices during the late nocturnal hours exhibit an upward trend compared to those observed in the late afternoon. Given that many sectors often decrease their production levels throughout the course of the week, it is plausible to anticipate a decline in overall electricity prices during this period.

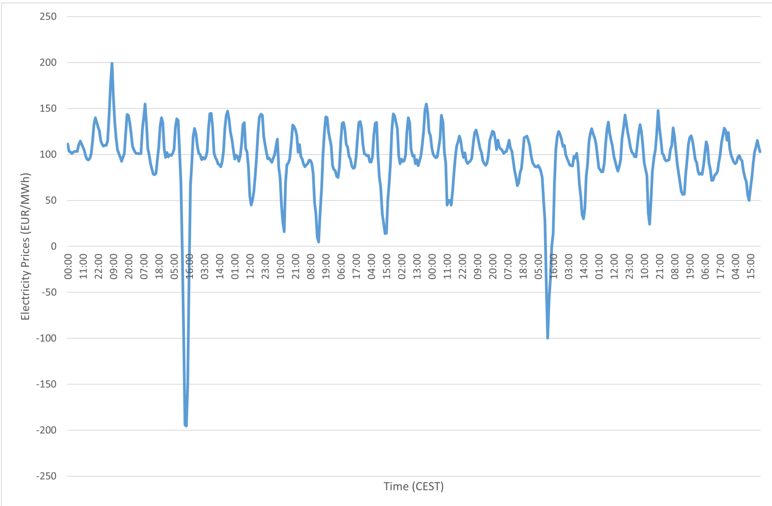

Figure 2.5: Electricity prices in the week of King's Day (2023) and the adjacent weeks.

The next period under discussion is the holiday season. There appears to be a noticeable decline in the mean electricity rates seen between the months of November and December. The period of Christmas (24^{th} December till 31^{st} January) is analysed and compared against the rest of the month. The data presented in Figure 2.6 indicates that the average electricity prices throughout the Christmas period in the years preceding 2021 exhibit minimal deviation from the rates recorded during the remainder of the month. A significant disparity is evident only in the years 2021 and 2022. The energy costs have experienced a notable escalation since the beginning of 2021, primarily attributed to the global impact of the COVID-19 epidemic and the expanding worldwide demand. The negative effects have been further exacerbated by the Russian invasion of Ukraine and the evolving climatic circumstances. The question remains as to whether the prices over this year's Christmas period will exhibit a similar trend to those observed in the past few years or if they will revert to the levels observed before the onset of the COVID-19 pandemic.

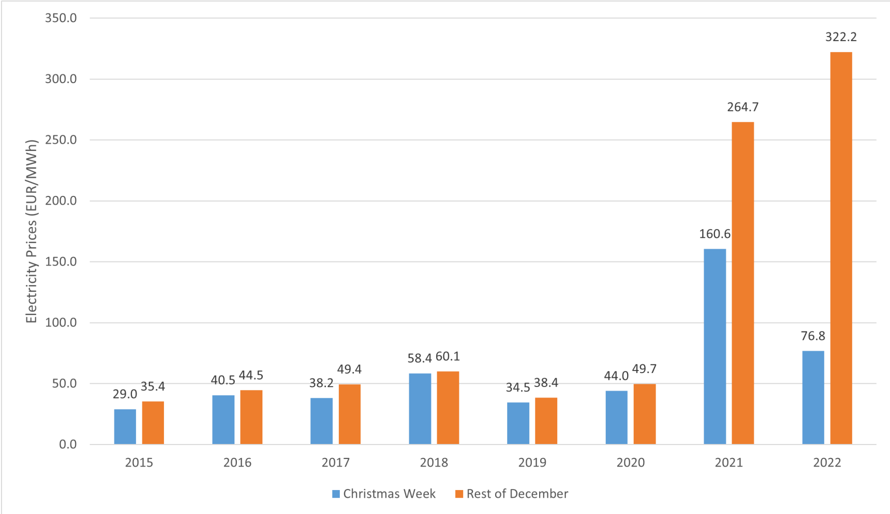

Figure 2.6: The effect of Christmas on the electricity prices

2.1.4. Negative electricity prices

During periods of high solar radiation and strong winds, there is an increased chance that electricity prices may decrease to below zero. A significant number of these occurrences take place on weekends, a period characterised by reduced demand on the power grid. A comprehensive analysis of the data obtained for the calendar year 2023 has been conducted. The term ”Renewable Ratio” is introduced as a distinct parameter, defined as the ratio between the total scheduled renewable generation from solar, onshore wind, and offshore wind and the total scheduled generation across all types. The utilisation of fossil fuel resources influences the pricing dynamics of the entire market in EU wholesale electricity markets to fulfil the overall demand (Climate Action Network Europe, 2021). Therefore, if renewable energy sources fulfil a substantial portion of the energy demand, the impact of fossil fuel output diminishes, resulting in a decline in the selling price of electricity. The main factor for determining the occurrence of negative prices in Figure 2.7 is the resulting ratio expressed as a percentage. Negative power prices are noticed during time slots when the percentage values of the ratio exceed 80%.

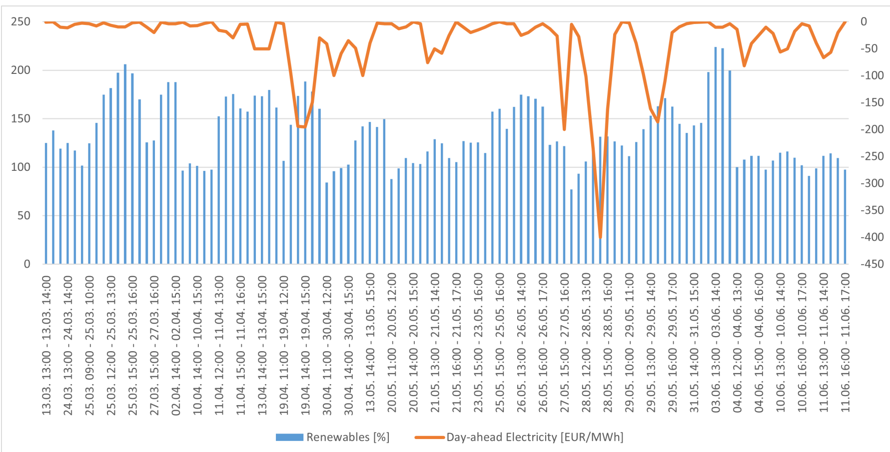

Figure 2.7: Observed negative electricity prices from March 2023 till June 2023.

For the time slots when the renewable ratio is above 100%, a portion of the excess power generated is exported to the neighbouring countries *viz.* Germany, Belgium, UK, Denmark and Norway. One such time slot is taken in Table 2.1 for the date and time 29/05/2023, 13:00 to 14:00. A negative electricity price of -161.70 was observed. The Renewable generation in this time slot was greater than the scheduled generation by a value of 1250 MW, thus giving a renewable ratio of 116%. The total day-ahead load can be met solely by renewable production. The excess power was partially offset by exporting 649 MW to Norway, 748 MW to Belgium, 697 MW to Denmark, 543 MW to the UK and 3952 MW to Germany.

Table 2.1: ENTSOE data for the period 13:00 to 14:00 on 29/05/2023

Parameter	**Unit**	**Value**
Day-ahead Electricity Price	EUR/MWh	-161.70
Scheduled Generation Day Ahead	MW	7757
Scheduled Generation (Wind and Solar) Day Ahead	MW	9007
Total Load Day Ahead	MW	6411
Cross-Border Physical Flow	MW	6589

In the year 2023, until the end of June, a total of 127 negative electricity time slots have been observed, and out of these, 53 were on the weekdays whilst the remaining 74 were on the weekends (as can be viewed in Figure 2.8). The prices below zero tend to occur mostly on Sundays, followed by Saturday and the workday, with the most negative prices observed on Monday.

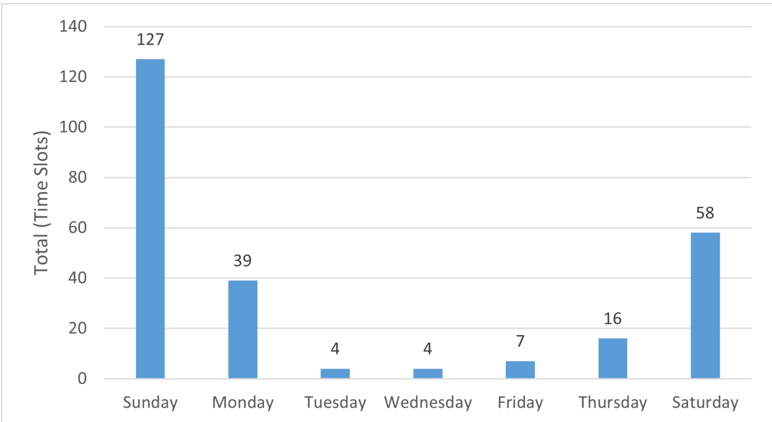

Figure 2.8: Occurrence of negative electricity prices on different days of the week from 2018-2022.

2.2. Power curve

This subsection compares the power curves of the turbines 3T-1, 3T-2 and 3T-3 turbines to the ideal power curve of a V90-3 MW turbine. The ideal 3MW turbine has a rated power of 3000 kW, and it produces the rated power at wind speeds of approximately 14.3 m/s and above until the cut-off velocity of 25 m/s. In Figure 2.9, the ideal power curve of a V90-3 MW turbine is plotted.

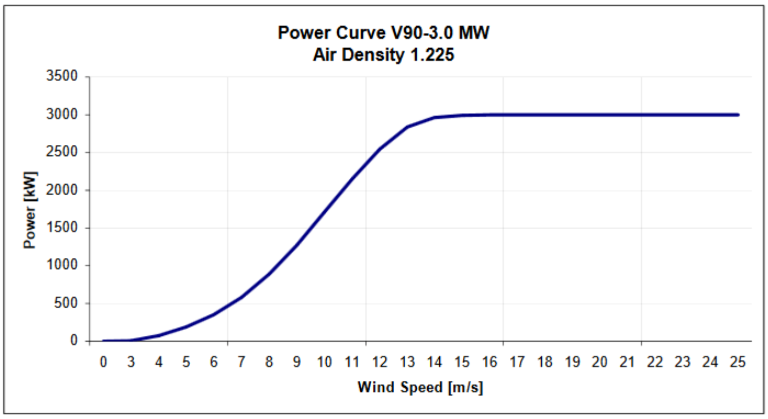

Figure 2.9: Ideal power curve of the Vestas 3MW turbine(Terziev et al., 2021).

The data was collected for the three turbines in the period from 01/01/2018 00:00 till 31/12/2023 23:00. Two of the chosen parameters, wind speed (m/s) and turbine power (kW), were used to construct the general power curve for each of the turbines which can be viewed in Figure 2.10.

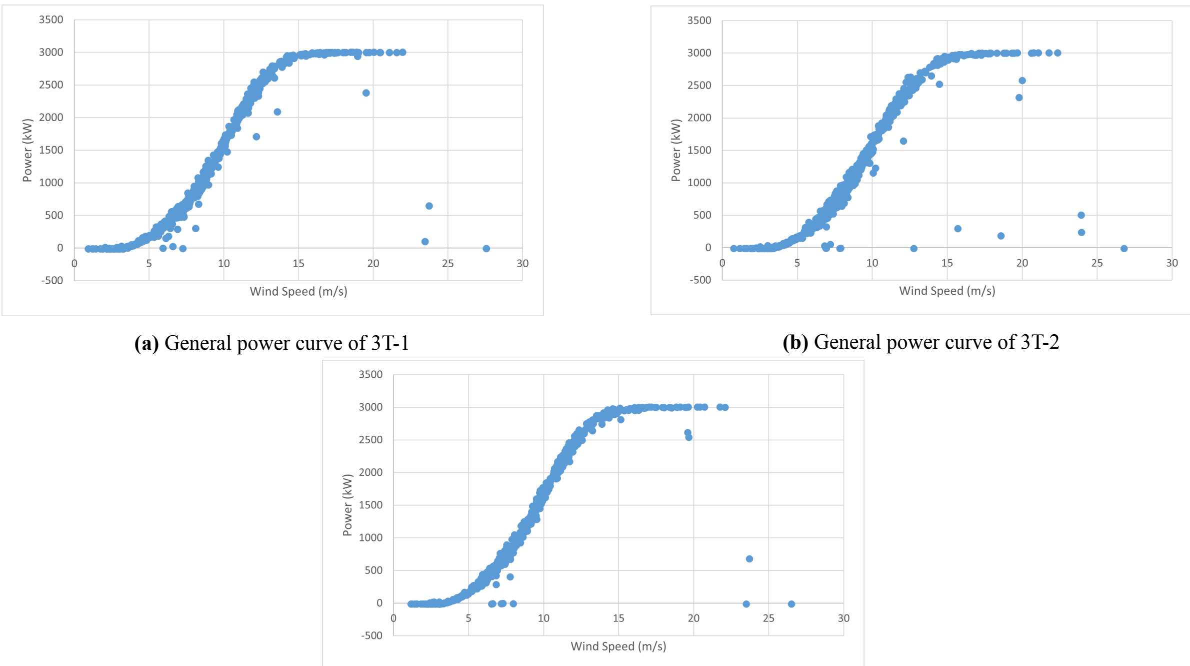

(a) General power curve of 3T-1

(b) General power curve of 3T-2

(c) General power curve of 3T-3

Figure 2.10: General power curves of wind turbines at the chosen wind farm

On one hand, all four graphs follow a similar kind of curve with the wind speeds from cut-in to the rated wind speed; there is a cubic relation between the wind speed and turbine power and a constant power output until the cut-off value of wind speed. On the other hand, the data points on the three chosen turbines show a deviation from the power curve seen in the ideal curve. Also, the observed values of the power between the rated wind speed and the cut-off wind speed are not the same as the rated power, i.e. 3000kW, but are a value slightly lesser than that. This is because of the electricity from the power grid to operate this turbine. This is also the reason why negative values of power can be observed when the turbine is not fully unavailable.

It can also be observed that the cut-out wind speed of the turbines is 22.5 m/s rather than the designed 25 m/s as above the speeds of 22.5 m/s, the power of the turbines does not match the rated power output. Moreover, there are multiple data points that neither follow the cubic relation between the wind speed and power in the cut-in till the rated wind speed section nor follow the constant power generation for wind speeds above the rated wind speed. The occurrence of these data points can be explained by a variable called Time-based Series Availability (TSA). In full turbine availability, the value ”1” is given with the TSA. Still, when the turbine is not fully available due to either scheduled maintenance or repair works, or exceedingly high winds, then the value of TSA is less than 1 with a minimum value of 0. In other words, the turbine was entirely unavailable in that specific time slot. Hence, the observed deviation in the power curve is observed as these data points do not represent the ideal turbine power production.

The wind turbine data is an intermediary in generating a forecast for the turbine output. The historical data obtained from the turbines loosely correlates with the archival forecast data pertaining to the specific site. The aforementioned correlation can be utilised in the context of real-time forecasting in order to make predictions regarding the production of the turbine. The next two parts provide an in-depth explanation of the two projections utilised to establish this correlation. The rationale for choosing a certain forecast type and the methodology for obtaining these forecasts are also elucidated.

2.3. MARS

MARS is ECMWF’s Meteorological Archival and Retrieval System. An API (Application Programming Interface) enables users to contact the ECMWF servers and retrieve data for a specific period. The data was gathered for the same period as in the previous section. MARS has its catalogue feature from which data from various models can be retrieved. Archival can be of 3 main classes: operational data, ECMWF-reanalyses data and Copernicus data. Operational data is the only class that allows the user to pick archival forecasts, as the other two classes are reanalysed data.

To retrieve the data, a request file (.req) is fed to the MARS interface and is executed by launching the API. An example of a REQ file for the year 2019 is shown in Figure 2.11. The operational version and surface level were chosen for the request file. The parameters requested were 100u and 100v, which are the u and v components of velocity measured at a height of 100m for the step range of 0-23, which represent the 24 hours of the day with these steps starting at 00:00:00.The area was narrowed to that encompassing the Netherlands. The requested data is received in a GRIB file (.grib) and converted to a CSV file (.csv). The data in the CSV file is altered with the formulae in Equation 2.1 and Equation 2.2 to give us the speed and direction of the forecasted winds from ECMWF. This data will be used to create the operational archive for each turbine.

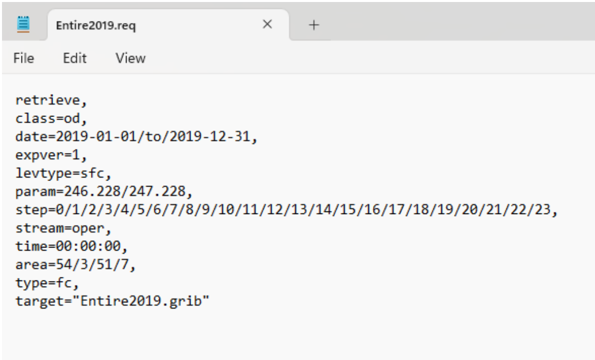
Entire2019.req
File Edit View

```
retrieve,
class=od,
date=2019-01-01/to/2019-12-31,
expver=1,
levtype=sfc,
param=246.228/247.228,
step=0/1/2/3/4/5/6/7/8/9/10/11/12/13/14/15/16/17/18/19/20/21/22/23,
stream=oper,
time=00:00:00,
area=54/3/51/7,
type=fc,
target="Entire2019.grib"
```

Figure 2.11: Request file for the data from 2019 for the Netherlands.

$$|\vec{V}| = \sqrt{u^2 + v^2} \tag{2.1}$$

$$\phi = mod\left(180 + \frac{180}{\pi} atan2(v, u), 360\right) \tag{2.2}$$

The entire process from the REQ file to the CSV file for the data from 1^{st} January 2018 is illustrated in Figure C.3 and Figure C.4. The MARS-API returns values on the closest four grid locations for the input location given in Figure C.4a. As seen in the section 2.4, the nearest grid location matching archival and real-time data will be used.

2.4. Real-time data

The real-time data provided by ECMWF is a 10-day forecast at the atmospheric level. ECMWF has the provision to provide the data via a few types of file transfer methods, which are FTP, SFTP, S3 and Google Cloud platform. Initially, an FTP file-transfer service called FileZilla was used to transfer the data onto a server created at the offices of Green Trust in Oosterbeek, Netherlands (FileZilla, 2023). The Real-time data generated in Bologna, Italy, is uploaded to the FTP server and can be downloaded onto any user device with the required login credentials. The chosen parameters were 10m, 100m and 200m u and v components of the wind velocity. Data is in the same GRIB format as the operational archive and also had to be converted to a CSV file so it can also be altered with the formulae in Equation 2.1 and Equation 2.2 to give the wind speed and wind direction. To match this data with the data from the operational archive, grid point 2 is chosen in Figure C.2, which has the location coordinates at a distance of 6.21km from the 3-Turbine wind farm.

Regrettably, the FTP server being employed by Green Trust exhibited chronic sluggishness in its communication with the ECMWF server. In addition, the geographical separation of the two servers presents a challenge in terms of establishing efficient networking pathways. The data was put onto the Green Trust server within two days following its generation. In addition, it has been seen that certain files are absent from the server due to a failure in the transfer process. Therefore, a different mechanism for transferring files has to be employed.

Following extensive contact with the support team at the European Centre for Medium-Range Weather Forecasts (ECMWF) using the Jira platform, a decision was reached on the 7^{th} of July 2023 to utilise Amazon's Simple Storage Service (S3). This meant that the real-time forecasts without any missing files were only made available from the 10^{th} of July 2023. The results presented in this study are derived exclusively from real-time data collected from the period starting on July 10^{th}, 2023, up until the present day.

Amazon Simple Storage Service (Amazon S3) is an object storage service that offers industry-leading scalability, data availability, security, and performance. It can store and retrieve any data anytime, from anywhere (AWS, 2023). By cutting out the need for a physical storage space, the transfer speed was significantly increased and enabled the user to receive files as soon as they were generated without any missing files.

The process of retrieving real-time data became much simpler. In Figure 2.12, a BASH code is visible in which a date filter ”T1D072300” is given that downloads all the files with that specific date filter. The values 07 represent the month, and the value 23 represents the date for which the 10-day forecast data is requested. These two values can be altered according to the desired input date. The value ”00” is when the steps start; in this case, it will be 00:00 on the 23^{rd} of July 2023. The next command attaches a GRIB extension to all the downloaded files in the folder. All the files are then copied onto a singular GRIB file. The final two commands read the merged file for the given location and convert the tab-separated GRIB file into the output CSV file.

```
aws s3 ls s3://thesisbucketdhruv | grep "T1D072300" | awk '{print $4}' > file_list.txt
rm -f ~/download_dir/*
#mkdir -p download.dir
while IFS= read -r file_name; do
aws s3 cp "s3://thesisbucketdhruv/$file_name" "download_dir/"
done < file_list.txt
rename 's/(.*)/$1.grib/' download_dir/*
grib_copy download_dir/* Real-TimeData.grib
grib_ls -F"%.2f" -l lat,long Real-TimeData.grib > Real-TimeData.tsv
sed "s/  */,/g" Real-TimeData.tsv > Real-TimeData.csv
```

Figure 2.12: Input file for real-time data

The data obtained in real-time exhibits a step range spanning from 0 to 240, corresponding to a 10-day forecast. However, it should be noted that the material is not distributed among 240 distinct files. In Figure C.5 and Table 2.2, it can be viewed that for the first 90 steps, the data is per hour and from step 93 till step 144, it is per 3 hours and 6 hours after 144 till 240. The data from this CSV file is converted into the wind speed and direction per step and then copied onto an Excel workbook (.xlsx). The missing steps are filled by averaging the known and unknown values. An example of the skeleton file with all the filled data is shown in Figure C.6 in Appendix C. This file will be the input for the turbine output forecast method in chapter 4.

Table 2.2: Dissemination schedule of the atmospheric model high-resolution 10-day forecast (HRES).

Step Frequency	Dissemination Schedule
0 to 90 by 1	5:45 –>6:12
93 to 144 by 3	6:12 –>6:27
150 to 240 by 6	6:27 –>6:55

2.5. Revenue generation

The objective at hand is to determine a time interval during which the minimal amount of revenue can be forfeited. One possible approach to optimise revenue is to choose a certain time window throughout the week that minimises the product of the power price, turbine output, and duration in hours. The product of the Average Turbine Output (ATP) in megawatts (MW) and the Day-ahead Electricity price (DEP) for a specific time slot is then calculated. This amount is thereafter multiplied by the overall duration of the time slot, which, for the purposes of this report, is considered to be one hour. The output of this calculation in Equation 2.3 gives the revenue generated by the specific turbine in that time slot in €. The revenue generated for each time slot of the day is calculated using the same method.

$$[ATP] * [DEP] * [t] = Revenue \tag{2.3}$$

Two distinct sets of time ranges are defined for the time parameter. The initial aspect pertains to the designated operational time frame, which spans from 0800 to 1800, during which the contractors possess the ability to engage in physical maintenance activities on the turbine. The second period under consideration is the overnight range, spanning from 1800 hours to 0800 hours. During this time, the turbine may be intentionally kept idle as a preliminary step before commencing work in the morning or for the purpose of turbine analysis. The graph below illustrates the suggested time periods for the first time range. The data has been taken for 2018 from the 1^{st} of January till the 5^{th} of January. i.e. The 1st work week of the year 2018. It is observed in Figure 2.13 that the working hour time range on the 1^{st} (Monday) results in a minor loss of money, and for the overnight time range, keeping the turbine idle on the night of the 1^{st} would result in the most minor loss of money.

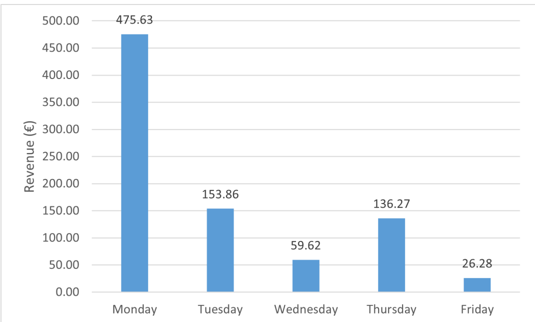

(a) 08:00 to 18:00.

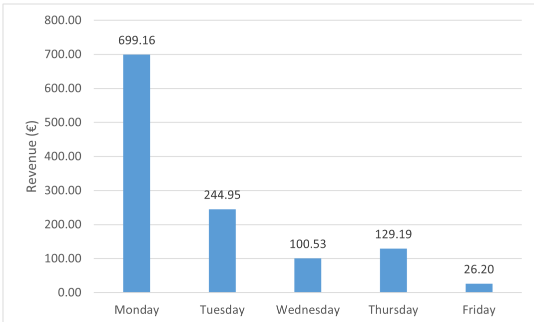

(b) 18:00 to 08:00 (next day)

Figure 2.13: Total revenue each day of a week in the winter of 2018.

A comparable analysis was performed during the summer times when the wind velocities were significantly lower. Typically, the cost of power tends to decrease in regions with higher levels of solar irradiation and significant wind resources. The data was collected for 2018 from the 2^{nd} of July till the 6^{th} of July. From Figure 2.14, it can be observed that for the working hours and the overnight periods on Friday, the 6^{th} of June showed the least loss in revenue for the specific week chosen.

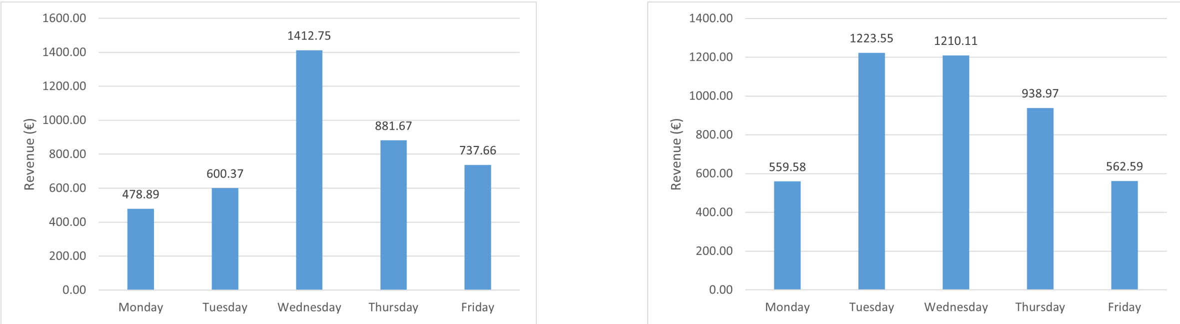

(a) 08:00 to 18:00.

(b) 18:00 to 08:00 (next day)

Figure 2.14: Total revenue each day a week in the summer of 2018.

3

Predictive Model for Electricity Prices (PMEP)

The fundamental workings of the PMEP are discussed in section 3.1, and multiple examples are provided to evaluate the model's performance. In section 3.2, an alternate working method is contemplated and compared to the first method. Lastly, a fully functional model is presented, and its workings and results are shown in section 3.3.

3.1. Fundamental working principal of the PMEP

The data collected by ENTSOE spans a period of seven years, namely from 2015 to the present. This dataset comprises day-ahead prices in the Netherlands for each hour of the day. The underlying concept revolves around utilising historical data to gain insights into the patterns of electricity costs across each day of the week. One important observation is that the specific date does not always occur on the same day every year. This is illustrated in the Figure C.9 in Appendix C.

Assume that a prediction will be made on the 3^{rd} of August 2023 for the forthcoming week encompassing the period from the 6^{th} of August to the 12^{th} of August, including Sunday until Saturday. The historical data about the above dates shows that the 6^{th} day of the month does not coincide with a Sunday in any of the specified years. Therefore, in this scenario, it is necessary to locate the nearest Sunday in the week where the 6^{th} of August occurs in the corresponding year. In the year 2022, the aforementioned date would correspond to the seventh day of August. Similarly, in the year 2021, it would correspond to the eighth day of August. In the year 2020, it would correspond to the ninth day of August. In the year 2019, it would have corresponded to the fourth day of August. Lastly, in the year 2018, it would have corresponded to the fifth day of August. The pattern in question has been allocated for implementation inside the PMEP.

The historical data is corrected with the data from recent weeks. The data from the past 3-4 weeks is then averaged into a singular column. The data for each day of the week is then averaged for the historical data set and the recent week's data. These are represented with ($\overline{P}_{day}$) and ($\overline{R}_{day}$). Then, the previous year's averaged value ($\overline{P}$) is multiplied by a correction factor (c_f), calculated using the Equation 3.1 to give the Predicted electricity price ($\overline{F}$) in Equation 3.2. This method of predicting electricity prices is termed the "Averaging Method".

$$c_f = \frac{\overline{P}_{day}}{\overline{R}_{day}} \tag{3.1}$$

$$\overline{F} = c_f * \overline{P} \tag{3.2}$$

Each predictive value obtained is compared to the observed values of the day-ahead prices from ENTSOE. The RMSE (Root-Mean Square Error) is calculated with Equation 3.3 to check the accuracy of the prediction where P_i and O_i represent the predicted and observed values, respectively, for the total of n values.

$$RMSE = \sqrt{\frac{\Sigma_{i=1}^{n}\left(P_i - O_i\right)^2}{n}} \tag{3.3}$$

The month of April was the first to be chosen for the price prediction model. Two predictions were made separately for the first two weeks of the month (02/04/2023 till 15/04/2023), and the results are displayed in Figure 3.1. To understand the relative closeness of the forecast values to the actual values, RMSE (root-mean-square error) analysis is performed, and it is observed that a value of 32.36 €/MWh and 49.66 €/MWh is obtained for the respective weeks.

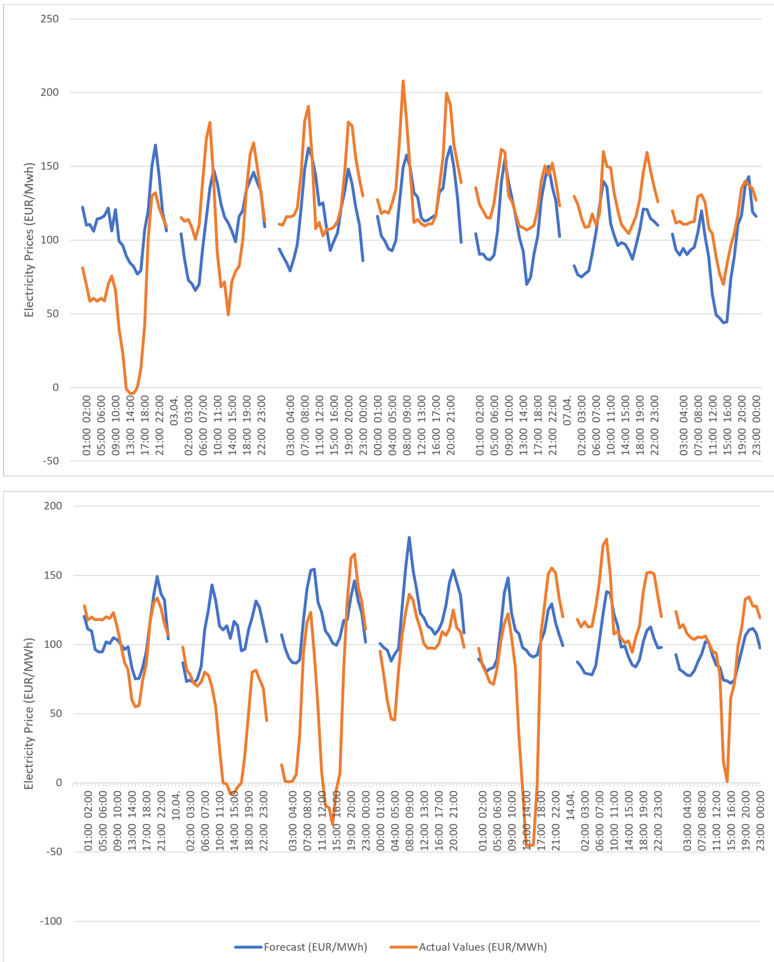

Figure 3.1: Forecast for 02-04-2023 till 08-04-2023 (top) and 09-04-2023 till 15-04-2023 (bottom).

3.2. An alternate method

An alternate "Normalised Method" was used to normalise electricity prices for different years on a level base. This is done by gathering the data from the previous years with the same method as discussed in the last section. Instead of averaging the historical values directly, these values are normalised using Equation 3.4. The normalised previous year average (P_{nom}) is defined as the ratio of the previous-year hourly electricity price (P) and the weekly average $\overline{P}_{week}$ of that particular week. These normalised values of previous years are then averaged to produce a single data set for historical values. This dataset is then multiplied with the recent 3-week average (R) to form the normalised forecast (F_{nom}) in Equation 3.5.

$$P_{nom} = \frac{P}{\overline{P}_{week}} \tag{3.4}$$

$$F_{nom} = P_{nom} * R \tag{3.5}$$

Figure 3.2 shows the two methods used to predict the day-ahead electricity price for the same week. The averaged method had a better RMSE of 29.76 €/MWh compared to the normalised method, with a value of 35.72 €/MWh, making it the better-performing method this week. Both methods face the familiar issue that neither method can predict negative prices.

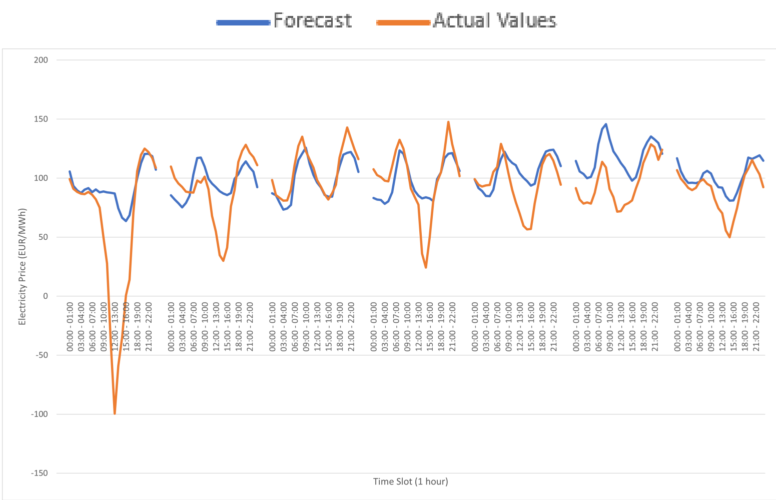

(a) Averaged forecast

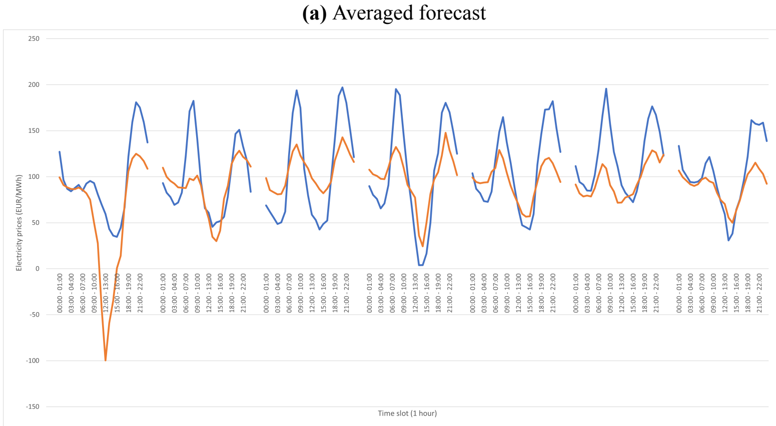

(b) Normalised forecast

Figure 3.2: Forecast for April 30th till May 5th 2023

Next, a further analysis was done to establish the better-performing method. The data range is extended to 2-weeks to get a better comparison. The graph is plotted and can be viewed in Figure 3.3. The top image is from 21^{st} May 2023 to 27^{th} May 2023. The negative prices observed throughout the week led to the RMSE of the forecast data with a higher than usual value of 40.76 €/MWh. The normalised method was also used for the same period, giving a slightly higher RMSE value of 42.78 €/MWh. The analysis period was then extended till the 3^{rd} of June 2023, and both methods resulted in similar but higher values of RMSE. The Averaged method (RMSE= 56.25 €/MWh) was pipped by the Normalised method (RMSE= 54.94 €/MWh).

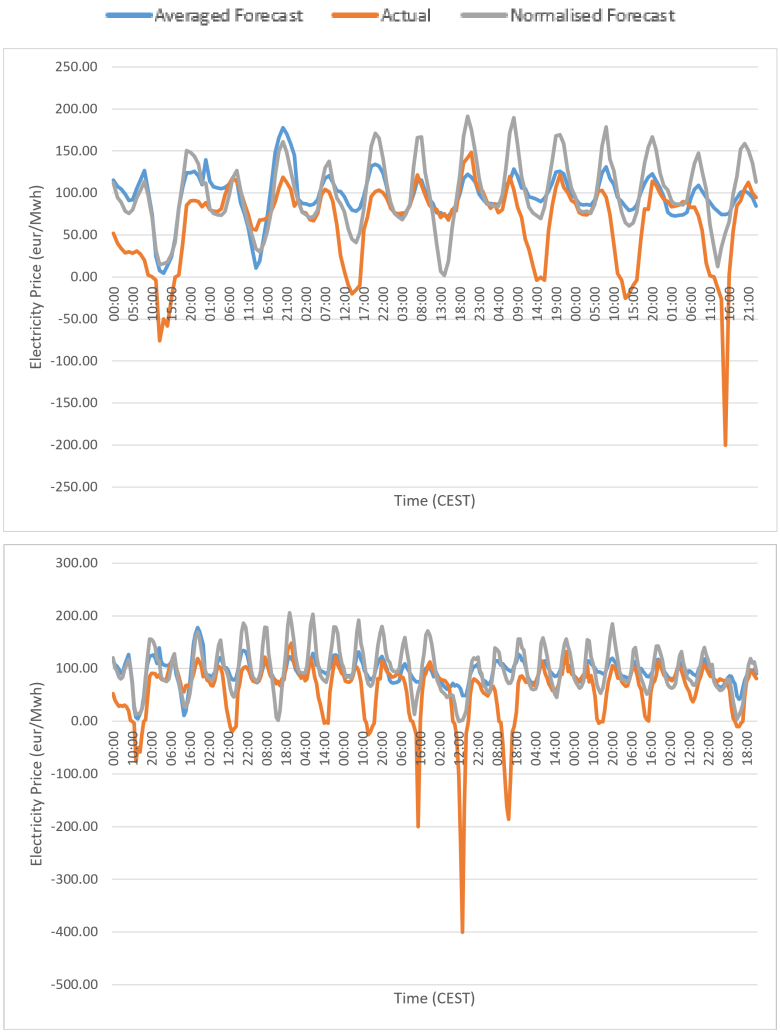

Figure 3.3: Averaged forecast vs. Normalised forecast 1-week comparison (top) and 2-week comparison (bottom)

The two methods are further examined, with the period under examination extended till the end of June 2023 and were compared in Table 3.1 and Table 3.2. For this period, the RMSE of the Averaged method was 43.69 €/MWh. The normalised method only slightly improved the RMSE value (RMSE= 41.81). For this comparison, the Averaged method performed marginally better in a 1-week scenario while the Normalised method was marginally better over a longer period. It can be concluded that either method would provide a similar performance in predicting electricity prices.

Table 3.1: RMSE (EUR/MWh) comparison of the Averaged and the Normalised method up to 3 weeks.

Method	RMSE (1-Week)	RMSE (2-Weeks)	RMSE (3-Weeks)
Averaged Method	40.76	56.25	48.16
Normalised Method	42.78	54.94	47.45

Table 3.2: RMSE (EUR/MWh) comparison of the Averaged and the Normalised method 4-weeks to 6-weeks

Method	RMSE (4-Weeks)	RMSE (5-Weeks)	RMSE (6-Weeks)
Averaged Method	47.01	46.53	43.69
Normalised Method	44.91	43.79	41.81

3.3. Fully functional PMEP

The subject week for the fully functional PMEP was chosen to be the week starting from the 9^{th} of July and ending on the 15^{th} of July in the year 2023. The forecasted electricity prices are matched against the actual values of the day-ahead electricity prices in Figure 3.4 for the subject week.

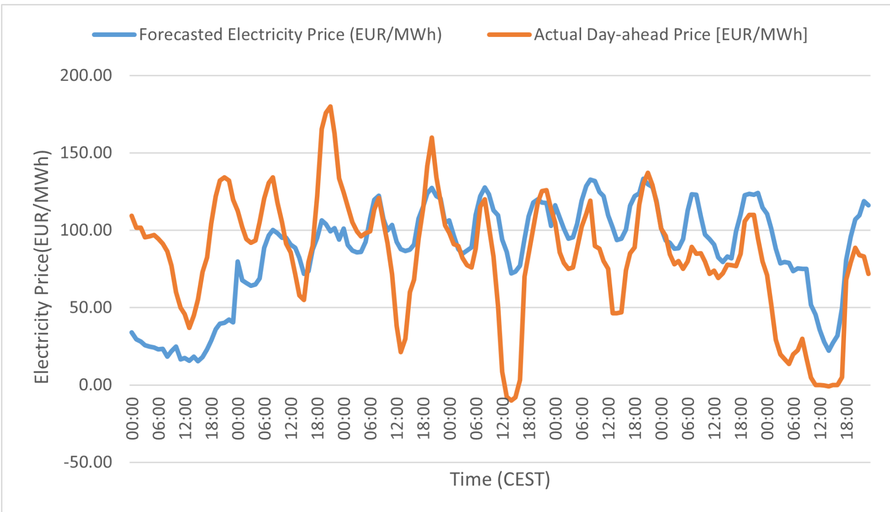

Figure 3.4: 7-day electricity price forecast from 09/07/2023 till 15/07/2023

The overall RMSE for the week was 40.26 €/MWh. Whilst the RMSE total for the weekdays reduces to 31.69 €/MWh, the RMSE total for the Weekend was 55.03 €/MWh. From Table 3.3, it can be observed that the RMSE on Sunday was 66.57 €/MWh while on the weekdays it ranges from 20 €/MWh to 42 €/MWh. This further emphasises that the model matches up well against the actual values during weekdays but struggles to do so on Sundays as the negative prices seem to creep in more often in the electricity market on the weekend,d causing the actual prices to deviate by large amounts to the natural trend. In Table 3.3, the RMSE

Table 3.3: RMSE per day; 09/07/2023 till 15/07/2023.

Date	Day of the Week	RMSE
09/07/2023	Sunday	66.57
10/07/2023	Monday	36.60
11/07/2023	Tuesday	26.27
12/07/2023	Wednesday	41.99
13/07/2023	Thursday	28.43
14/07/2023	Friday	20.51
15/07/2023	Saturday	43.50

The same model is run for multiple subject weeks before it is automated in the section 5.2. The week from the 12^{th} of February 2023 to the 18^{th} of February 2023 is another example to run this model. The forecasted electricity prices are matched up against the actual values of the day-ahead electricity prices in Figure 3.5 for this week.

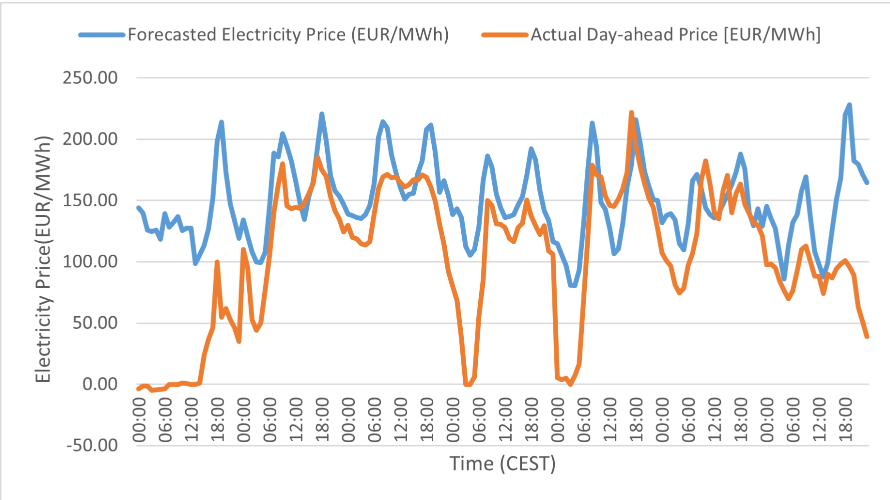

Figure 3.5: 7-day electricity price forecast from 12/02/2023 till 18/02/2023

The overall RMSE was 63.27 €/MWh. Whilst the weekday RMSE was reduced to 42.05 €/MWh, the RMSE for the Weekend was 94.51 €/MWh. On Sunday, the 12^{th} of February, the model had an RMSE of 120.21 €/MWh due to the negative prices observed that day. Such negative prices were uncommon in previous years.

Table 3.4: RMSE per day; 12/02/2023 till 18/02/2023.

Date	Day of the Week	RMSE
12/02/2023	Sunday	120.21
13/02/2023	Monday	32.11
14/02/2023	Tuesday	30.39
15/02/2023	Wednesday	57.15
16/02/2023	Thursday	52.29
17/02/2023	Friday	29.74
18/02/2023	Saturday	68.81

4

Forecast Model for Wind Turbine Power (FMWTP)

A Sanity check is performed on the data from ECMWF in section 4.1. In the last section, data filtering ensures the most appropriate values are used to correlate the archival and real-time data to the turbine data. Lastly, insection 4.3, the methodology is established for the FMWTP, and some examples of its performance are provided.

4.1. Sanity checks

As discussed in section 2.4, the real-time data from ECMWF gives the wind velocity at heights of 10m, 100m and 200m for four separate grid locations. Given that the hub height of the three selected turbines is 105m, it is advantageous to employ real-time and archive data collected at a height of 100m to establish correlations with the turbine data. Before the data is correlated, a sanity check is performed to evaluate whether the data provided by ECMWF is accurate quickly. This is done by plotting the wind rose for the archival data against all three turbines. A wind rose gives you information on the relative wind speeds in different directions. The archival dataset is the forecast dataset retrieved using the MARS-API, and the real-time data set is the forecast dataset provided by ECMWF as soon as it is generated in real-time. Since both archival and real-time data sets belong to the same category of forecast datasets, it is logical to utilise the historical data in conjunction with the existing turbine data for swift verification. Thus, by clearing the archival dataset, the real-time data can also be assumed to have earned the same sanity check.

The data obtained from the three turbines is considered a unified dataset, and it can be viewed in the Figure 4.1. Both datasets have a step range of 1 hour and are taken for the period from 0:00 on the 1^{st} of January 2018 till 23:00 on the 31^{th} of December 2022, thus, making the comparison of their Wind rose more convenient. There are large similarities in the Wind Rose of all four diagrams. Although a small difference can be noticed that the operational archive skews a bit more towards the 270° direction, all four diagrams show more or less the same relative frequency of wind directions.

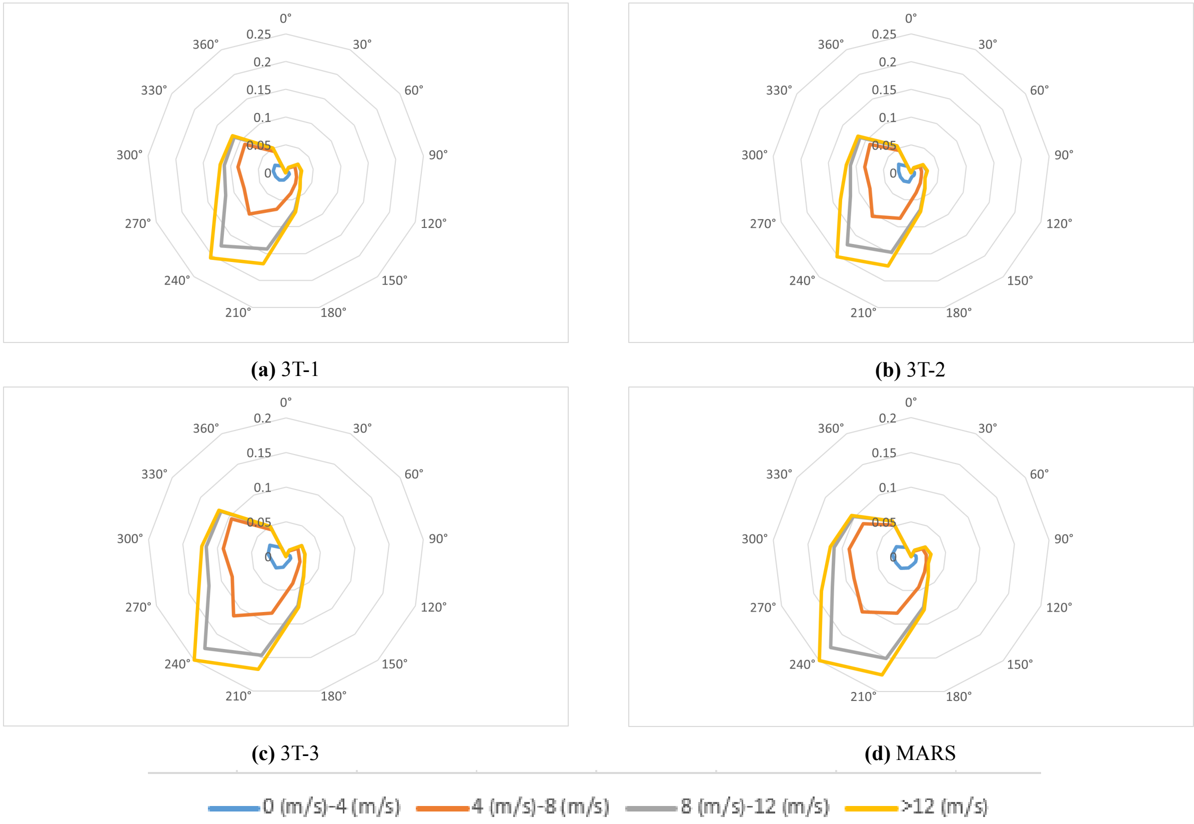

(a) 3T-1

(b) 3T-2

(c) 3T-3

(d) MARS

Figure 4.1: Wind rose diagram for the 3T wind farm

4.2. Filtering the data

A separate Excel workbook titled ”Operational Archive vs 3T” was created for every individual turbine. The operational data’s wind speeds and wind directions are recorded alongside the wind turbine data in this workbook. Three critical parameters were not considered when performing a sanity check on the data in section 4.1. These are the TSA of the turbines, the direction matching and the wind ratio. Each parameter has been assigned a column in the workbook. A single value or a range of values is established for these parameters to filter the data. Filtering the data before it is used for the correlation to reduce the forecasted wind turbine power inaccuracy.

4.2.1. TSA

The TSA is bounded by the interval of 0 and 1, with each turbine possessing a distinct TSA value. The turbine’s availability is not full for any number below 1, indicating that the representative turbine output should not be considered. In Figure 4.2, the data points are plotted for turbine 3T-1 for the values of TSA not equal to 1, i.e. When the turbine is not fully available. The power curve in the two situations exhibits minimal resemblance to the power curve depicted in Figure 2.10. Thus, the filtration is done with the value of TSA=1.

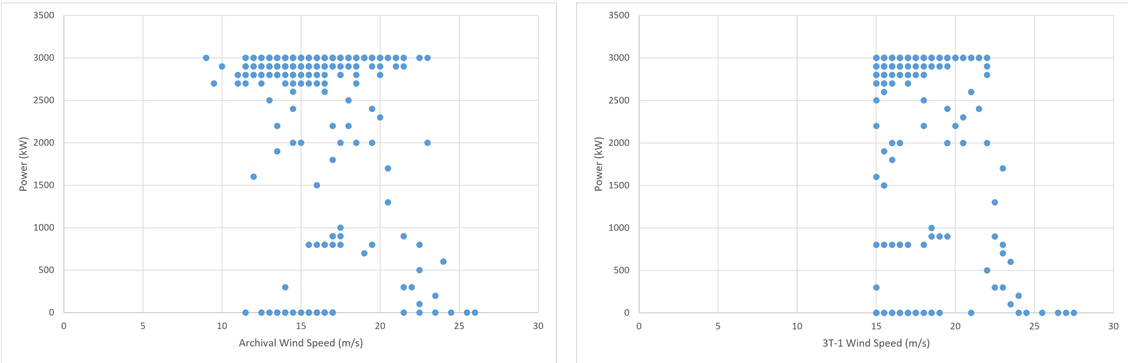

Figure 4.2: Power curve for 3T-1 with data points having TSA ≠ 1.

4.2.2. Direction matching

The selection process for direction matching involves choosing datasets where the exact wind direction is recorded for both the archival and turbine data. This is indicated by a direction match value of 1. In Figure 4.3, the average wind direction per turbine is shown. For the particular comparison, the wind directions are rounded to the closest 30° to form 12 wind direction bins. It can be observed that with the slightest change in the wind direction, the power observed for the individual can vary by a significant amount. From the orientation of the wind farm in Figure 1.5 and the average turbine output in Figure 4.3, the wake effects on the turbines can be better understood. For the wind directions, 30° and 60°, the wake effects on the turbines 3T-1 and 3T-2 can be observed by the reduction in the average power output compared to that of turbine 3T-1. Similar observations can be made for the wind directions 210° and 240°. The power output turbines 3T-2 and 3T-3 are greatly affected by the presence of the wakes from turbine 3T-1. Thus, ensuring that the archival and turbine data for every chosen data point have the same wind direction when rounded off is essential.

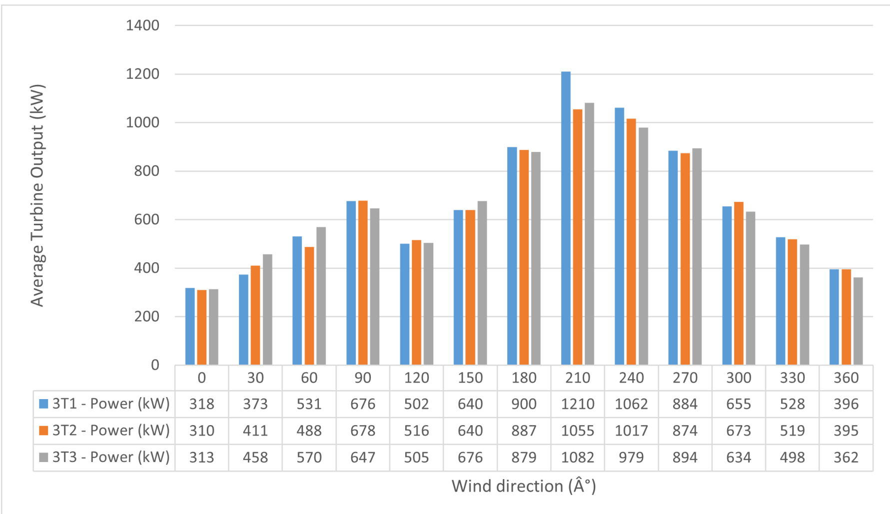

Figure 4.3: Averaged turbine output per wind direction

4.2.3. Wind ratio

The wind ratio is defined as the ratio of the archival wind speed and the observed turbine wind speed for the same time slot. Based on the marginal disparity between the hub height of 105m and the real-time data recorded at the height of 100m, it is probable that the wind speeds measured at the selected grid point and the turbine will exhibit a negligible discrepancy and remain largely consistent. The wind ratio was initially assigned a solitary value of 1. However, when calculating the average number of valid points per cell for the region between the cut-in wind speed and rated wind speed in the Matrix depicted in Figure 4.5, it was discovered that the average number of valid points per cell was only 13. The objective of the ”wind ratio” filter is to generate a power curve that is as smooth as feasible while maximising the number of data points.

Following that, the wind ratio was assessed within the range of 0.95 to 1.055. In this particular instance, the curve exhibited a consistent level of smoothness, although it did not yield a substantial rise in the average quantity of valid points per cell. In order to achieve an adequate number of acceptable data points for the averaging process, it is necessary for the average valid points per cell to approach a value of 50. This outcome was achieved by selecting a wind ratio range spanning from 0.9 to 1.1, resulting in an average of 40 valid data points inside the Matrix. In Figure 4.4, the effect of the filter on the power curve established between the archival wind speed and the turbine output for the same turbine can be observed for all the different values of the wind ratio.

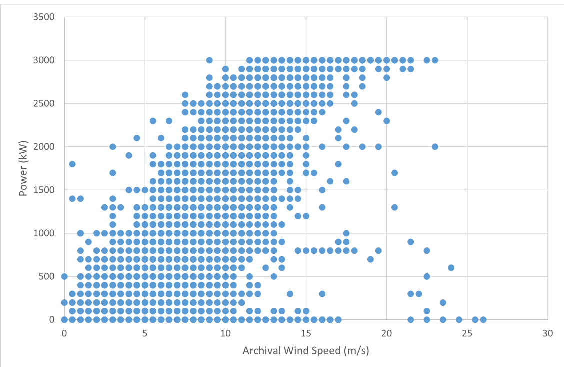

(a) [TSA, Direction Match, Wind Ratio]= undefined

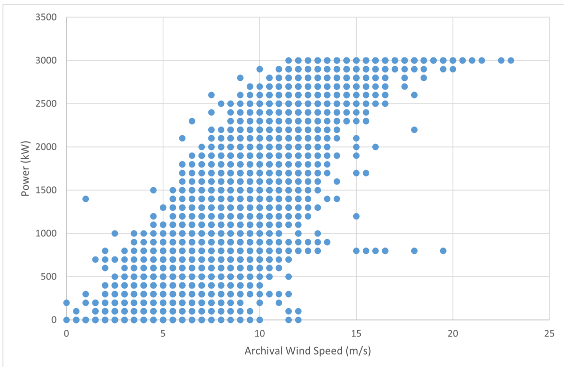

(b) TSA=1, Direction Match=1, Wind Ratio= undefined

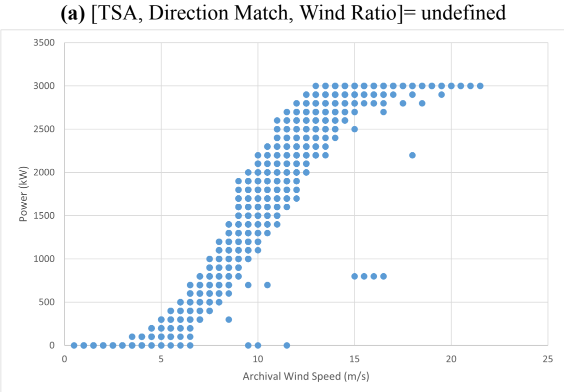

(c) TSA=1, Direction Match=1, Ratio= [0.9,1.1]

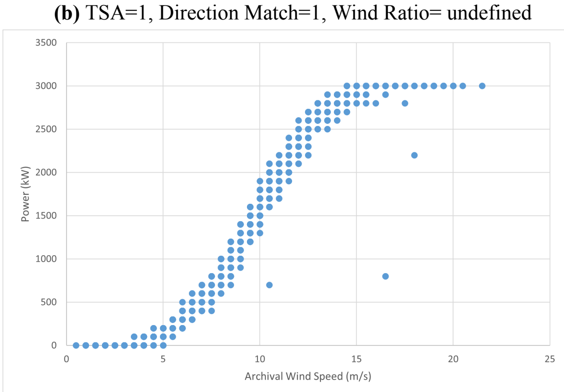

(d) TSA=1, Direction Match=1, Ratio=1

Figure 4.4: Power curve made with archival wind speed for turbine 3T-1

4.3. The workings of the FMWTP

The archival and the turbine wind speeds are rounded off to the nearest 0.5 m/s values, and the respective wind directions are rounded off to the nearest 30°. The wind speed and wind direction datasets are thus binned per 0.5 m/s and 30° to create the matrix Figure 4.5 with the archival wind speed column ranging from 0 m/s to 22.5 m/s and the archival wind direction row ranging from 0° to 360°. The averaged values of the power output are rounded off to the closest 10 kW.

Archive Wind Sector (Â°)													
Archive Wind Speed (m/s)	0	30	60	90	120	150	180	210	240	270	300	330	360
0													
0.5			0										
1	0	0	0		0		0						0
1.5	0	0	0	0	0		0		0	0	0	0	0
2	0	0	0	0	0	0	0	0	0	0	0	0	0
2.5	0	0	0	0	0	0	0	0	0	0	0	0	0
3	0	0	0	0	0	0	0	0	0	0	0	0	0
3.5	0	0	0	0	0	0	0	10	0	10	0	0	0
4	30	50	60	60	50	70	40	30	50	50	60	20	30
4.5	100	100	100	100	100	100	110	100	100	100	100	100	100
5	140	160	170	180	160	160	160	120	160	160	160	160	140
5.5	230	240	250	240	230	230	220	230	230	220	230	220	230
6	340	350	380	380	370	370	360	360	350	350	360	370	340
6.5	450	460	500	480	480	490	450	460	460	450	510	440	450
7	540	530	550	520	580	560	540	500	520	560	560	510	540
7.5	630	660	660	690	690	680	680	650	640	680	710	700	630
8	830	830	870	870	900	840	800	820	830	830	800	790	830
8.5	1020	990	1060	1000	1010	1010	990	1010	1010	1000	1020	1010	1020
9	1190	1190	1260	1250	1100	1270	1180	1180	1190	1190	1190	1220	1190
9.5	1340	1330	1450	1490	1450	1380	1340	1380	1380	1360	1400	1380	1340
10	1600	1570	1590	1610	1700	1530	1560	1560	1550	1620	1580	1560	1600
10.5	2030	1750	1810	1790	1800	1750	1770	1760	1770	1780	1830	1490	2030
11	1950	2050	2050	1950	1960	1900	1940	1980	1990	1990	2050	1920	1950
11.5	2150	1970	2330	2190	2100	2280	2060	2210	2230	2210	2280	2180	2150
12	2000	2300	2510	2510	2250	2280	2350	2420	2430	2410	2400	2510	2000
12.5	2600	2400	2720	2410	2400		2500	2580	2540	2540	2580	2660	2600
13	2700	2550	2800	2680	2800		2600	2720	2700	2670	2700	2630	2700
13.5	2900	2660	2820	2800		2500	2600	2770	2740	2730	2640	2720	2900
14		2500		2800			2800	2820	2850	2790	2830	2880	
14.5			2900	2800			2850	2890	2900	2890	3000		
15							2970	2890	2920	2950	2940	2900	
15.5	3000						2900	2880	2900	2960	3000		3000
16	2800						2900	2970	2980	2990	2970	3000	2800
16.5							3000	2760	2980	2990	3000		
17								3000	3000	3000	3000	3000	
17.5								3000	3000	3000	3000		
18								3000	3000	3000	3000	3000	
18.5								3000	3000	3000	3000		
19								3000	3000	3000	3000		
19.5								3000	3000	3000	3000	3000	
20							3000	3000	3000	3000			
20.5								3000	3000	3000			
21								3000	3000				
21.5									3000				
22									3000				
22.5									3000				

Figure 4.5: Matrix consisting of the averaged turbine power output (in kW) for 3T-1

The forecasted wind speed and wind directions are rounded off to the nearest 0.5 m/s and 30°, respectively. These are then used as the input values for the XLOOKUP function in Excel (Stockton, 2021). The model employs a nested XLOOKUP function to perform both VLOOKUP and HLOOKUP operations for the purpose of looking up the averaged wind speed and averaged wind direction, respectively. Consequently, it retrieves the average turbine output value by referencing the two parameters at each time step. The values obtained from implementing the XLOOKUP function represent the forecasted turbine output.

For example, in Figure 4.5, to look up the value of the average turbine power for the archival wind speed and wind direction of 7.5 m/s and 210°, The XLOOKUP function initially does a horizontal lookup of the wind speed within the vertical column, and subsequently records the associated power values for all wind directions (shown by the blue highlighting). Subsequently, the model vertically scans for the specific column encompassing the entire power values corresponding to a wind direction of 210° (shown by the yellow highlighting). The resulting value of the intended power output is determined by identifying the row and column (highlighted in green).

The vacant cells are needed to be selectively filled. As the Netherlands predominantly experiences wind in the South-West direction (Wingfeet, 2015) i.e. 210° and, 240° and 270° , the cells in those wind direction columns are filled out to completion. Before the cut-in wind speed, the power values in each sector are denoted as 0 kW, while the absent values between the rated power and the cut-out wind speed are denoted as 3000 kW, corresponding to the rated power of these turbines. A power curve for the matrix is established for the 240° and depicted in Figure 4.6.

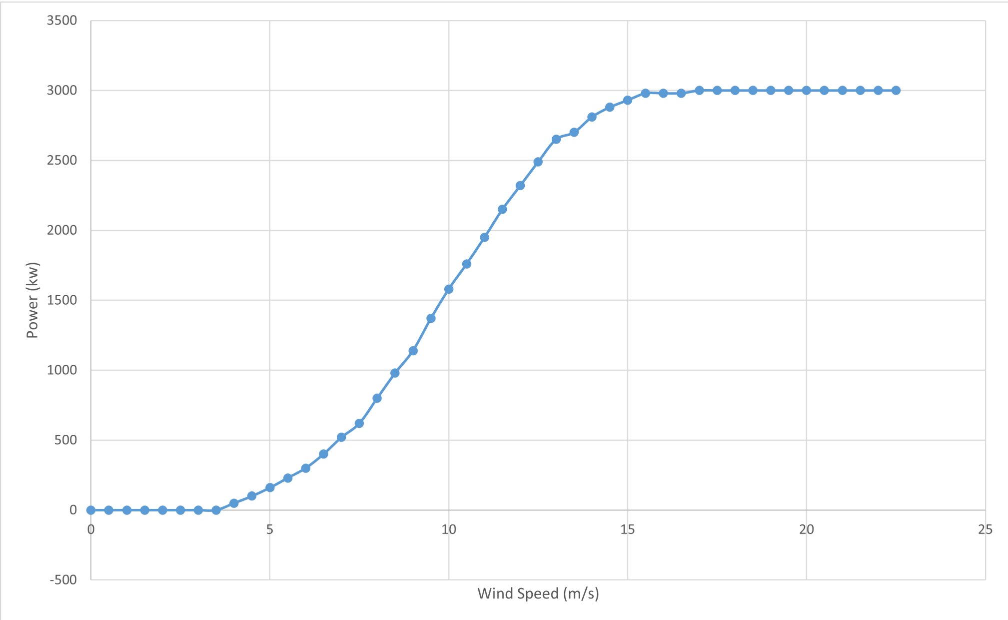

Figure 4.6: Matrix power curve for 3T-1 for the dominant wind direction 240°.

In the Figure 4.7, the 7-day forecast executed on the 9^{th} of July 2023 is measured against the actual turbine power observed by the three chosen turbines. In order to evaluate the accuracy of the forecast values derived from the matrix averaging approach compared to the actual turbine output, a Root Mean Square Error (RMSE) study is conducted. The turbines 3T-1, 3T-2, and 3T-3 exhibit root mean square errors (RMSE) of 483 kW, 481 kW, and 695 kW, respectively. There was a notable disparity between the observed and forecasted statistics of turbine 3T-3. During this time period, the turbine had a time-based system availability (TSA) value of 0 during the initial 106 out of the 168 time slots.

A similar 7-day forecast is done for the 1st of January 2023. The forecast turbine output is compared to the observed output and plotted in the Figure 4.8. It is observed that there is an RMSE of 721 kW, 727 kW and 746 kW for the turbines 3T-1, 3T-2 and 3T-3 turbines respectively. In the Table 4.1, the 7-day forecasts are compared to the 10-day forecasts.

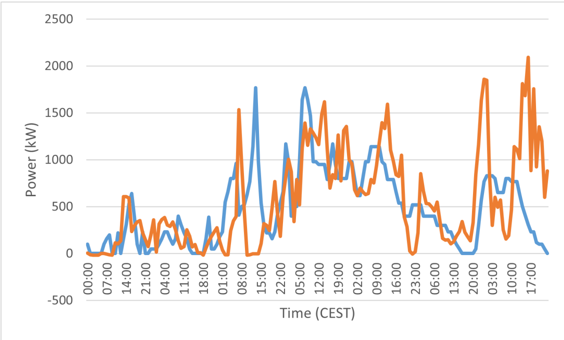

(a) 3T-1 turbine output: actual vs forecast

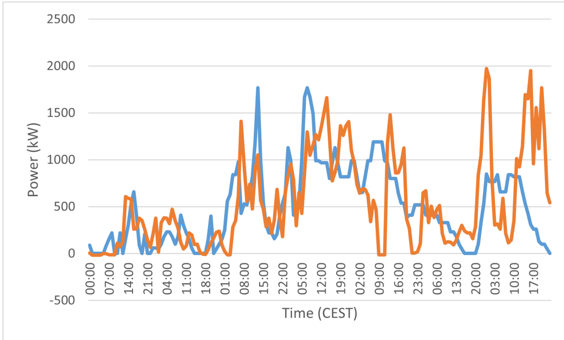

(b) 3T-2 turbine output: actual vs forecast

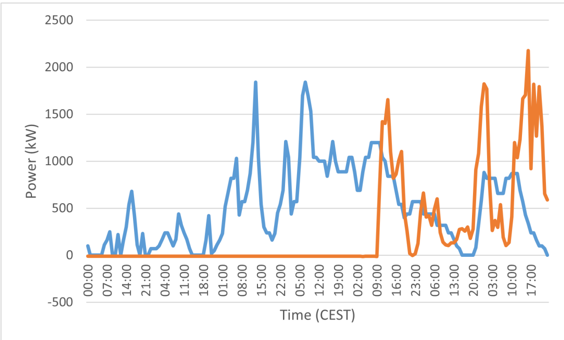

(c) 3T-3 turbine output: actual vs forecast

Figure 4.7: 7-day turbine output forecast for the 9^{th} of July, 2023.

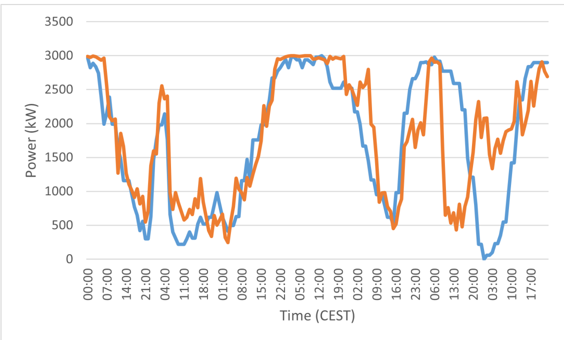

(a) 3T-1 turbine output: actual vs forecast

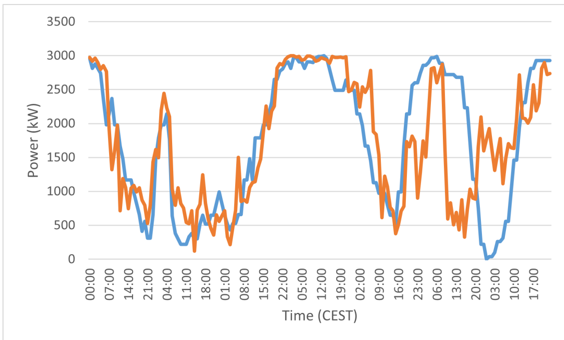

(b) 3T-2 turbine output: actual vs forecast

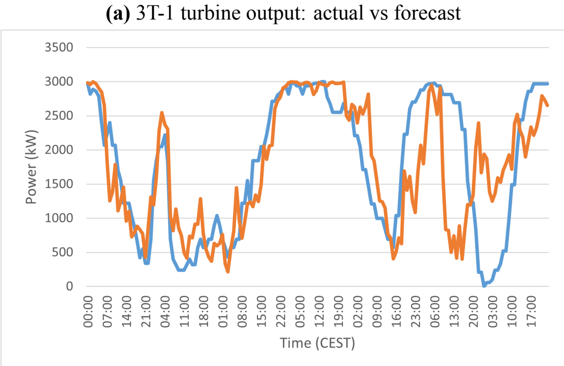

(c) 3T-3 turbine output: actual vs forecast

Figure 4.8: 7-day turbine output forecast for the 1^{st} of January, 2023.

Table 4.1: Summary table: FMWTP vs. Observed turbine output (3T-1) for January 2023

Date of Forecast	**RMSE 7-Day (EUR)**	**RMSE 10-Day (EUR)**
01/01/2023	721.00	843.14
08/01/2023	757.82	827.57
15/01/2023	656.77	583.86
22/01/2023	325.20	614.46
29/01/2023	623.25	674.10

The root-mean-square error (RMSE) for the turbine 3T-1, 3T-2 and 3T-3 as a function of the lead time (0-240 hours) is plotted in Figure 4.9. The RMSE is derived from the difference in the FMWTP output and the actual turbine output for each time slot. Data was collected from individual forecasts spanning the period of 42 days starting from the 10^{th} of July 2023 till the 20^{th} of August 2023. As the time step value increases from zero to 240 a sharp increase in the RMSE value of the turbine output can be clearly observed in all three graphs. The accuracy of the FMWTP gradually decreases from the 1^{st} day of the forecast till the 10^{th} day. This can be partially explained by the increase in inaccuracy of the meteorological wind speed and wind directions with respect to the lead time for the same period under observation. These can be viewed in Figure D.3 and Figure D.4 in Appendix D.

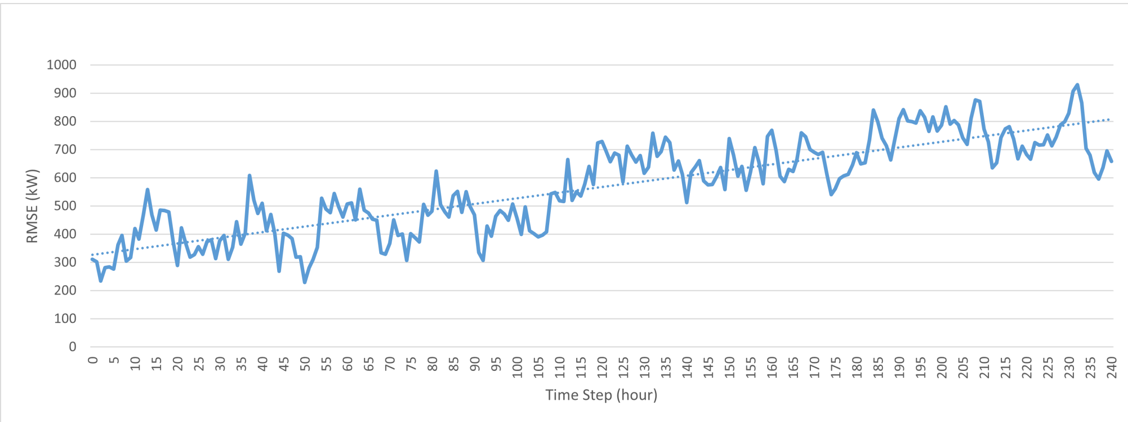

(a) 3T-1

Figure 4.9: RMSE (in kW) as a function of lead time for all three turbines

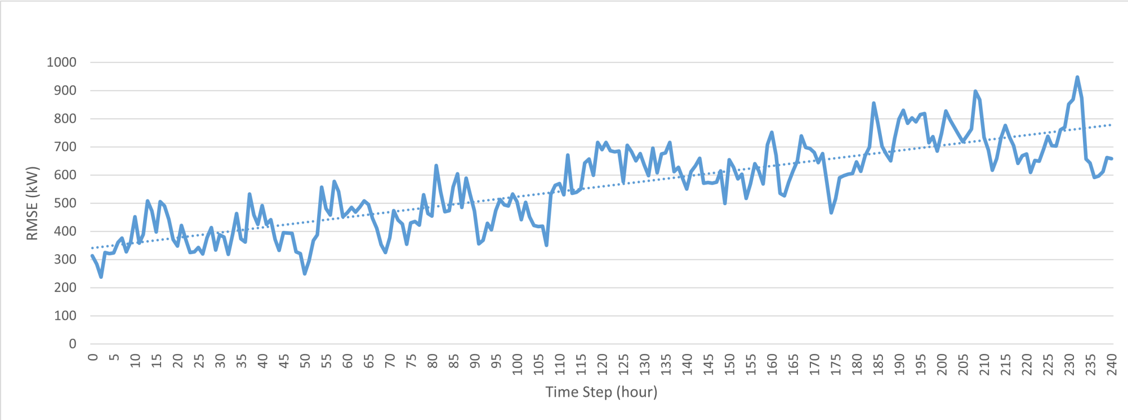

(b) 3T-2

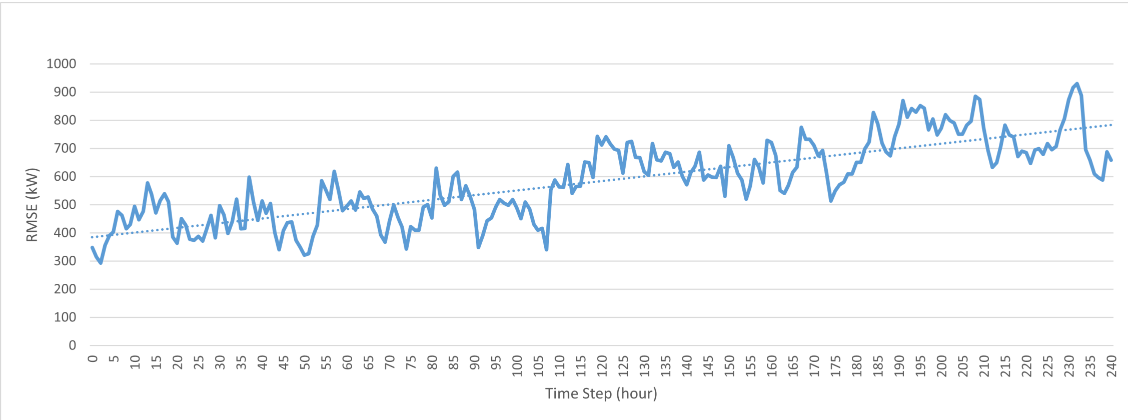

(c) 3T-3

Figure 4.9: RMSE (in kW) as a function of lead time for all three turbines

5
Revenue Model for Wind Turbines (RMWT)

First, in section 5.1, the methodology of the RMWT is presented. This is compared to the actual revenue generated by the 3-turbine wind farm. Next, the automation process of the RMWT is discussed section 5.2. The RMWT is evaluated in comparison to the standard operating procedure (SOP) for master maintenance, as outlined in section 5.3. In section 5.4, the model is compared to the actual revenue of the turbine in multiple weeks. Lastly, in section 5.5, the model is compared to the recommendation given by the ASM team at Green Trust.

5.1. Methodology

The prediction models for electricity prices and turbine output constructed in chapter 3 and chapter 4 will be used to generate the revenue of the turbines. The period chosen for this model is the week starting from the 9^{th} of July 2023 and ending on the 15^{th} of July 2023. The forecasted values of the FMWTP and PMEP for the 9^{th} of July 2023 till the 15^{th} of July 2023 are fed to the RMWT, which uses Equation 2.3 the total forecasted revenue is calculated for each turbine for the entire week. The product of the Forecast Turbine Power (ATP$_{forecast}$), the predictive electricity price (DEP$_{predicted}$) and the time step duration give the forecasted revenue.

$$[ATP_{forecast}] * [DEP_{predicted}] * [t] = [Revenue_{forecast}] \tag{5.1}$$

The forecasted revenues for different periods, specifically during working hours and overnight, are compared to the actual revenue figures that would have been observed if the turbine output and day-ahead electricity prices were considered. The actual values of the turbines do not factor in the TSA values. In Figure 5.1c, illustrates the observed revenue of turbine 3T-3, which is found to be negative. This negative revenue can be attributed to the turbine's non-operational state, resulting from continuing maintenance activities. Hence, these data will not be considered during the analysis of the forecast's performance. In Figure 5.1a and Figure 5.1b, the RMWT performs better overnight than during working hours. This can be either because of the better performance of the FMWTP, the PMEP, or both for the specific period.

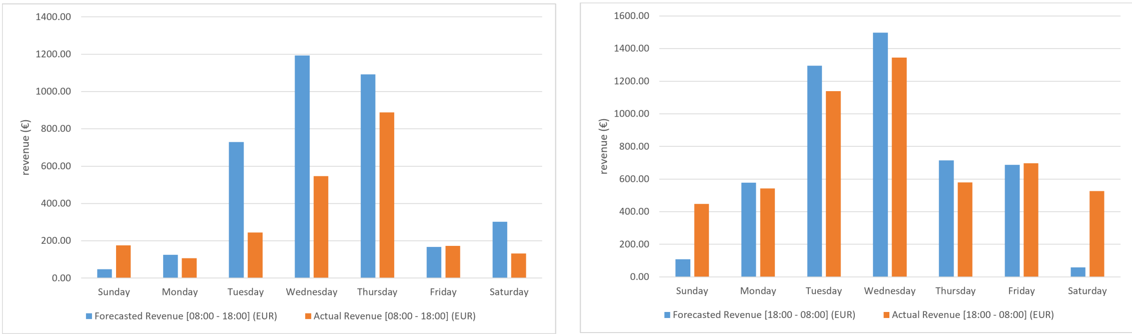

(a) 3T-1

(b) 3T-2

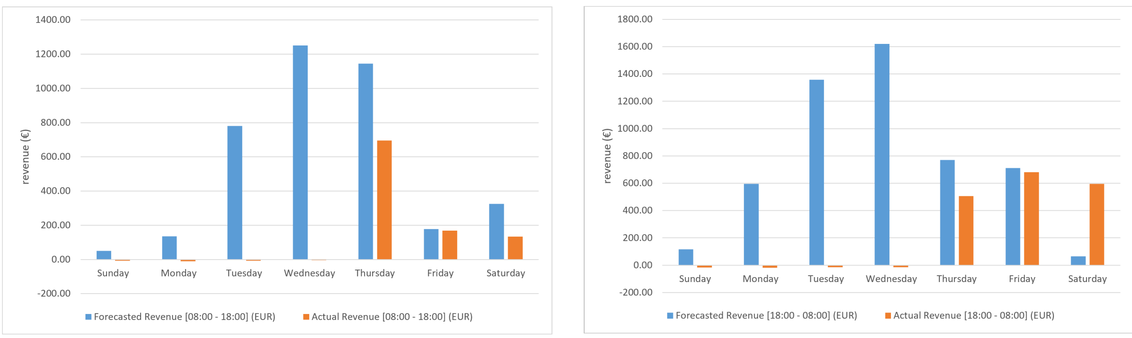

(c) 3T-3

Figure 5.1: Forecast revenue vs. Actual revenue of the chosen turbines from 09/07/2023 till 15/07/2023

5.2. Automation

This section discusses the automated process of the RMWT. The first step involves supplying the model with a specific date in order to get the forecasted revenue estimate. The first date randomly selected for the RMWT was the 23^{rd} of July 2023. After giving the input date filter ”T1D072300”, the 10-day HRES forecast provided by ECMWF is downloaded for the corresponding date. The values of the wind speeds for each 1-hour time step from 0:00 hours on the 23^{rd} of July 2023 till 0:00 hours on the 2^{nd} of August 2023. A few examples of the output are illustrated in Figure C.7. In parallel, the specified date of 23^{th} of July 2023 is inputted into the PMEP, a system designed to forecast hourly electricity prices for the subsequent seven-day period, spanning from 0:00 hours on 23^{rd} to 23:00 on 29^{th} of July 2023. The FMWTP and PMEP output values are inputted into the RMWT to get the forecasted revenue.

In Figure 5.2a, Figure 5.2b and Figure 5.2c, the revenue that would be lost for each of the turbines if any form of maintenance were to be scheduled on these days can be seen. The forecast revenue for the working hours and the overnight period are then calculated.

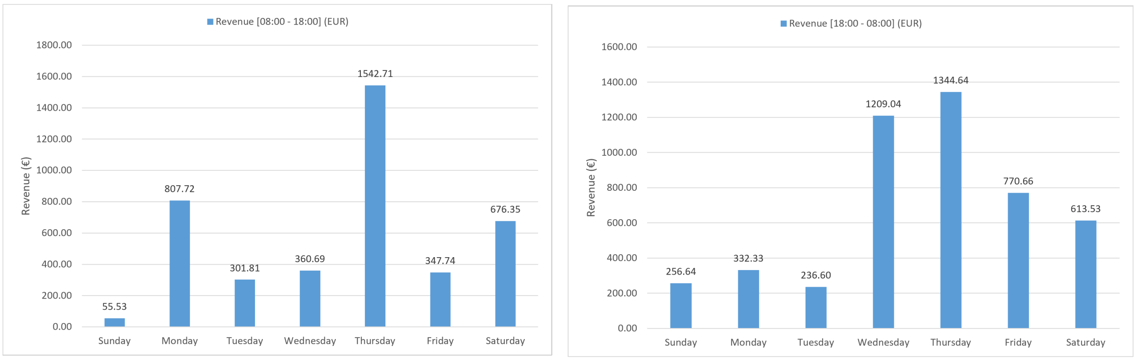

(a) 3T-1

Figure 5.2: Forecasted revenue of the chosen turbines from 23/07/2023 till 29/07/2023.

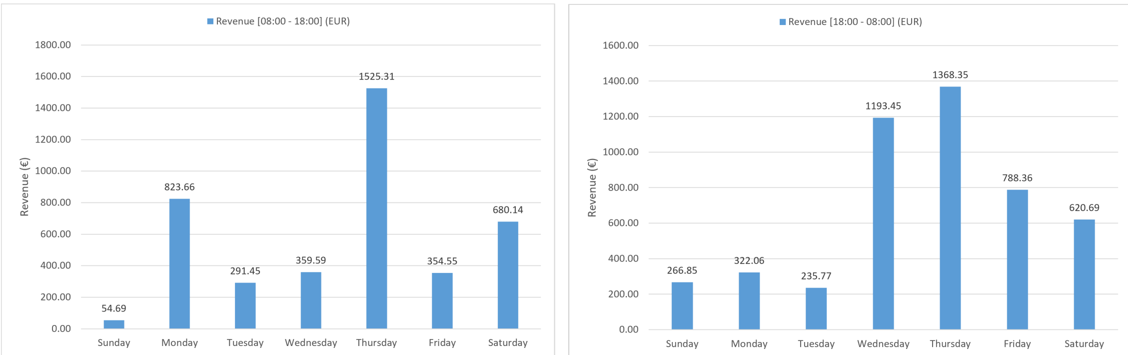

(b) 3T-2

(c) 3T-3

Figure 5.2: Forecasted revenue of the chosen turbines from 23/07/2023 till 29/07/2023.

5.3. Hypothetical master maintenance

The turbine 3T-3 is the subject of analysis in this particular case study. The turbine has been reported to undergo the process of comprehensive master maintenance. This would necessitate the turbine undergoing service for two consecutive days and remaining inactive overnight. The designated dates for the task in the present year were the 23^{rd} and the 24^{th} of May. The model was employed to calculate the forecasted loss of revenue for the specified time frame. Based on the findings, technicians will be provided with an alternative date for carrying out this task. The model methodology will be used for the 19^{th} of May 2023, the Friday of the week before the scheduled dates. In this case, the archival forecast will be taken for the date 19^{th} of May 2023. The figure below presents the forecasted revenue generated on the 19^{th} for the forthcoming week. Based on the provided information, the user can make informed decisions regarding the recommended dates for the master maintenance. .

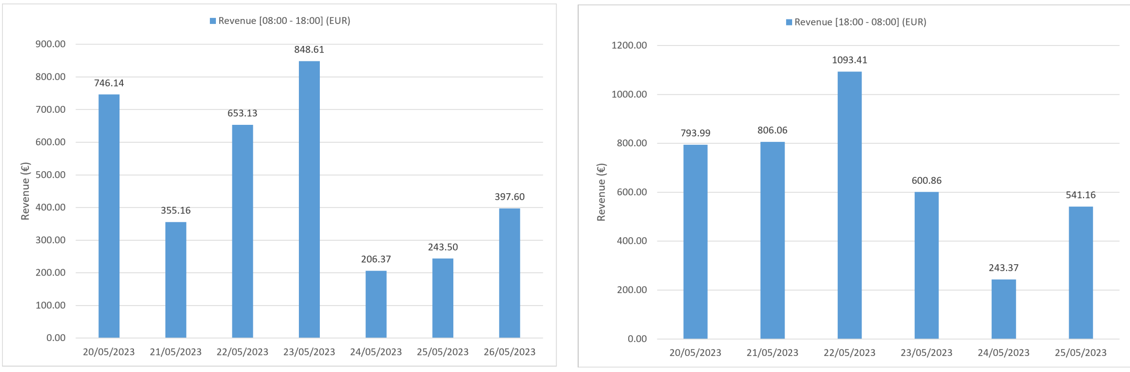

(a) RMWT output

(b) Actual revenue

Figure 5.3: Revenue for the week 21/05/2023 till 26/05/2023 for turbine 3T-3

According to the results obtained from the model, if the master maintenance were to be performed on the 23^{rd} and the 24^{th}, it would lead to a revenue loss of €1655.54. Rather than doing the task on the dates 24^{th} and 25^{th}, it suggests forecasting a revenue loss of €693.24. When comparing the forecast to the actual revenue, the dates 23^{rd} and 24^{th} give out a revenue loss of €717.97 and a loss of €858.55 for the dates 24^{th} and 25^{th}. Either of the date ranges would lead to a lesser loss of revenue, which is ideal for understanding the benefit of using this model, which lacks accuracy at the moment but still provides a valid indication.

5.4. Comparing with actual revenue

In this specific section, a comparison is presented between the forecasted revenue and the realised revenue of turbine 3T-1 over a span of several weeks. The objective is to ascertain the degree of correspondence between the model and the revenue across multiple instances. The model's input date filter for each week under observation is determined by selecting the day corresponding to the Friday of the preceding week. In the first example, the input date of the model is the 21^{st} of July 2023. The corresponding forecast and the actual revenue are plotted in Figure 5.4. From Figure 5.4a, it can be inferred that the model would suggest performing any 2-day task on Monday and Tuesday with a forecasted revenue of €490.06. According to the actual revenue, the master maintenance should also be performed on the same two days, but the money lost would be much higher than what is predicted by the model. The model was run on the input dates 14^{th} of July, 28^{th} of July, and 04^{th} of August 2023 for the turbine 3T-1, and the results can be viewed in Figure 5.5.

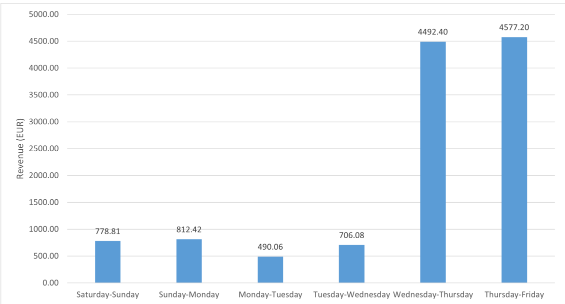

(a) Revenue forecast

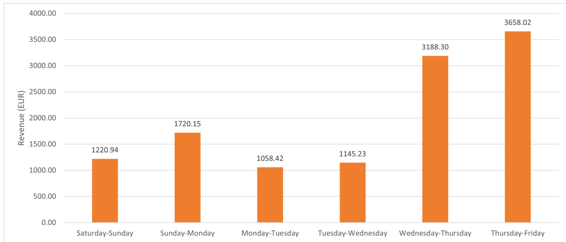

(b) Actual revenue

Figure 5.4: Forecast vs. Actual revenue for turbine 3T-1 from 22/07/2023 till 28/07/2023.

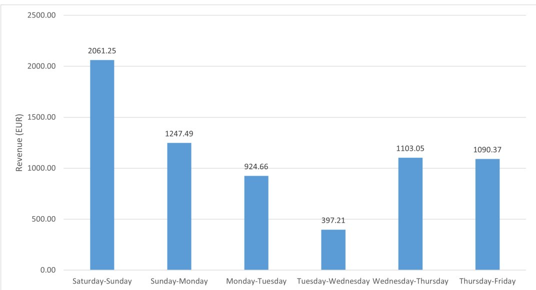

(a) Revenue forecast (14/07/2023)

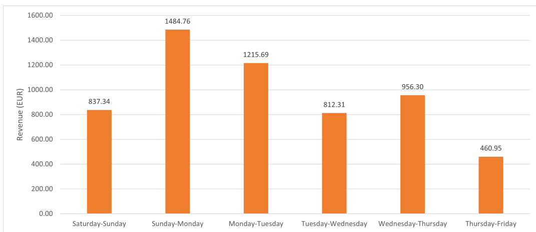

(b) Actual revenue (14/07/2023)

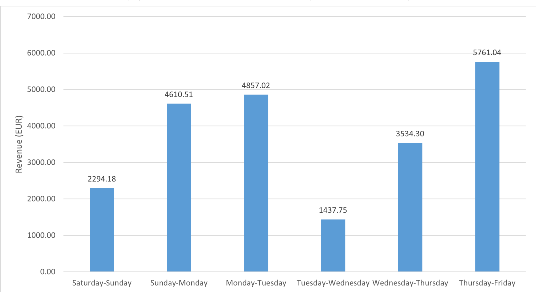

(c) Revenue forecast (28/07/2023)

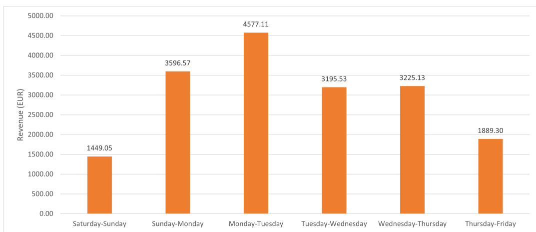

(d) Actual revenue (28/07/2023)

Figure 5.5: Forecast vs. Actual revenue for turbine 3T-1 for multiple weeks

In the first case, the model suggests Tuesday and Wednesday with forecast revenue of €397.21. The actual revenue on that day was €812.31. According to the Figure 5.5b, the days Thursday and Friday would result in the least loss of revenue of €460.95 while the €812.31 would be lost if the decision were to be made using the model. In the next case, the model again suggests Tuesday and Wednesday as the days with forecast revenue of €1437.75, whilst the actual revenue on those days is €3195.53. The optimum days would be. Thursday and Friday when the actual revenue is €1889.30. The model indicates a significantly higher value of €5761.04. In the final scenario, both the model and the actual revenue align, indicating that Wednesday and Thursday are the recommended days. However, both sources yield notably distinct values of €1651.76 and €179.43.

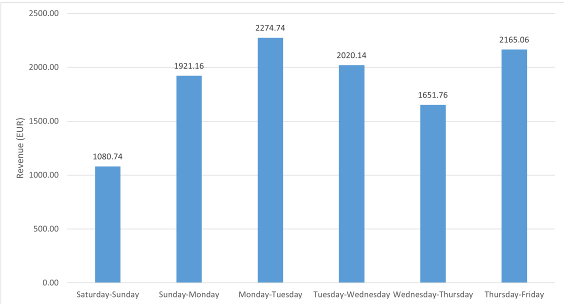

(e) Revenue forecast (04/08/2023)

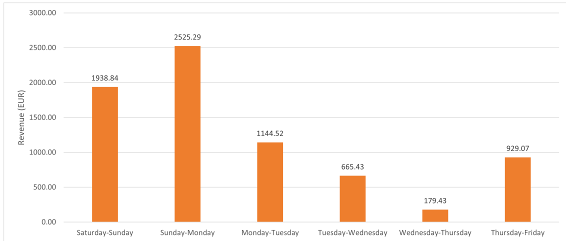

(f) Actual revenue (04/08/2023)

Figure 5.5: Forecast vs. Actual revenue for turbine 3T-1 for multiple weeks

In the 4 cases presented above, the model gives the correct indication 2 out of 4 times when compared to the actual revenue. Despite the model's correct indication, it cannot forecast revenue accurately. Therefore, the model would function as a more reliable indicator rather than an exact income prediction. In the subsequent section, a comparison is made between the model and the conventional approach of human input in determining the optimal dates for a 2-day maintenance task.

Table 5.1: Summary table: RMWT vs. Retrospect

Date of Forecast	**RMWT Revenue Forecast (EUR)**	**RMWT Revenue Actual (EUR)**	**Retrospect Revenue Forecast (EUR)**	**Retrospect Revenue Actual (EUR)**
14/07/2023	397.21	812.31	1090.37	460.95
22/07/2023	490.06	1058.42	490.06	1058.42
28/07/2023	1437.75	3195.53	5761.04	1889.30
04/08/2023	1651.76	179.43	1651.76	179.43

5.5. Comparing with regular method

In this case study, each member of the 3-man Asset Management team of Green Trust identified the ideal dates for performing a maintenance task on turbine 3T-1. They were given the situation as follows: On Friday, the 11^{th} of August, they will receive a call from the technicians who want to perform a specific task on the turbine, for example, retrofitting or blade maintenance, and they want to be told two consecutive dates in the next week when they can come to the wind farm and perform this task i.e the same time range in section 5.3. The ASM member must then look at the weather forecast on the spot on Windy (shown in Figure 5.6), make up their mind and provide a suggestion. This will be pitted against the advice of the RMWT. The response given to the technician by members A and B was to come on Wednesday the 16th and work until the evening of the 17th (Thursday), whilst member C instructed the technician to come on Monday the 14th and work until the evening of the 15th (Tuesday).

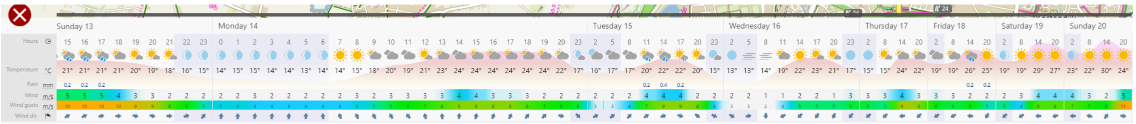

Figure 5.6: Windy Forecast (ECMWF) mid-day on 11/08/2023.

According to RMWT, the forecasted revenue for Wednesday and Thursday (as shown in Figure 5.7 is €738.16. Alternatively, if Monday and Tuesday were suggested, the revenue loss would be €348.76. If Tuesday and Wednesday were suggested, the revenue loss would be €125.83, which is a much better value. If the decision were to be made for the dates based on the RMWT, it would have given an additional saving of €612.33. The values obtained via RMWT were cross-checked with the actual values of the revenue of the turbine in Table 5.2 to understand the benefit of using the RMWT and what improvements can be made to get closer to the actual values.

Table 5.2: Summary table: Decision making (case 1)

Decision maker	**Forecast revenue (EUR)**	**Actual revenue (EUR)**	**2-Day period suggestion**
Team ASM	738.16	944.75	Wednesday and Thursday
RMWT	125.83	552.45	Tuesday and Wednesday

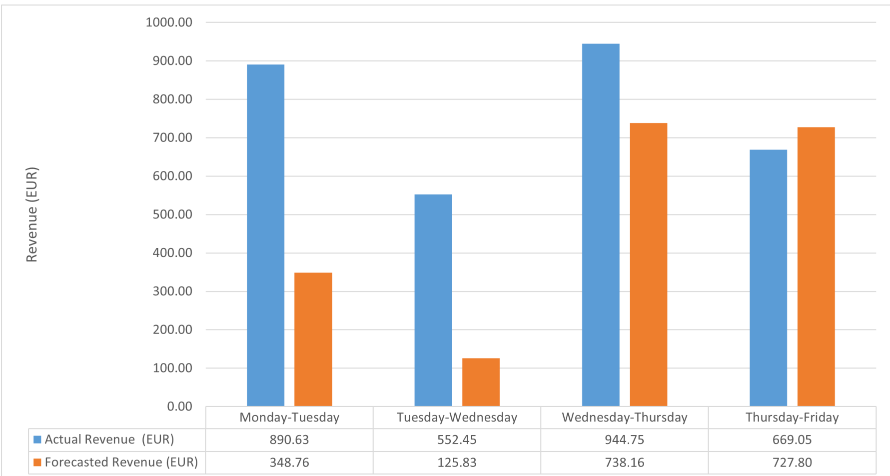

Figure 5.7: Forecasted vs. Actual Revenue for the input date 11/08/2023

The 3-man team was again asked for their services on the following Friday, i.e. 18^{th} of August 2023. The situation posed to them was the same, and they made their respective decisions based on the image in Figure 5.8. There was a unanimous agreement to suggest the days Monday and Tuesday to the technicians for the 2-day task to be performed. As shown in Figure 5.9, the forecasted revenue for Monday and Tuesday is €101.65. In this case, the model agrees with the decision made by the 3-man team. The actual revenue for the two days is €300.78. Based on the model, the suggestions for the days Tuesday and Wednesday are made, with the forecasted revenue being €165.00. In retrospect, it is evident from Table 5.3 that if these two days were recommended instead of Monday and Tuesday, the owner would have realised a cost savings of around €50, compared to the actual income of €249.16.

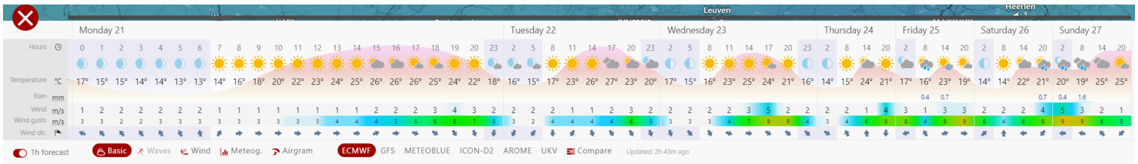

Figure 5.8: Windy forecast (ECMWF) mid-day on 18/08/2023.

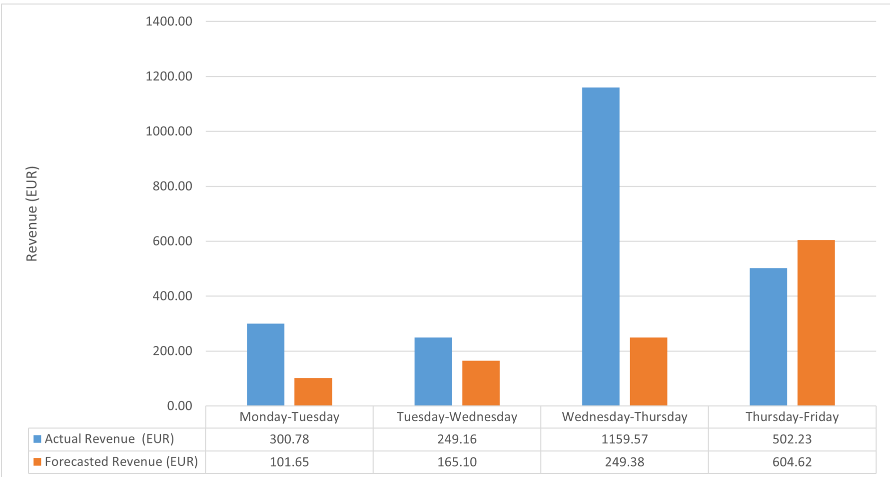

Figure 5.9: Forecasted vs. Actual Revenue for the input date 18/08/2023

Table 5.3: Summary table: Decision making (case 2)

Decision maker	Forecast revenue (EUR)	Actual revenue (EUR)	2-Day period suggestion
Team ASM	101.65	300.78	Tuesday and Wednesday
RMWT	101.65	300.78	Tuesday and Wednesday
Retrospect	165.10	249.16	Monday and Tuesday

6
Alternate onshore wind farm

The layout of onshore wind farms varies regarding the overall number of turbines and their alignment. Therefore, evaluating the effectiveness of the FMWTP and RMWT models by their application to a distinct wind farm case study is imperative. The first section describes the layout of the newly chosen wind farm. In the next section, the turbines of the newly established wind farm undergo data checks and filtering processes, followed by the construction of a power curve that correlates the archival wind speed with the corresponding turbine output. Finally, the RMWT is run for the new wind farm with the required changes, and the forecast revenue is shown graphically.

6.1. 5-turbine wind farm

To evaluate the effectiveness of the FMWTP and RMWT models in an alternative wind farm, a wind farm consisting of five turbines has been selected for testing purposes. The wind farm configuration can be observed in the Figure 6.1.

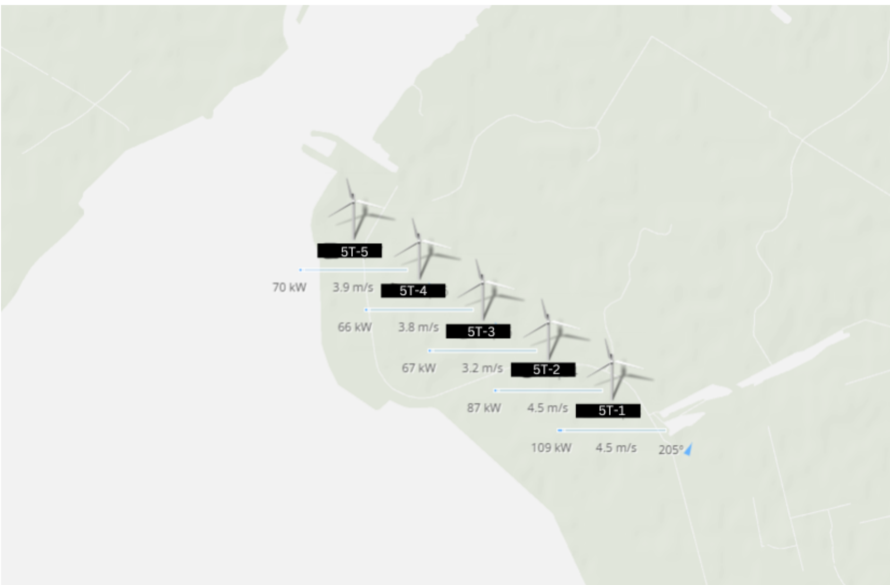

Figure 6.1: Terrain map of the 5-turbine wind farm

Similar to the 3-T turbines, the power curve of Enercon E82 (2.3 MW) turbines of the 5-T wind farm are plotted in Figure 6.2a. The figure shows that the 5T turbines have a cut-in wind speed of around 2 m/s, a rated wind speed of 14 m/s with its rated power of 2300 kW and a cut-out wind speed of over 28 m/s.

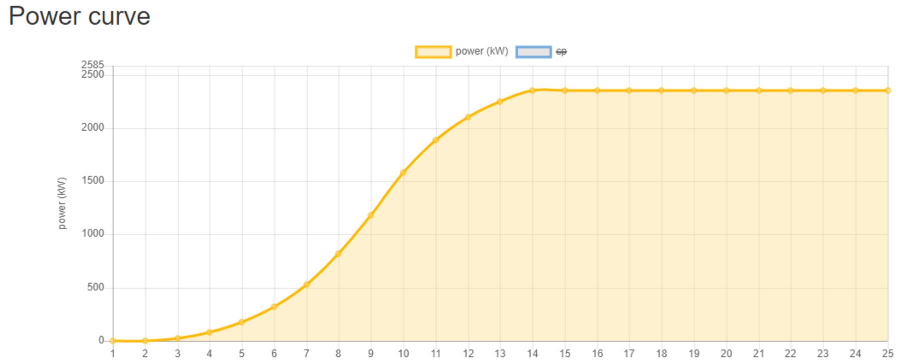

(a) Ideal power curve

(b) Nacelle

Figure 6.2: 2.3 MW Enercon turbine (Wind Turbine Models, 2023a)

The turbines have a hub height of 78m. The wind speeds measured at the anemometer behind the turbine's nacelle in Figure 6.2b are comparable to the wind speeds retrieved from the closest grid point at 100m. But, to ensure uniform comparison, the wind speeds measured at 100m height are translated to 78m height. This is done using the Power Law equation shown in Equation 6.1. It states that for altitudes above 60m, the influence of surface roughness is not present. To find the wind speed at 78m, the wind speed at 100m is multiplied by the ratio of the heights (78/100) to the power alpha (α), which is generally considered to be 0.143 over land (Zaaijer & Viré, 2021).

$$U(h) = U(h_{ref}) * \left(\frac{h}{h_{ref}}\right)^{\alpha} \tag{6.1}$$

6.2. Check, filter and plot the power curve

Prior to using this wind park as a subject for the two models, it is necessary to conduct sanity tests and data filtering. In Figure 6.3 below, the wind rose diagrams of the turbine and the archival data for the closest grid point, which is at a distance of 1.41km from the input location of the wind farm, can be observed.

Figure 6.3: Wind rose diagram for the 5T wind farm

On the one hand, it can be observed that the turbines 5T-1, 5T-3, and 5T-4 exhibit a strong correspondence with the historical data. In contrast, there are notable disparities between the wind rise diagrams of turbines 5T-2 and 5T-5 when compared to the archive data and the remaining three turbines. After conducting a more thorough analysis, the turbines 5T-2 and 5T-5 appear misaligned by almost 30° for the wind speeds in the Southwest direction. This is a general occurrence in many wind farms where the North of more than one turbine can be skewed significantly, causing it to show the wrong wind direction readings. This is another aspect to be considered when running these turbines in the FMWTP and RMWT models. To compensate for this, the rounded-off values for the wind directions are altered based on the average difference for the period under consideration for the archival data.

The grid connection for the 5T wind turbines has a total capacity of 10MW, which means the turbines with full availability can not produce more than 2MW each at any given time. Keeping this in mind, the archival wind speeds correlate to the Turbine Power with a maximum attainable value of 2MW per turbine. Thus, compared to the ideal power curve, the Figure 6.4 and the Figure 6.5 have their rated power at 2000kW. For the data filtering, the chosen wind ratio is 0.78 to 1.22. This gives an average of 46 valid data points between the cut-in wind speed to the rated wind speed for the 5T-1 turbine and a smooth power curve for the same region compared to 10 valid data points obtained when the ratio is 1.

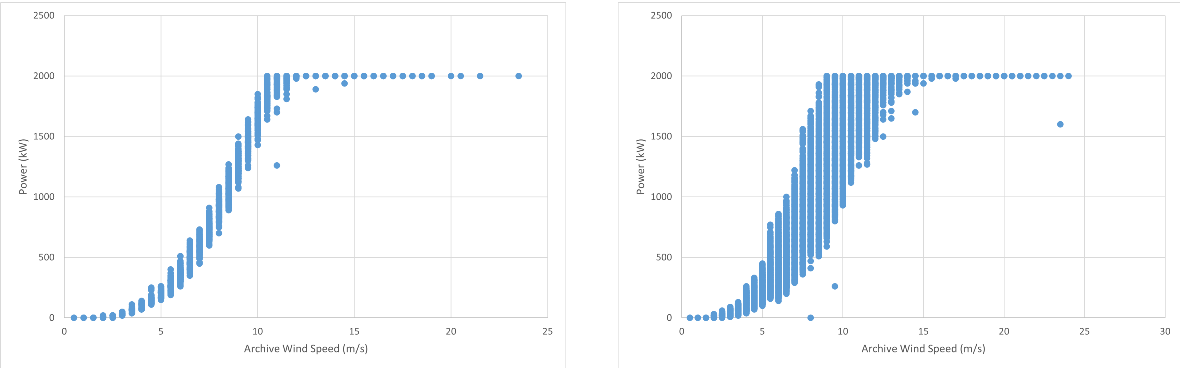

(a) TSA= 1, Direction Match= 1, Ratio= [1]

(b) TSA= 1, Direction Match= 1, Ratio= [0.78: 1.22]

Figure 6.4: Power curve made with archival wind speed for turbine 5T-1

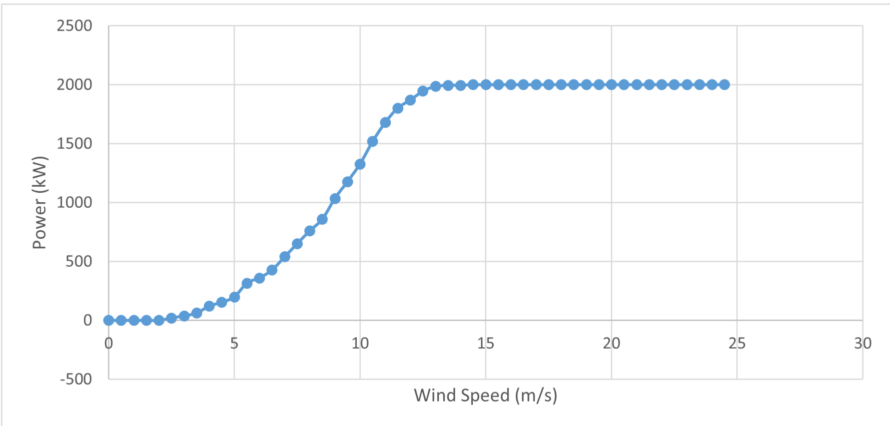

Figure 6.5: Matrix power curve for 5T-1 for the dominant wind direction 210°

6.3. Using the RMWT on the 5T wind farm

The forecasted revenue of the 5T turbines from 22^{nd} till 28^{th} of July 2023 is presented in Figure 6.6. Therefore, it has been demonstrated in this section that both the FMWTP and the RMWT exhibit effective utilisation across multiple wind farms.

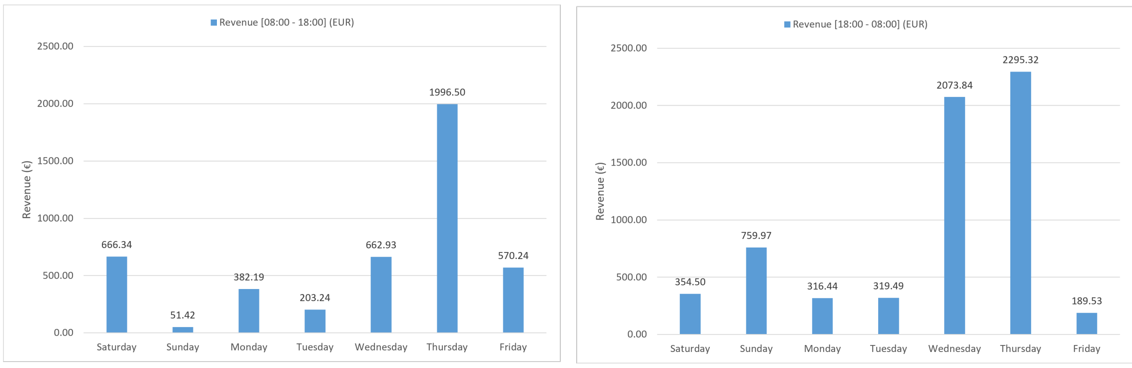

(a) 5T-1

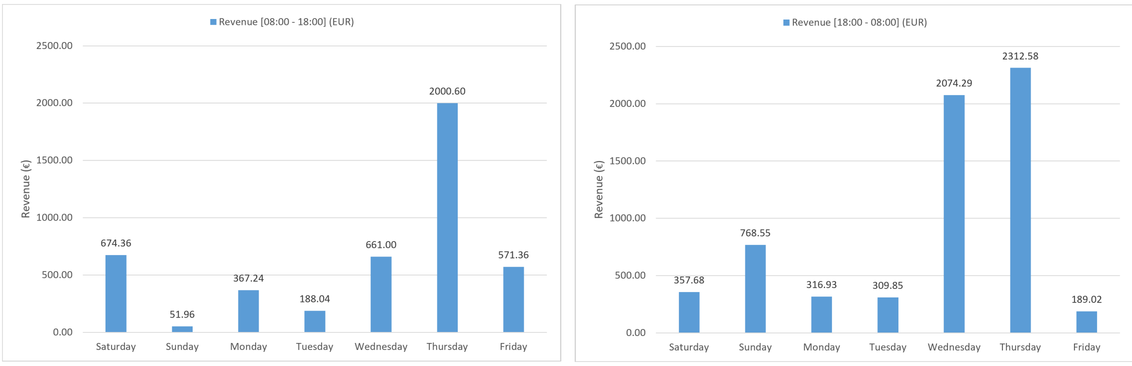

(b) 5T-2

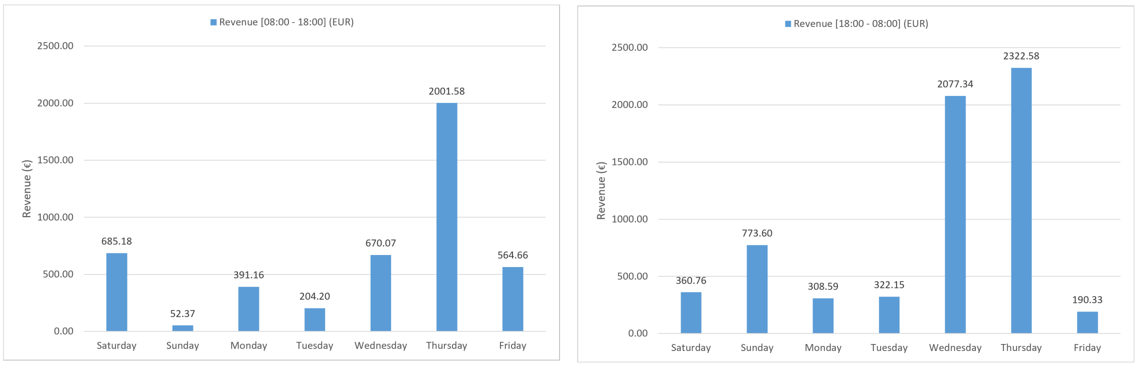

(c) 5T-3

Figure 6.6: Forecasted 5T wind farm turbine revenue from 22/07/2023 till 28/07/2023.

(d) 5T-4

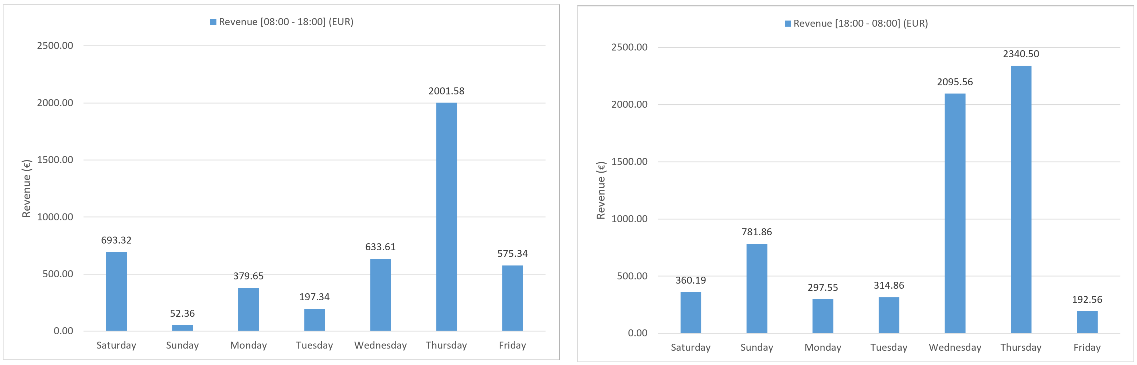

(e) 5T-5

Figure 6.6: Forecasted 5T wind farm turbine revenue from 22/07/2023 till 29/07/2023.

6.4. Comparing RMWT with actual revenue

The forecasted revenue for the week mentioned in section 6.3 for turbine 5T-3 is compared to the actual revenue of the turbine for the week. The performance of the RMWT for turbine 5T-3 can be viewed in 6.7. The depicted figure showcases the utilisation of an input date filter set to the 23^{rd} of July 2023. As a result, the model exhibits enhanced performance in relation to the real income as the FMWTP is using the more accurate wind speeds of the first seven days rather than the data from the forecasts from the 3^{rd} day till the 8^{th} day.

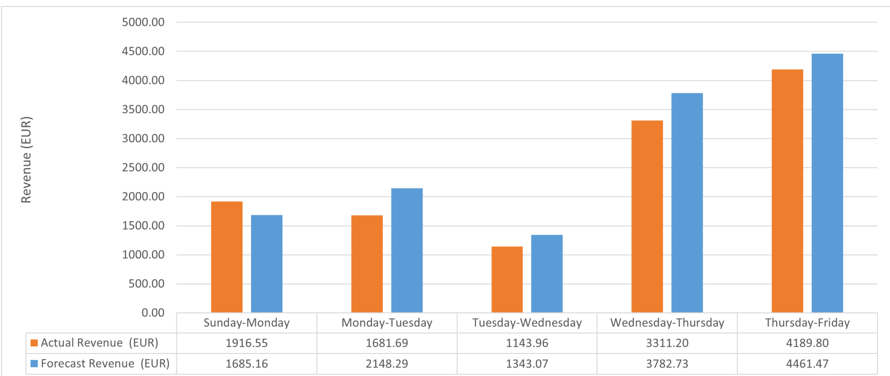

Figure 6.7: Forecast revenue vs. Actual revenue of 5T-3 from 23/07/2023 till 28/07/202

In order to obtain a more precise evaluation of the RMWT for the 5T wind farm. The data from the same date range is taken, but this time, the input data filter is assumed to be 21^{st} of July 2023. As can be observed from Figure 6.8, choosing the input date as the 21^{st}, as opposed to the 23^{rd}, significantly impacts the resulting output of the RMWT. In this instance, the prediction values exhibit higher inaccuracy than the forecast depicted in Figure 6.7.

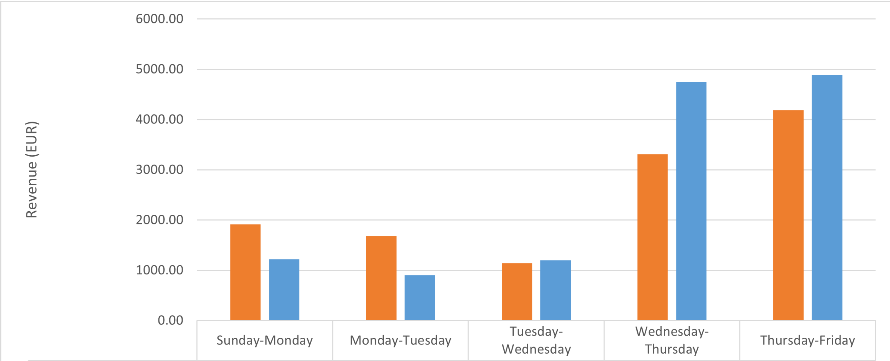

	Sunday-Monday	Monday-Tuesday	Tuesday-Wednesday	Wednesday-Thursday	Thursday-Friday
Actual Revenue (EUR)	1916.55	1681.69	1143.96	3311.20	4189.80
Forecast Revenue (EUR)	1217.13	903.94	1196.41	4748.98	4888.81

Figure 6.8: Forecast revenue vs. Actual revenue of 5T-3 with input date 21/07/2023.

7

Limitations of the model and scope for improvement

In the first section, the limitations of the PMEP will be mentioned. In section 2, the same would be done for the FMWTP and in the final section, the impact of the limitations of the two models on the RMWT is discussed. The reasoning for the constraints and limitations is presented in each section, and possible improvements are explored.

7.1. PMEP

The major limitation of the PMEP is the inability of the model to predict negative energy prices. This leads to the RMSE of the model being higher on the weekends compared to the weekdays. In subsection 2.1.4, it was observed that these prices are most often on weekends, but on rare occasions, they also occur on weekdays. Being able to predict these negative prices or even identify when a possibility may arise can help the accuracy of the model.

The first step is understanding the correlation of electricity prices with renewable generation and load on the grid. In subsection 2.1.4, it was discovered that when the contribution of renewable production is more than 80%, then there is a chance that negative electricity prices will occur. The second variable in understanding these prices is the demand or, in this case, the load on the system. When the market on the system is low, and it can supply the demand with renewables to a large extent, it is possible to expect negative prices. The issue arises for the prediction of the load. In ENTSOE, the load data is provided on a day-ahead basis. Although there is an option to retrieve the week-ahead forecast, only singular values are given for the week-ahead load, which would have to be split into day-ahead loads, which then would have to be divided into loads per hour.

The same ”Averaged Method” used to predict the day-ahead electricity prices was used to predict the day-ahead load using the actual load values from previous years and correcting it with the recent weeks' load. The RSME ranged around the values 20-50 €/MWh for the electricity prices. However, the RSME was roughly around the 1000-2000 MW region for the load data, which was a significant difference. But this prediction could well be used to anticipate negative prices as long as the generation of renewable sources and the total generation could be predicted. Similar to load data, these values were only available in the day-ahead format.

For the renewables, a different approach was chosen. The forecast for the parameters *viz.* Wind speed, direct solar radiation and total cloud cover were considered values that could be used to predict renewable production. The Operational data used these parameters from a singular location, the KNMI headquarters (De Bilt, Utrecht), to correlate them to the actual load. The idea was to use real-time data with the parameters mentioned above and be able to predict the negative prices using a linear regression curve. This would, at the least, indicate the possibility of negative prices.

The first limitation of this method is that it cannot be expected that one location could represent the weather of all of the Netherlands. This can be rectified by using multiple locations to create a correlation with the actual historical load and then using the real-time forecast from the exact locations and the predictive bag to create a predictive model for negative electricity prices. The second limitation was insufficient time to convince the people at ECMWF to alter the chosen parameters for the HRES order and implement these changes.

Another limitation of the PMEP is that the recent 3-week average does not always correct the previous year's average. If, in the summer period, solar and wind availability is abundant for a few weeks, that would reflect in the recent 3-week average and would affect the forecasted electricity price regardless of the weather forecast of the upcoming week. A similarity analysis of the forecast for the recent three weeks and the forthcoming forecast can help establish if the recent 3-week average should be used to correct the previous-year standard. This can also be applied to periods like Christmas or the end of the summer. In both cases, the industries close operations, affecting electricity prices. At the end of these periods, the reopening of the industries and offices also results in prices that do not reflect the previous week's prices.

7.2. FMWTP

The main limitation of the FMWTP is the accuracy of the weather forecast. Depending on what day of the week the model is run can make a massive difference in the accuracy of the output. Suppose the model is run on a Sunday, and the result is calculated from that particular Sunday till the upcoming Saturday. In that case, the model uses the weather forecast for the 1st seven days. But, if the model is made to run on Friday rather than Sunday, then the model uses the forecast from the 3^{rd} till the 8^{th} day for the 1-week forecast.

The accuracy of the weather forecast reduces with the increase in the time step. If the model is run on Sunday, the forecast accuracy will be considerably higher than if it were run on Friday. An example of the impact of the chosen day can be viewed in the results in chapter 4 where the input date was always a Sunday, but in chapter 5, the model was run on a Friday, and that led to the turbine output being less accurate than that in the previous chapter. The same comparison was tested in section 6.4.

A limitation of using the real-time weather forecast is that if the wind speed for a particular time step is below the cut-in wind speed, the model will give the turbine power output of 0 KW. In some cases, the actual wind speed might be slightly above the cut-in wind speed, or a wind gust may increase the incoming wind speed. In both cases, the turbine would produce power, but the forecast would show the produced power as zero. One rectification for this is to include the parameter for wind gusts and the u and v components of electricity.

Another limitation of the FMWTP is in filling the wind speed and direction of the missing time steps from the real-time data. This is done by averaging the known values to find the unknown values in between, but wind speeds do not follow such a predictable pattern. This can be observed in Figure D.5 and Figure D.6. A better understanding has to be developed to fill in the missing wind speeds.

7.3. RMWT

The culmination of the limitations of the PMEP and the FMWTP leads to the poor performance of the RMWT in terms of accuracy with the actual revenue of the turbine. The revenue model uses Equation 2.3 to calculate the total revenue per time step. Nothing can be done to improve the performance of the RMWT without making considerable changes to the PMEP and FMWTP. When comparing the performance of the RMWT for the overnight period and the working hours period, it generally performs better in the overnight period, which is counterproductive as most work on the turbine will be done during the working period. Thus, the model's accuracy during that period has to take priority in terms of improvement.

8 Conclusion and recommendation

8.1. Conclusion

The objective of this academic research is to develop a statistical model for the scheduling of maintenance tasks for onshore wind turbines. The methodology involves the development of two predictive models, which utilise historical data to estimate electricity prices and weather API data to predict turbine output. The predicted revenue of the turbines is calculated in a model called RMWT by combining the outputs of the PMEP and FMWTP. The calculations have been conducted for a wind farm consisting of three turbines, as outlined in this paper, and have been compared with the actual revenue data.

The operational mechanisms of the PMEP were formed through the implementation of two distinct processes, with both methods demonstrating similar performance in terms of RSME. Subsequently, the root mean square error (RMSE) of 40.26 €/MWh was computed for the predictive electricity prices. Notably, the predictive model's electricity pricing (PMEP) performance exhibited a superior RMSE on weekdays of 31.69 €/MWh compared to 55.03 €/MWh on the weekends. In instances where negative prices were recorded, the model exhibited an inability to forecast such negative prices accurately. Consequently, this increases the root mean square error (RMSE) to 66.57 €/MWh. The weekends exhibited a greater frequency of negative pricing, resulting in higher RSME values on Saturdays and Sundays.

Following the use of data filtration techniques, a significant correlation was seen between the wind speed of the turbine and its power output. This correlation facilitated the creation of a matrix comprising the averaged values of the archival wind speed, archival wind direction, and the corresponding turbine power. The above-mentioned relationship is subsequently employed to generate a power value that is the foundation for predicting the turbine power associated with the real-time data. The projected power figure is compared with the actual measurement of turbine output power. The RMSE was observed in the range €300 till €850. The study revealed that weather forecast data exhibited a decline in accuracy as time progressed, resulting in a lack of consistency between the predicted power levels and the actual power output of the turbines.

The outputs of both models were merged to yield a single output representing the turbine's revenue. The forecast revenue was evaluated against the actual revenue in several situations. The indication accurately suggested the need for a 2-day maintenance activity in 2 of the four chosen cases with an actual revenue loss of only €1237.85 in the two cases. The model was further evaluated against the implemented technique, wherein AMT members were assigned consecutive workdays for the same task based on a weather forecast obtained from Windy. The model proposed more favourable outcomes than what the members could offer, and a comparison was made between the projected revenue and the actual revenue to verify the accuracy of the model's prediction. The suggestions based on the output of the RMWT led to an actual revenue loss of €853.23. Subsequently, an alternate wind farm was used to evaluate the model. The model underwent essential modifications and was successfully executed for the newly established wind farm. Finally, the limitations of both models were discussed. The major limitation of the PMEP is its inability to predict negative prices, while the FMWTP's main limitation is the inaccuracy of weather forecast data.

In conclusion, the RMWT effectively serves as an indicator for the scheduling of maintenance operations. The model demonstrates a high level of accuracy in predicting electricity costs, albeit encountering challenges in reliably predicting negative prices. The level of accuracy in weather forecasting significantly influences the model's inconsistent prediction of turbine output. Both of these models collectively contribute to the lack of precision in estimating the revenue generated by the turbines. The model exhibits versatility in its applicability, as it can effectively be employed for many wind farms rather than being restricted to a singular wind farm.

8.2. Recommendations for future work

The ultimate objective of this project is to develop the capability to anticipate and project the financial losses incurred by a turbine for the forthcoming week. The procedure should prioritise user-friendliness and minimise the number of components involved, aiming for instantaneity or continuity. The model should be able to update itself while in operation, maintaining continuous functionality dynamically.

The first recommendation pertains to the European Network of Transmission System Operators for Electricity ENTSOE. The website offers the capability to utilise its application programming interface (API), which can then be merged with the API of the real-time data from ECMWF, resulting in a unified command file. This would facilitate the complete automation of the RMWT. Updating electricity pricing for the PMEP involves manual weekly updates in the Excel spreadsheet.

The second recommendation concerns the selection of parameters for the data arrangement in the HRES 10-day forecast and the operational archive. The correlation between the turbine and forecast data can be more detailed by choosing certain parameters like temperature and pressure. These two parameters can be used to predict the air density, determining if the turbine will produce a higher or lower power value for the same wind speed and direction.

The third recommendation is also in regard to the parameters in the data order for real-time and archival data. The parameters of direct solar radiation and total cloud cover can be used along with the wind speeds across multiple locations in the Netherlands to establish the weather for the nation per date and time. Through this process, a study can be done with the archival data, the historical negative prices and the load on the system. This understanding can be applied to the PMEP to increase the accuracy of the models about its ability to identify the negative price occurrences in the energy market.

The fourth and final recommendation is to invest in storage solutions for producers and consumers alike. By implementing this approach, renewable energy producers would no longer need to curb their production whenever there is a decrease in demand. The surplus electricity can be stored and subsequently utilised to power the corresponding wind or solar farms. Consumers can utilise stored electricity as an alternative to procuring electricity at excessively high costs. This will ultimately result in stabilising power prices, benefiting both parties involved and reducing the frequency of negative electricity prices, consequently enhancing the precision of the PMEP.

References

AWS. (2023). *Amazon s3*. Retrieved June 28, 2023, from https://aws.amazon.com/s3/

Bashir, M. B. A. (2022). Principle parameters and environmental impacts that affect the performance of wind turbine: An overview. *Arabian Journal for Science and Engineering*, *47*(7), 7891–7909. https://doi.org/10.1007/s13369-021-06357-1

Besnard, F., Patriksson, M., Strömberg, A. B., Wojciechowski, A., & Fischer, K. (2011). A review of wind turbine operation and maintenance: State of the art and future challenges. *Renewable and Sustainable Energy Reviews*, *15*(8), 4189–4204.

Central Bureau van Statistiek. (2022). The netherlands in numbers: Infographics inspired by 36 questions. *Nederland in cijfers*.

Climate Action Network Europe. (2021). *High electricity prices*. Retrieved August 24, 2023, from https://caneurope.org/high-electricity-prices-links-fossil-gas-need-shift-to-renewables/

Costa, Á. M., Orosa, J. A., Vergara, D., & Fernández-Arias, P. (2021). New tendencies in wind energy operation and maintenance. *Applied Sciences*, *11*(4). https://doi.org/10.3390/app11041386

Ding, F., Tian, Z., & Jin, T. (2013). Maintenance modeling and optimization for wind turbine systems: A review. *2013 International Conference on Quality, Reliability, Risk, Maintenance, and Safety Engineering (QR2MSE)*, 569–575. https://doi.org/10.1109/QR2MSE.2013.6625648

ECMWF. (2023). *Ecmwf-advancing global nwp through international collaboration*. Retrieved March 6, 2023, from https://www.ecmwf.int/

Enel. (2023). *Self-hoisting crane at rocky ridge wind farm*. Retrieved July 26, 2023, from https://www.enelnorthamerica.com/newsroom/news/search-photos/photo/2019/12/self-hoisting-crane-at-rocky-ridge-wind-farm/

ENTSOE. (2023). *Entsoe-e transparency platform*. Retrieved February 24, 2023, from https://transparency.entsoe.eu/dashboard/show

FileZilla. (2023). *Filezilla - the free ftp solution*. Retrieved June 9, 2023, from https://filezilla-project.org/

Froger, A., Gendreau, M., Mendoza, J., Eric, P., & Rousseau, L.-M. (2018). Solving a wind turbine maintenance scheduling problem. *Journal of Scheduling*, *21*, 53–76. https://doi.org/10.1007/s10951-017-0513-5

Heijden, T. V. D., Lago, J., Palensky, P., & Abraham, E. (2021). Electricity price forecasting in european day ahead markets: A greedy consideration of market integration. *IEEE Access*, *9*, 119954–119966. https://doi.org/10.1109/ACCESS.2021.3108629

Hesselink, M. M. J. (2018). Developing a forecasting model for the power production of wind turbines. http://essay.utwente.nl/74895/

In Statista. (2023). *Average monthly electricity wholesale price in the netherlands from january 2019 to june 2023 (in euros per megawatt-hour) [graph]*. Retrieved August 2, 2023, from https://www.statista.com/statistics/1314549/netherlands-monthly-wholesale-electricity-price/

Iseh.A., J., & Woma.T., Y. (2013). Weather forecasting models, methods and applications. *International journal of engineering research and technology*, *2*. https://api.semanticscholar.org/CorpusID:128549920

Johnsen, A. M. (2019). Forecasting day-ahead electricity spot prices, with applications to the german electricity market. https://api.semanticscholar.org/CorpusID:207997516

Lago, J., Marcjasz, G., De Schutter, B., & Weron, R. (2021). Forecasting day-ahead electricity prices: A review of state-of-the-art algorithms, best practices and an open-access benchmark. *Applied Energy*, *293*, 116983. https://doi.org/https://doi.org/10.1016/j.apenergy.2021.116983

Liu, M., Liu, G., & Liu, K. (2019). Standard modeling practice research for a safety technical disclosure of wind turbine maintenance systems. In Y. Tan, Y. Shi, & B. Niu (Eds.), *Advances in swarm intelligence* (pp. 301–308). Springer International Publishing.

Lu, B., Li, Y., Wu, X., & Yang, Z. (2009). A review of recent advances in wind turbine condition monitoring and fault diagnosis. *2009 IEEE Power Electronics and Machines in Wind Applications*, 1–7. https://doi.org/10.1109/PEMWA.2009.5208325

Manfre Jaimes, D., Zamudio López, M., Zareipour, H., & Quashie, M. (2023). A hybrid model for multi-day-ahead electricity price forecasting considering price spikes. *Forecasting*, *5*(3), 499–521. https://doi.org/10.3390/forecast5030028

Marsh, G. (2011). Meeting the challenge of wind turbine blade repair. *Reinforced Plastics*, *55*(4), 32–36. https://doi.org/https://doi.org/10.1016/S0034-3617(11)70112-6

Peng, H., Li, S., Shangguan, L., Fan, Y., & Zhang, H. (2023). Analysis of wind turbine equipment failure and intelligent operation and maintenance research. *Sustainability*, *15*(10). https://doi.org/10.3390/su15108333

Reder, M. D., Gonzalez, E., & Melero, J. J. (2016). Wind turbine failures - tackling current problems in failure data analysis. *Journal of Physics: Conference Series*, *753*(7), 072027. https://doi.org/10.1088/1742-6596/753/7/072027

Sabir, M., Koetse, M., & Rietveld, P. (2007). The impact of weather conditions on mode choice: Empirical evidence for the netherlands. In P. Hilferink, P. Rietveld, & T. van den Hanenberg (Eds.), *Proceedings of the bivec-gibet transport research day 2007* (pp. 512–527).

Sareen, A., Sapre, C. A., & Selig, M. S. (2014). Effects of leading edge erosion on wind turbine blade performance. *Wind Energy*, *17*(10), 1531–1542. https://doi.org/https://doi.org/10.1002/we.1649

Sayam, A., Rahman, A. N. M. M., Rahman, M. S., Smriti, S. A., Ahmed, F., Rabbi, M. F., Hossain, M., & Faruque, M. O. (2022). A review on carbon fiber-reinforced hierarchical composites: Mechanical performance, manufacturing process, structural applications and allied challenges. *Carbon Letters*, *32*(5), 1173–1205. https://doi.org/10.1007/s42823-022-00358-2

Schouten, T. N., Dekker, R., Hekimoğlu, M., & Eruguz, A. S. (2022). Maintenance optimization for a single wind turbine component under time-varying costs. *European Journal of Operational Research*, *300*(3), 979–991. https://doi.org/https://doi.org/10.1016/j.ejor.2021.09.004

Senn, M. (2022). *Lightning damage to wind turbine*. Retrieved August 22, 2023, from https://www.envistaforensics.com/en-au/knowledge-centre/insights/articles/lightning-damage-to-wind-turbine/

Stockton, B. (2021). *How to use the xlookup function in excel*. Retrieved June 26, 2023, from https://careerfoundry.com/en/blog/data-analytics/xlookup-function-excel/

Terziev, A., Iliev, I., Beloev, H., & Panteleev, Y. (2021). Impact assessment of terrain specifics on wind energy production over semi-complex terrains. *IOP Conference Series: Earth and Environmental Science*, *664*, 012042. https://doi.org/10.1088/1755-1315/664/1/012042

Tschora, L., Pierre, E., Plantevit, M., & Robardet, C. (2022). Electricity price forecasting on the day-ahead market using machine learning. *Applied Energy*, *313*, 118752. https://doi.org/https://doi.org/10.1016/j.apenergy.2022.118752

Vivablast. (2023). *The importance of blade repair and the stages of wind turbine maintenance*. Retrieved July 26, 2023, from https://vivablast.com/news-and-media/the-importance-of-blade-repair-wind-turbine-maintenance/

Wang, Y., Liu, Y., Li, J., & Zhang, X. (2019a). Lightning strike damage assessment of wind turbine blade based on acoustic emission testing. *Renewable Energy*, *132*, 1238–1248.

Wang, Y., Liu, Y., Li, J., & Zhang, X. (2019b). Maintenance modeling and optimization for wind turbine systems: A review. *IEEE Transactions on Reliability*, *68*(2), 517–535.

Wind Turbine Models. (2023a). *Enercon e-82 e2 2.300*. Retrieved August 14, 2023, from https://en.wind-turbine-models.com/turbines/550-enercon-e-82-e2-2.300

Wind Turbine Models. (2023b). *Vestas v90-3.0*. Retrieved August 17, 2023, from https://en.wind-turbine-models.com/turbines/603-vestas-v90-3.0#datasheet

Windy. (2023). Retrieved July 26, 2023, from https://www.windy.com/multimodel/51.555/4.437?51.360,4.436,8,m:e48agiv

Wingfeet. (2015). *Wind in netherlands*. Retrieved July 31, 2023, from https://www.r-bloggers.com/2015/11/wind-in-netherlands/#:~:text=In%20the%20Netherlands%20there%20is,in%20turn%20will%20bring%20rain.

Yan, X., She, D., Xu, Y., & Jia, M. (2021). Application of generalized composite multiscale lempel–ziv complexity in identifying wind turbine gearbox faults. *Entropy*, *23*(11), 1372.

Yang, D., Wang, W., & Hong, T. (2022). A historical weather forecast dataset from the european centre for medium-range weather forecasts (ecmwf) for energy forecasting. *Solar Energy*, *232*, 263–274. https://doi.org/https://doi.org/10.1016/j.solener.2021.12.011

Zaaijer, M., & Viré, A. (2021). *Introduction to wind turbines: Physics and technology*.

Zhang, P., & Lu, D. (2019). A survey of condition monitoring and fault diagnosis toward integrated o&m for wind turbines. *Energies*, *12*(14), 2801.

A

Windy comparison

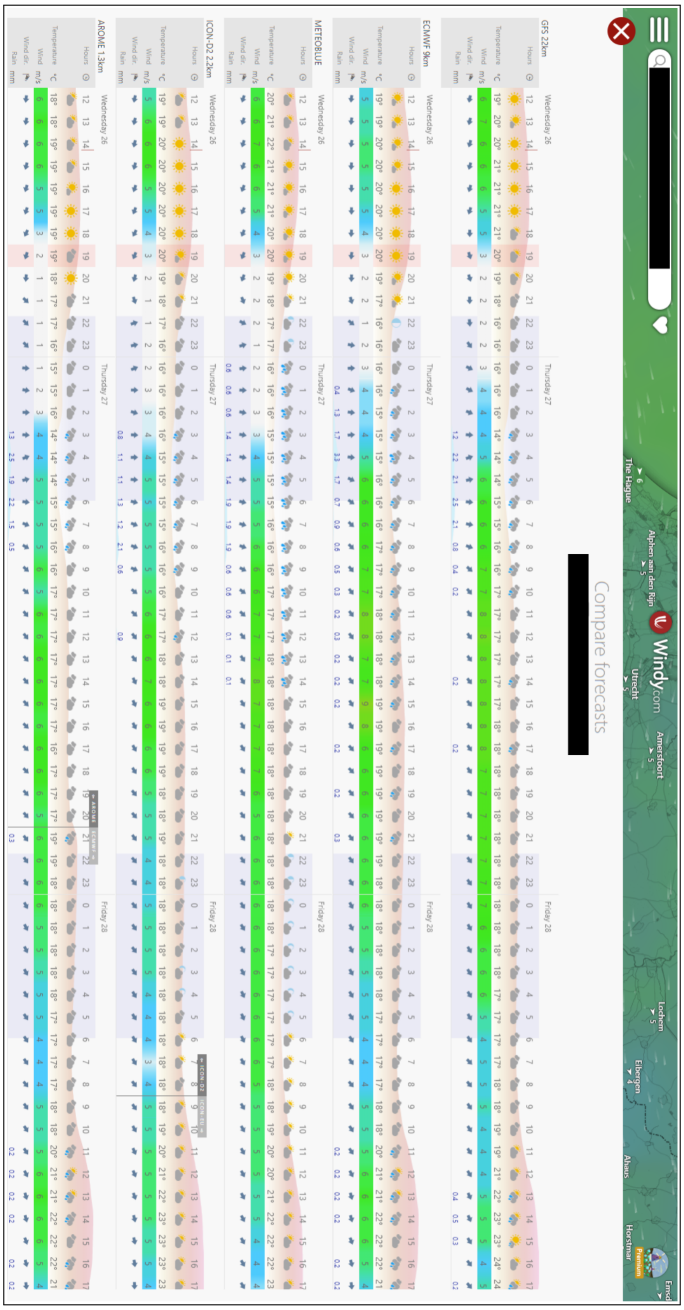

Figure A.1: Location: Comparison of all different weather forecast models for the location of 3T wind farm(1)

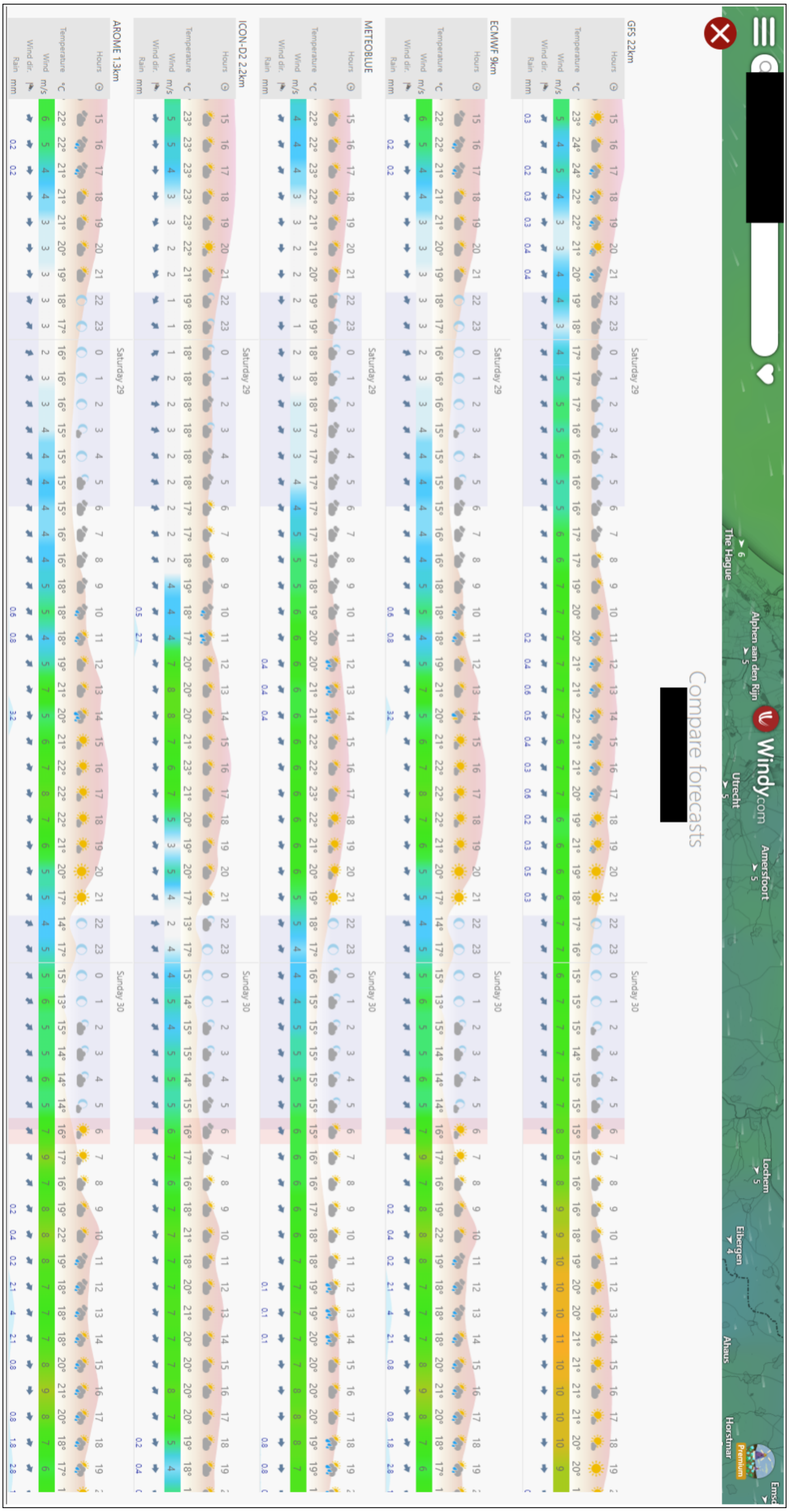

Figure A.2: Location: Comparison of all different weather forecast models for the location of 3T wind farm (2)

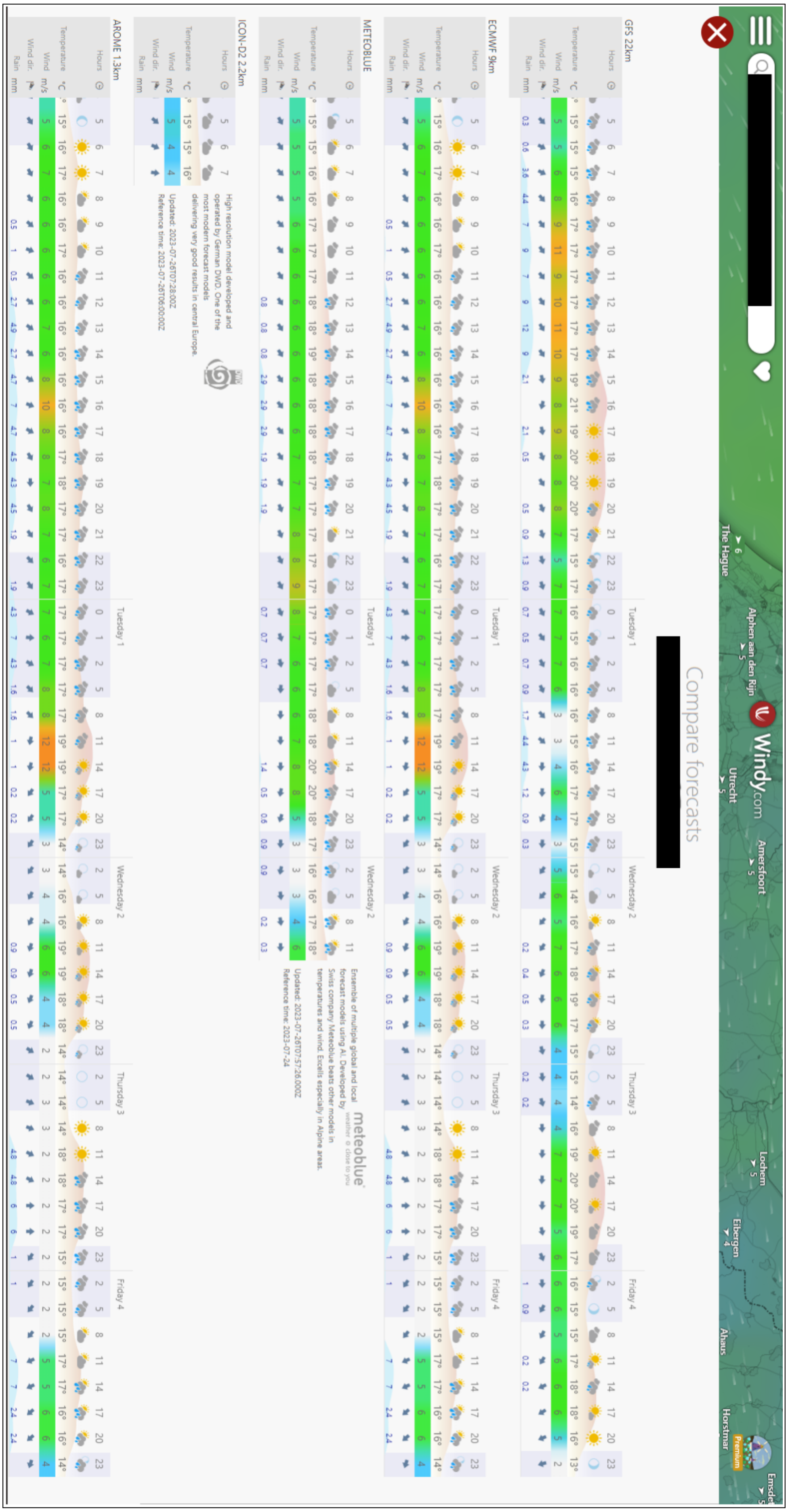

Figure A.3: Location: Comparison of all different weather forecast models for the location of 3T wind farm (3)

B

Datasheets

B.1. Vestas V-90 3MW

Power	
Rated power:	3,000.0 kW
Flexible power ratings:	-
Cut-in wind speed:	4.0 m/s
Rated wind speed:	15.0 m/s
Cut-out wind speed:	25.0 m/s
Survival wind speed:	-
Wind zone (DIBt):	-
Wind class (IEC):	-

Rotor	
Diameter:	90.0 m
Swept area:	6,362.0 m²
Number of blades:	3
Rotor speed, max:	18.4 U/min
Tipspeed:	87 m/s
Type:	-
Material:	-
Manufacturer:	-
Power density 1:	471.5 W/m²
Power density 2:	2.1 m²/kW

(a)

Gear box	
Type:	spur/planetary
Stages:	3.0
Ratio:	-
Manufacturer:	-

Generator	
Type:	Asynchronus
Number:	1
Speed, max:	-
Voltage:	1,000.0 V
Grid connection:	OptiSpeed
Grid frequency:	50 Hz
Manufacturer:	-

Tower	
Hub height:	80/105 m
Type:	Steel tube
Shape:	conical
Corrosion protection:	painted
Manufacturer:	-

Weight	
Single blade:	-
Hub:	-
Rotor:	41.0 t
Nacelle:	70.0 t
Tower, max:	285.0 t
Total weight:	396.0 t

(b)

Figure B.1: Datasheet for the Vestas V-90 3MW turbine (Wind Turbine Models, 2023b).

B.2. Enercon E-82 2.3MW

Datasheet

Power

Rated power:	2,350.0 kW
Flexible power ratings:	-
Cut-in wind speed:	2.0 m/s
Rated wind speed:	14.0 m/s
Cut-out wind speed:	34.0 m/s
Survival wind speed:	-
Wind zone (DIBt):	-
Wind class (IEC):	Ia

Rotor

Diameter:	82.0 m
Swept area:	5,281.0 m²
Number of blades:	3
Rotor speed, max:	18.0 U/min
Tipspeed:	77 m/s
Type:	-
Material:	GFRP
Manufacturer:	Enercon
Power density 1:	445.0 W/m²
Power density 2:	2.2 m²/kW

Gear box

Type:	direct drive
Stages:	-
Ratio:	-
Manufacturer:	-

(a)

Generator

Type:	synchronous
Number:	1
Speed, max:	18.0 U/min
Voltage:	690.0 V
Grid connection:	inverters
Grid frequency:	50 Hz
Manufacturer:	Enercon

Tower

Hub height:	59/69/78/84 m
Type:	steel tube / hydrid
Shape:	conical
Corrosion protection:	painted
Manufacturer:	Enercon

Weight

Single blade:	-
Hub:	-
Rotor:	-
Nacelle:	-
Tower, max:	-
Total weight:	-

(b)

Figure B.2: Datasheet for the Vestas V-90 3MW turbine(Wind Turbine Models, 2023a)

C

Miscellaneous (screenshots)

C.1. ENTSOE-webpage

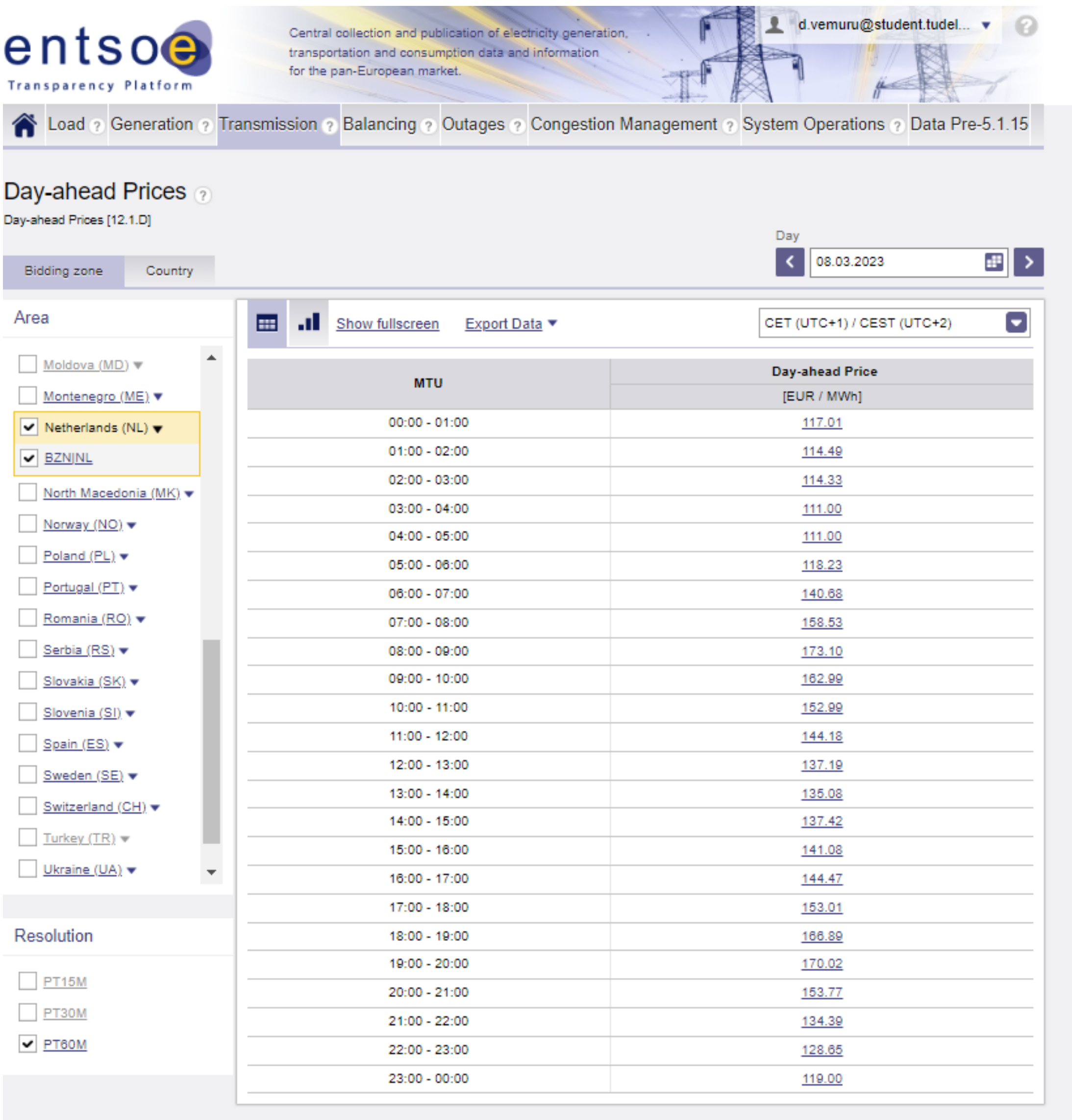

Figure C.1: Day-ahead prices for the Netherlands on 08/03/2023 (ENTSOE, 2023).

C.2. Real-time data

```
dvemuru@Andrew:~$ grib_ls -F"%.2f" -l [redacted]T1D07071200070906001.grib
T1D07071200070906001.grib
edition      centre       typeOfLevel  level        dataDate     stepRange    dataType     shortName    packingType  gridType          value1  value2  value3  value4
1            ecmf         surface      0            20230707     42           fc           100u         grid_simple  regular_ll   1.33 1.34 1.82 1.85
1            ecmf         surface      0            20230707     42           fc           100v         grid_simple  regular_ll   -0.21 -0.07 -0.08 0.04
1            ecmf         surface      0            20230707     42           fc           10v          grid_simple  regular_ll   0.46 0.48 0.46 0.44
1            ecmf         surface      0            20230707     42           fc           10u          grid_simple  regular_ll   0.50 0.50 0.77 0.81
1            ecmf         surface      0            20230707     42           fc           200v         grid_simple  regular_ll   -0.91 -0.73 -0.85 -0.64
1            ecmf         surface      0            20230707     42           fc           200u         grid_simple  regular_ll   1.07 1.06 1.77 1.77
6 of 6 messages in T1D07071200070906001.grib

6 of 6 total messages in 1 files
Input Point: latitude=[redacted]  longitude=[redacted]
Grid Point chosen #4 index=[redacted] latitude=[redacted] longitude=[redacted] distance=6.21 (Km)
Other grid Points
- 1 - index=[redacted] latitude=[redacted] longitude=[redacted] distance=6.93 (Km)
- 2 - index=[redacted] latitude=[redacted] longitude=[redacted] distance=6.21 (Km)
- 3 - index=[redacted] latitude=[redacted] longitude=[redacted] distance=6.93 (Km)
- 4 - index=[redacted] latitude=[redacted] longitude=[redacted] distance=6.21 (Km)
```

(a) Real-time data in GRIB format

	A	B	C	D	E	F	G	H	I	J	K	L	M	N	O
1	T1D07071200070906001.grib														
2	edition	centre	typeOfLe\	level	dataDate	stepRange	dataType	shortNam	packingTy	gridType	value1	value2	value3	value4	
3	1	ecmf	surface	0	20230707	42	fc	100u	grid_simp	regular_ll	1.33	1.34	1.82	1.85	
4	1	ecmf	surface	0	20230707	42	fc	100v	grid_simp	regular_ll	-0.21	-0.07	-0.08	0.04	
5	1	ecmf	surface	0	20230707	42	fc	10v	grid_simp	regular_ll	0.46	0.48	0.46	0.44	
6	1	ecmf	surface	0	20230707	42	fc	10u	grid_simp	regular_ll	0.5	0.5	0.77	0.81	
7	1	ecmf	surface	0	20230707	42	fc	200v	grid_simp	regular_ll	-0.91	-0.73	-0.85	-0.64	
8	1	ecmf	surface	0	20230707	42	fc	200u	grid_simp	regular_ll	1.07	1.06	1.77	1.77	
9	6 of 6 messages in T1D07071200070906001.grib														
10															
11	6 of 6 total messages in 1 files														
12	Input Point: latitude=[redacted] longitude=[redacted]														
13	Grid Point chosen #4 index=[redacted] latitude=[redacted] longitude=[redacted] distance=6.21 (Km)														
14	Other grid Points														
15	- 1 - index=[redacted]	latitude=[redacted]	longitude=[redacted]	distance=6.93 (Km)											
16	- 2 - index=[redacted]	latitude=[redacted]	longitude=[redacted]	distance=6.21 (Km)											
17	- 3 - index=[redacted]	latitude=[redacted]	longitude=[redacted]	distance=6.93 (Km)											
18	- 4 - index=[redacted]	latitude=[redacted]	longitude=[redacted]	distance=6.21 (Km)											
19															

(b) Real-time CSV data (altered)

Figure C.2: Real-time data from ECMWF

C.3. MARS interface and Excel output

```
01-01-2018.req
File   Edit   View

retrieve,
class=od,
date=2018-01-01,
expver=1,
levtype=sfc,
param=246.228/247.228,
step=0/1/2/3/4/5/6/7/8/9/10/11/12/13/14/15/16/17/18/19/20/21/22/23,
stream=oper,
time=00:00:00,
area=54/3/51/7,
type=fc,
target="01-01-2018.grib"
```

(a) Request file for the date 01/01/2018

```
dvemuru@Andrew:~$ chmod +x ~/mars/bin/mars
dvemuru@Andrew:~$ export PATH=~/mars/bin/:$PATH
dvemuru@Andrew:~$ mars 01-01-2018.req
2023-07-28 04:40:41 ECMWF API python library 1.6.3
2023-07-28 04:40:41 ECMWF API at https://api.ecmwf.int/v1
2023-07-28 04:40:43 Welcome Dhruv Vemuru
2023-07-28 04:40:48 In case of problems, please check https:/
2023-07-28 04:40:51 Request submitted
2023-07-28 04:40:51 Request id: 64c397a7502cf04c22151728
2023-07-28 04:40:51 Request is submitted
2023-07-28 04:40:54 Request is active
```

(b) MARS interface

Figure C.3: The input for the process of generating the data using the MARS-API.

	A	B	C	D	E	F	G	H	I	J	K	L	M	N
1	29Feb2020.grib													
2	edition	centre	ypeOfLeve	level	dataDate	stepRange	dataType	shortName	packingType	gridType	value			
3	1	ecmf	surface	0	20200229	1	fc	10u	grid_simple	reduced_gg	4.27	7.454193	speed	
4	1	ecmf	surface	0	20200229	1	fc	10v	grid_simple	reduced_gg	6.11	214.9479	direction	
5	1	ecmf	surface	0	20200229	2	fc	10u	grid_simple	reduced_gg	3.99	7.305785	speed	
6	1	ecmf	surface	0	20200229	2	fc	10v	grid_simple	reduced_gg	6.12	213.1028	direction	
7	1	ecmf	surface	0	20200229	3	fc	10u	grid_simple	reduced_gg	3.54	7.182903	speed	
8	1	ecmf	surface	0	20200229	3	fc	10v	grid_simple	reduced_gg	6.25	209.5272	direction	
9	1	ecmf	surface	0	20200229	4	fc	10u	grid_simple	reduced_gg	3.3	7.245171	speed	
10	1	ecmf	surface	0	20200229	4	fc	10v	grid_simple	reduced_gg	6.45	207.0956	direction	
11	1	ecmf	surface	0	20200229	5	fc	10u	grid_simple	reduced_gg	3	7.286261	speed	
12	1	ecmf	surface	0	20200229	5	fc	10v	grid_simple	reduced_gg	6.64	204.3138	direction	
13	1	ecmf	surface	0	20200229	6	fc	10u	grid_simple	reduced_gg	2.39	7.019409	speed	
14	1	ecmf	surface	0	20200229	6	fc	10v	grid_simple	reduced_gg	6.6	199.9064	direction	
15	1	ecmf	surface	0	20200229	7	fc	10u	grid_simple	reduced_gg	1.13	7.100493	speed	
16	1	ecmf	surface	0	20200229	7	fc	10v	grid_simple	reduced_gg	7.01	189.1572	direction	
17	1	ecmf	surface	0	20200229	8	fc	10u	grid_simple	reduced_gg	0.3	7.665872	speed	
18	1	ecmf	surface	0	20200229	8	fc	10v	grid_simple	reduced_gg	7.66	182.2428	direction	
19	1	ecmf	surface	0	20200229	9	fc	10u	grid_simple	reduced_gg	0.31	6.747125	speed	
20	1	ecmf	surface	0	20200229	9	fc	10v	grid_simple	reduced_gg	6.74	182.6334	direction	
21	1	ecmf	surface	0	20200229	10	fc	10u	grid_simple	reduced_gg	0.07	7.560324	speed	
22	1	ecmf	surface	0	20200229	10	fc	10v	grid_simple	reduced_gg	7.56	180.5305	direction	
23	1	ecmf	surface	0	20200229	11	fc	10u	grid_simple	reduced_gg	0.21	8.502594	speed	
24	1	ecmf	surface	0	20200229	11	fc	10v	grid_simple	reduced_gg	8.5	181.4153	direction	
25	1	ecmf	surface	0	20200229	12	fc	10u	grid_simple	reduced_gg	2.74	10.35894	speed	
26	1	ecmf	surface	0	20200229	12	fc	10v	grid_simple	reduced_gg	9.99	195.3376	direction	
27	1	ecmf	surface	0	20200229	13	fc	10u	grid_simple	reduced_gg	10.47	11.76225	speed	
28	1	ecmf	surface	0	20200229	13	fc	10v	grid_simple	reduced_gg	5.36	242.8903	direction	
29	1	ecmf	surface	0	20200229	14	fc	10u	grid_simple	reduced_gg	8.45	8.702235	speed	
30	1	ecmf	surface	0	20200229	14	fc	10v	grid_simple	reduced_gg	2.08	256.1713	direction	
31	1	ecmf	surface	0	20200229	15	fc	10u	grid_simple	reduced_gg	7.79	8.793776	speed	
32	1	ecmf	surface	0	20200229	15	fc	10v	grid_simple	reduced_gg	4.08	242.3568	direction	
33	1	ecmf	surface	0	20200229	16	fc	10u	grid_simple	reduced_gg	7.91	9.226625	speed	
34	1	ecmf	surface	0	20200229	16	fc	10v	grid_simple	reduced_gg	4.75	239.0149	direction	
35	1	ecmf	surface	0	20200229	17	fc	10u	grid_simple	reduced_gg	5.86	7.651536	speed	
36	1	ecmf	surface	0	20200229	17	fc	10v	grid_simple	reduced_gg	4.92	229.9835	direction	
37	1	ecmf	surface	0	20200229	18	fc	10u	grid_simple	reduced_gg	5.16	7.725807	speed	
38	1	ecmf	surface	0	20200229	18	fc	10v	grid_simple	reduced_gg	5.75	221.9045	direction	
39	1	ecmf	surface	0	20200229	19	fc	10u	grid_simple	reduced_gg	5.62	8.729651	speed	
40	1	ecmf	surface	0	20200229	19	fc	10v	grid_simple	reduced_gg	6.68	220.0745	direction	
41	1	ecmf	surface	0	20200229	20	fc	10u	grid_simple	reduced_gg	5.25	8.48831	speed	
42	1	ecmf	surface	0	20200229	20	fc	10v	grid_simple	reduced_gg	6.67	218.2065	direction	
43	1	ecmf	surface	0	20200229	21	fc	10u	grid_simple	reduced_gg	5.01	8.334009	speed	
44	1	ecmf	surface	0	20200229	21	fc	10v	grid_simple	reduced_gg	6.66	216.9524	direction	
45	1	ecmf	surface	0	20200229	22	fc	10u	grid_simple	reduced_gg	5.02	8.452242	speed	
46	1	ecmf	surface	0	20200229	22	fc	10v	grid_simple	reduced_gg	6.8	216.4361	direction	
47	1	ecmf	surface	0	20200229	23	fc	10u	grid_simple	reduced_gg	4.79	8.473736	speed	
48	1	ecmf	surface	0	20200229	23	fc	10v	grid_simple	reduced_gg	6.99	214.4215	direction	
49	1	ecmf	surface	0	20200229	24	fc	10u	grid_simple	reduced_gg	4.75	8.459462	speed	
50	1	ecmf	surface	0	20200229	24	fc	10v	grid_simple	reduced_gg	7	214.1597	direction	
51	48 of 48 messages in 29Feb2020.grib													
52														
53	48 of 48 total messages in 1 files													
54	Input Point: latitude=[redacted] longitude=[redacted]													
55	Grid Point chosen #1 index=[redacted]titude=[redacted]longitude=[redacted] distance=2.96 (Km)													
56	Other grid Points													
57	- 1 - index=[redacted] latitude=[redacted] longitude=[redacted]distance=2.96 (Km)													

(a) 01-01-2023.grib

Figure C.4: The output for the process of generating the data using the MARS-API.

	A	B	C	D	E	F	G	H	I	J	K	L	M	N	O
1	01-01-2018.grib														
2	edition	centre	typeOfLe	level	dataDate	stepRan	dataTyp	shortNar	packingT	gridType	value1	value2	value3	value4	
3	1	ecmf	surface	0	2E+07	0	fc	100u	grid_sim	reduced_	10.24	10.14	9.97	10.38	
4	1	ecmf	surface	0	2E+07	0	fc	100v	grid_sim	reduced_	11.16	11.21	10.77	11.17	
5	1	ecmf	surface	0	2E+07	1	fc	100u	grid_sim	reduced_	11.36	11.26	10.64	11.44	
6	1	ecmf	surface	0	2E+07	1	fc	100v	grid_sim	reduced_	12.81	12.49	12.38	12.91	
7	1	ecmf	surface	0	2E+07	2	fc	100u	grid_sim	reduced_	14.59	14.19	14.29	14.66	
8	1	ecmf	surface	0	2E+07	2	fc	100v	grid_sim	reduced_	8.34	8.32	8.88	8.3	
9	1	ecmf	surface	0	2E+07	3	fc	100u	grid_sim	reduced_	13.81	13.09	13.13	14.52	
10	1	ecmf	surface	0	2E+07	3	fc	100v	grid_sim	reduced_	6.33	6.7	6.47	5.86	
11	1	ecmf	surface	0	2E+07	4	fc	100u	grid_sim	reduced_	12.49	12.09	12.28	13.03	
12	1	ecmf	surface	0	2E+07	4	fc	100v	grid_sim	reduced_	6.41	6.63	6.37	5.85	
13	1	ecmf	surface	0	2E+07	5	fc	100u	grid_sim	reduced_	11.03	10.74	10.91	11.46	
14	1	ecmf	surface	0	2E+07	5	fc	100v	grid_sim	reduced_	5.65	5.89	5.62	5.3	
15	1	ecmf	surface	0	2E+07	6	fc	100u	grid_sim	reduced_	9.71	9.81	9.66	9.62	
16	1	ecmf	surface	0	2E+07	6	fc	100v	grid_sim	reduced_	6.75	6.73	6.35	6.65	
17	1	ecmf	surface	0	2E+07	7	fc	100u	grid_sim	reduced_	8.86	9.07	8.89	8.73	
18	1	ecmf	surface	0	2E+07	7	fc	100v	grid_sim	reduced_	8.55	8.51	8.18	8.49	
19	1	ecmf	surface	0	2E+07	8	fc	100u	grid_sim	reduced_	8.64	8.54	8.45	8.58	
20	1	ecmf	surface	0	2E+07	8	fc	100v	grid_sim	reduced_	9.02	8.88	8.75	9.22	
21	1	ecmf	surface	0	2E+07	9	fc	100u	grid_sim	reduced_	8.39	8.09	8.22	8.55	
22	1	ecmf	surface	0	2E+07	9	fc	100v	grid_sim	reduced_	9.22	9.19	8.88	9.28	
23	1	ecmf	surface	0	2E+07	10	fc	100u	grid_sim	reduced_	6.81	6.7	6.67	6.8	
24	1	ecmf	surface	0	2E+07	10	fc	100v	grid_sim	reduced_	9.37	9.3	9.02	9.33	
25	1	ecmf	surface	0	2E+07	11	fc	100u	grid_sim	reduced_	4.81	4.54	4.88	5.16	
26	1	ecmf	surface	0	2E+07	11	fc	100v	grid_sim	reduced_	8.41	8.4	8.4	8.59	
27	1	ecmf	surface	0	2E+07	12	fc	100u	grid_sim	reduced_	3.62	3.24	3.61	3.79	
28	1	ecmf	surface	0	2E+07	12	fc	100v	grid_sim	reduced_	8.22	8.12	7.89	8.11	
29	1	ecmf	surface	0	2E+07	13	fc	100u	grid_sim	reduced_	1.84	1.7	1.56	1.98	
30	1	ecmf	surface	0	2E+07	13	fc	100v	grid_sim	reduced_	7.52	7.75	6.95	7.34	
31	1	ecmf	surface	0	2E+07	14	fc	100u	grid_sim	reduced_	1.6	1.37	1.97	1.74	
32	1	ecmf	surface	0	2E+07	14	fc	100v	grid_sim	reduced_	8.38	8.47	8.3	8.1	
33	1	ecmf	surface	0	2E+07	15	fc	100u	grid_sim	reduced_	0.79	0.48	1.01	0.78	
34	1	ecmf	surface	0	2E+07	15	fc	100v	grid_sim	reduced_	8	8.01	7.99	7.64	
35	1	ecmf	surface	0	2E+07	16	fc	100u	grid_sim	reduced_	-1.95	-2.72	-1.65	-1.19	
36	1	ecmf	surface	0	2E+07	16	fc	100v	grid_sim	reduced_	4.98	4.31	5.32	5.58	
37	1	ecmf	surface	0	2E+07	17	fc	100u	grid_sim	reduced_	-3.14	-3.58	-2.87	-2.19	
38	1	ecmf	surface	0	2E+07	17	fc	100v	grid_sim	reduced_	2.12	1.22	1.96	2.49	
39	1	ecmf	surface	0	2E+07	18	fc	100u	grid_sim	reduced_	-0.77	-0.64	-1.1	-0.27	
40	1	ecmf	surface	0	2E+07	18	fc	100v	grid_sim	reduced_	-1.93	-2.76	-1.87	-1.38	
41	1	ecmf	surface	0	2E+07	19	fc	100u	grid_sim	reduced_	2.28	2.46	1.89	2.62	
42	1	ecmf	surface	0	2E+07	19	fc	100v	grid_sim	reduced_	-3.67	-4.95	-4.44	-2.2	
43	1	ecmf	surface	0	2E+07	20	fc	100u	grid_sim	reduced_	5.17	5.13	4.15	5.24	
44	1	ecmf	surface	0	2E+07	20	fc	100v	grid_sim	reduced_	-2.44	-2.8	-2.18	-1.88	
45	1	ecmf	surface	0	2E+07	21	fc	100u	grid_sim	reduced_	8.14	8.15	7.08	7.93	
46	1	ecmf	surface	0	2E+07	21	fc	100v	grid_sim	reduced_	-1.45	-1.61	-1.3	-1.17	
47	1	ecmf	surface	0	2E+07	22	fc	100u	grid_sim	reduced_	9.13	9.31	8.63	8.67	
48	1	ecmf	surface	0	2E+07	22	fc	100v	grid_sim	reduced_	-1.81	-1.71	-1.63	-1.72	
49	1	ecmf	surface	0	2E+07	23	fc	100u	grid_sim	reduced_	8.96	9.12	8.47	8.68	
50	1	ecmf	surface	0	2E+07	23	fc	100v	grid_sim	reduced_	-0.67	-0.64	-0.54	-0.61	
51	48 of 48 messages in 01-01-2018.grib														
52															
53	48 of 48 total messages in 1 files														
54	Input Point: latitude=[redacted]longitude=[redacted]														
55	Grid Point chosen #1 index[redacted] latitude=[redacted] longitude=[redacted] distance=2.59 (Km)														
56	Other grid Points														
57	- 1 - index=[redacted]latitude=[redacted] longitude=[redacted]distance=2.59 (Km)														
58	- 2 - index[redacted]latitude[redacted] longitude[redacted] distance=6.77 (Km)														
59	- 3 - index[redacted] latitude=[redacted] longitude[redacted]distance=9.36 (Km)														
60	- 4 - index[redacted] latitude[redacted] longitude[redacted] distance=9.50 (Km)														
61															

(b) 01-01.2018.csv

Figure C.4: The output for the process of generating the data using the MARS-API.

C.4. Excel files for real-time data

09-07-2023.grib

edition	centre	typeOf	level	dataDa	stepRa	dataTy	shortN	packing	gridTyp	value1	value2	value3	value4
1	ecmf	surface	0	20230709	0	fc	100u	grid_simp	regular_ll	3.74	3.74	4.46	4.33
1	ecmf	surface	0	20230709	0	fc	100v	grid_simp	regular_ll	-1.62	-2.21	-1.27	-1.88
1	ecmf	surface	0	20230709	1	fc	100v	grid_simp	regular_ll	-2.11	-2.4	-2.77	-2.95
1	ecmf	surface	0	20230709	1	fc	100u	grid_simp	regular_ll	1.77	1.52	2.36	2.1
1	ecmf	surface	0	20230709	2	fc	100v	grid_simp	regular_ll	-1.54	-1.84	-2.25	-2.53
1	ecmf	surface	0	20230709	2	fc	100u	grid_simp	regular_ll	1.06	1.24	1.57	1.87
1	ecmf	surface	0	20230709	3	fc	100u	grid_simp	regular_ll	0.4	0.48	0.51	0.67
1	ecmf	surface	0	20230709	3	fc	100v	grid_simp	regular_ll	-1.22	-1.36	-1.35	-1.43
1	ecmf	surface	0	20230709	4	fc	100v	grid_simp	regular_ll	-1.76	-2.04	-1.51	-1.69
1	ecmf	surface	0	20230709	4	fc	100u	grid_simp	regular_ll	-1.15	-1.33	-0.71	-0.79
1	ecmf	surface	0	20230709	5	fc	100v	grid_simp	regular_ll	-1.62	-2.1	-1.69	-2.3
1	ecmf	surface	0	20230709	5	fc	100u	grid_simp	regular_ll	-2.2	-1.24	-1.23	-0.25
1	ecmf	surface	0	20230709	6	fc	100v	grid_simp	regular_ll	-2.67	-3.57	-2.59	-3.19
1	ecmf	surface	0	20230709	6	fc	100u	grid_simp	regular_ll	1.76	3.08	1.99	3.28
1	ecmf	surface	0	20230709	7	fc	100v	grid_simp	regular_ll	-2.75	-2.44	-3	-2.53
1	ecmf	surface	0	20230709	7	fc	100u	grid_simp	regular_ll	3.77	4.09	3.55	3.75
1	ecmf	surface	0	20230709	8	fc	100u	grid_simp	regular_ll	1.97	0.85	2.72	1.4
1	ecmf	surface	0	20230709	8	fc	100v	grid_simp	regular_ll	-5.6	-5.29	-5.59	-5.5
1	ecmf	surface	0	20230709	9	fc	100u	grid_simp	regular_ll	-1.8	-1.88	-1.76	-1.84
1	ecmf	surface	0	20230709	9	fc	100v	grid_simp	regular_ll	-3.14	-2.7	-3.11	-2.71
1	ecmf	surface	0	20230709	10	fc	100u	grid_simp	regular_ll	-2.4	-2.52	-2.58	-2.73
1	ecmf	surface	0	20230709	10	fc	100v	grid_simp	regular_ll	-1.19	-0.87	-1.23	-0.96
1	ecmf	surface	0	20230709	11	fc	100u	grid_simp	regular_ll	0.66	0.64	-0.64	-0.27
1	ecmf	surface	0	20230709	11	fc	100v	grid_simp	regular_ll	4.64	5.35	2.09	2.7
1	ecmf	surface	0	20230709	12	fc	100v	grid_simp	regular_ll	1.36	0.34	1.94	0.93
1	ecmf	surface	0	20230709	12	fc	100u	grid_simp	regular_ll	2.13	2.3	3.19	3.94
1	ecmf	surface	0	20230709	13	fc	100v	grid_simp	regular_ll	-0.6	-1.34	-1.15	-1.74
1	ecmf	surface	0	20230709	13	fc	100u	grid_simp	regular_ll	4.73	4.99	5.16	5.47
1	ecmf	surface	0	20230709	14	fc	100u	grid_simp	regular_ll	5.01	5.07	4.84	4.93
1	ecmf	surface	0	20230709	14	fc	100v	grid_simp	regular_ll	-3.03	-2.97	-2.85	-2.61
1	ecmf	surface	0	20230709	15	fc	100v	grid_simp	regular_ll	-4.48	-4.65	-4.3	-4.56
1	ecmf	surface	0	20230709	15	fc	100u	grid_simp	regular_ll	4.91	5.16	4.67	4.92
1	ecmf	surface	0	20230709	16	fc	100u	grid_simp	regular_ll	4.96	4.67	5.33	5.02
1	ecmf	surface	0	20230709	16	fc	100v	grid_simp	regular_ll	-5.97	-6.03	-5.85	-5.92
1	ecmf	surface	0	20230709	17	fc	100u	grid_simp	regular_ll	4.38	3.91	4.69	4.19
1	ecmf	surface	0	20230709	17	fc	100v	grid_simp	regular_ll	-5.54	-5.45	-5.35	-5.25

(a)

1	ecmf	surface	0	20230709	84	fc	100v	grid_simp	regular_ll	1.97	1.72	2.14	1.97
1	ecmf	surface	0	20230709	85	fc	100v	grid_simp	regular_ll	1.38	1.26	1.73	1.67
1	ecmf	surface	0	20230709	85	fc	100u	grid_simp	regular_ll	8.63	8.56	8.86	8.77
1	ecmf	surface	0	20230709	86	fc	100u	grid_simp	regular_ll	8.57	8.38	8.88	8.7
1	ecmf	surface	0	20230709	86	fc	100v	grid_simp	regular_ll	0.75	0.76	1.58	1.59
1	ecmf	surface	0	20230709	87	fc	100u	grid_simp	regular_ll	8.18	8.1	8.46	8.47
1	ecmf	surface	0	20230709	87	fc	100v	grid_simp	regular_ll	0.38	0.5	0.87	0.92
1	ecmf	surface	0	20230709	88	fc	100v	grid_simp	regular_ll	1.28	1.26	1.53	1.62
1	ecmf	surface	0	20230709	88	fc	100u	grid_simp	regular_ll	8.23	8.5	8.83	9.02
1	ecmf	surface	0	20230709	89	fc	100v	grid_simp	regular_ll	0.87	1.06	1.6	1.89
1	ecmf	surface	0	20230709	89	fc	100u	grid_simp	regular_ll	8.77	8.95	9.12	9.32
1	ecmf	surface	0	20230709	90	fc	100v	grid_simp	regular_ll	1.45	1.74	1.83	2.13
1	ecmf	surface	0	20230709	90	fc	100u	grid_simp	regular_ll	8.01	8.22	8.85	9.03
1	ecmf	surface	0	20230709	93	fc	100v	grid_simp	regular_ll	4.15	4.14	4.46	4.56
1	ecmf	surface	0	20230709	93	fc	100u	grid_simp	regular_ll	6.95	6.92	7.2	7.28
1	ecmf	surface	0	20230709	96	fc	100v	grid_simp	regular_ll	5.29	5.24	5.49	5.56
1	ecmf	surface	0	20230709	96	fc	100u	grid_simp	regular_ll	6.62	6.51	6.63	6.67
1	ecmf	surface	0	20230709	99	fc	100v	grid_simp	regular_ll	4.07	4.05	4.26	4.19
1	ecmf	surface	0	20230709	99	fc	100u	grid_simp	regular_ll	6.04	6.1	6.01	6.2
1	ecmf	surface	0	20230709	102	fc	100u	grid_simp	regular_ll	7.23	7.17	6.72	6.78
1	ecmf	surface	0	20230709	102	fc	100v	grid_simp	regular_ll	5.04	5	4.96	4.97
1	ecmf	surface	0	20230709	105	fc	100v	grid_simp	regular_ll	3.76	3.66	3.49	3.41
1	ecmf	surface	0	20230709	105	fc	100u	grid_simp	regular_ll	7.98	8.37	8.47	8.85
1	ecmf	surface	0	20230709	108	fc	100u	grid_simp	regular_ll	8.08	8.32	8.85	9.1
1	ecmf	surface	0	20230709	108	fc	100v	grid_simp	regular_ll	2.19	1.97	2	1.75
1	ecmf	surface	0	20230709	111	fc	100u	grid_simp	regular_ll	7.61	7.75	8	8.05
1	ecmf	surface	0	20230709	111	fc	100v	grid_simp	regular_ll	0.31	0.56	0.72	0.82
1	ecmf	surface	0	20230709	114	fc	100u	grid_simp	regular_ll	6.6	6.77	6.66	6.78
1	ecmf	surface	0	20230709	114	fc	100v	grid_simp	regular_ll	0.27	0.35	0.62	0.79
1	ecmf	surface	0	20230709	117	fc	100u	grid_simp	regular_ll	5.73	5.81	6.14	6.3
1	ecmf	surface	0	20230709	117	fc	100v	grid_simp	regular_ll	2.67	2.88	3.22	3.41
1	ecmf	surface	0	20230709	120	fc	100u	grid_simp	regular_ll	6.12	6.01	6.16	6.16
1	ecmf	surface	0	20230709	120	fc	100v	grid_simp	regular_ll	3.79	3.78	4.07	4.17
1	ecmf	surface	0	20230709	123	fc	100v	grid_simp	regular_ll	3.77	3.74	4.16	4.25
1	ecmf	surface	0	20230709	123	fc	100u	grid_simp	regular_ll	5.31	5.23	5.28	5.26
1	ecmf	surface	0	20230709	126	fc	100u	grid_simp	regular_ll	5.22	5.18	5.29	5.39
1	ecmf	surface	0	20230709	126	fc	100v	grid_simp	regular_ll	3.63	3.52	3.72	3.7
1	ecmf	surface	0	20230709	129	fc	100u	grid_simp	regular_ll	4.88	4.97	5.36	5.66
1	ecmf	surface	0	20230709	129	fc	100v	grid_simp	regular_ll	3.58	3.49	3.19	3

(b)

1	ecmf	surface	0	20230709	156	fc	100u	grid_simp	regular_ll	3.3	3.21	3.42	3.41
1	ecmf	surface	0	20230709	156	fc	100v	grid_simp	regular_ll	7.31	7.25	7.24	7.1
1	ecmf	surface	0	20230709	162	fc	100u	grid_simp	regular_ll	2.24	2.42	2.72	2.81
1	ecmf	surface	0	20230709	162	fc	100v	grid_simp	regular_ll	4.59	4.87	3.95	4.26
1	ecmf	surface	0	20230709	168	fc	100u	grid_simp	regular_ll	1.53	0.73	1.13	0.86
1	ecmf	surface	0	20230709	168	fc	100u	grid_simp	regular_ll	3.44	3.17	3.39	3.61
1	ecmf	surface	0	20230709	174	fc	100u	grid_simp	regular_ll	7.26	7.29	7.87	7.96
1	ecmf	surface	0	20230709	174	fc	100v	grid_simp	regular_ll	2.56	2.54	2.85	2.88
1	ecmf	surface	0	20230709	180	fc	100v	grid_simp	regular_ll	2.08	1.72	1.51	1.36
1	ecmf	surface	0	20230709	180	fc	100u	grid_simp	regular_ll	7.74	7.76	8.35	8.45
1	ecmf	surface	0	20230709	186	fc	100u	grid_simp	regular_ll	6.32	6.75	7.21	7.55
1	ecmf	surface	0	20230709	186	fc	100v	grid_simp	regular_ll	-2.06	-1.43	-0.52	-0.21
1	ecmf	surface	0	20230709	192	fc	100u	grid_simp	regular_ll	2.33	2.65	3.23	3.39
1	ecmf	surface	0	20230709	192	fc	100v	grid_simp	regular_ll	3.14	3.45	3.74	3.96
1	ecmf	surface	0	20230709	198	fc	100u	grid_simp	regular_ll	4.23	4.15	4.66	4.58
1	ecmf	surface	0	20230709	198	fc	100v	grid_simp	regular_ll	2.39	2.53	2.53	2.76
1	ecmf	surface	0	20230709	204	fc	100u	grid_simp	regular_ll	3.69	3.41	3.08	2.56
1	ecmf	surface	0	20230709	204	fc	100v	grid_simp	regular_ll	5.36	5.63	5.8	6.05
1	ecmf	surface	0	20230709	210	fc	100v	grid_simp	regular_ll	0.36	0.58	0.31	0.62
1	ecmf	surface	0	20230709	210	fc	100u	grid_simp	regular_ll	7.09	7.16	7.16	7.34
1	ecmf	surface	0	20230709	216	fc	100u	grid_simp	regular_ll	3.36	3.54	3.83	4.1
1	ecmf	surface	0	20230709	216	fc	100u	grid_simp	regular_ll	7.58	7.42	7.62	7.52
1	ecmf	surface	0	20230709	222	fc	100v	grid_simp	regular_ll	6.31	6.47	6.31	6.31
1	ecmf	surface	0	20230709	222	fc	100u	grid_simp	regular_ll	4.24	4.39	4.8	5.02
1	ecmf	surface	0	20230709	228	fc	100u	grid_simp	regular_ll	7.69	7.47	6.91	6.65
1	ecmf	surface	0	20230709	228	fc	100u	grid_simp	regular_ll	8.96	9.2	9.68	9.9
1	ecmf	surface	0	20230709	234	fc	100u	grid_simp	regular_ll	9.25	9.27	9.95	10.12
1	ecmf	surface	0	20230709	234	fc	100v	grid_simp	regular_ll	2.69	2.48	2.41	2.49
1	ecmf	surface	0	20230709	240	fc	100u	grid_simp	regular_ll	4.85	4.79	5.15	5.18
1	ecmf	surface	0	20230709	240	fc	100u	grid_simp	regular_ll	8.13	8.13	8.43	8.55

750 of 750 total messages in 1 files
Input Point: latitude=[redacted] longitude=[redacted]
Grid Point chosen #4 index=[redacted] latitude=[redacted] longitude=[redacted] distance=6.21 (Km)
Other grid Points
- 1 - index[redacted] latitude=[redacted] longitude=[redacted] distance=6.93 (Km)
- 2 - index[redacted] latitude=[redacted] longitude=[redacted] distance=6.21 (Km)
- 3 - index[redacted] latitude=[redacted] longitude=[redacted] distance=6.93 (Km)
- 4 - index[redacted] latitude=[redacted] longitude=[redacted] distance=6.21 (Km)

09-07-2023

(c)

Figure C.5: Real-time data CSV file for the 9^{th} of July 2023.

D+3	17	T1D07090000071217001.grib	12/07/2023	17:00	1.06	8.95	9.012552358	263.2455953	WEST	Wednesday
D+3	18	T1D07090000071218001.grib	12/07/2023	18:00	1.74	8.22	8.402142584	258.0481249	WEST	Wednesday
D+3	19		12/07/2023	19:00			8.233006311	248.5787404		Wednesday
D+3	20		12/07/2023	20:00			8.233006311	248.5787404		Wednesday
D+3	21	T1D07090000071221001.grib	12/07/2023	21:00	4.14	6.92	8.063870039	239.1093559	SOUTH-WEST	Wednesday
D+3	22		12/07/2023	22:00			8.210382698	235.1391141		Wednesday
D+3	23		12/07/2023	23:00			8.283639027	233.1539933		Wednesday
D+4	0	T1D07090000071300001.grib	13/07/2023	00:00	5.24	6.51	8.356895357	231.1688724	SOUTH-WEST	Thursday
D+4	1		13/07/2023	01:00			7.839475539	233.7936597		Thursday
D+4	2		13/07/2023	02:00			7.580765631	235.1060534		Thursday
D+4	3	T1D07090000071303001.grib	13/07/2023	03:00	4.05	6.1	7.322055722	236.4184471	SOUTH-WEST	Thursday
D+4	4		13/07/2023	04:00			8.031637086	235.7642265		Thursday
D+4	5		13/07/2023	05:00			8.386427768	235.4371162		Thursday
D+4	6	T1D07090000071306001.grib	13/07/2023	06:00	5	7.17	8.741218451	235.1100059	SOUTH-WEST	Thursday
D+4	7		13/07/2023	07:00			8.938226219	240.7457011		Thursday
D+4	8		13/07/2023	08:00			9.036730103	243.5635486		Thursday
D+4	9	T1D07090000071309001.grib	13/07/2023	09:00	3.66	8.37	9.135233987	246.3813962	SOUTH-WEST	Thursday

(a)

D+5	17		14/07/2023	17:00			2.912084931	220.8036405		Friday
D+5	18	T1D07090000071418001.grib	14/07/2023	18:00	2.1	1.46	2.557655176	214.8084981	SOUTH-WEST	Friday
D+5	19		14/07/2023	19:00			3.343851801	163.5754519		Friday
D+5	20		14/07/2023	20:00			3.736950113	137.9589288		Friday
D+5	21	T1D07090000071421001.grib	14/07/2023	21:00	1.57	-3.82	4.130048426	112.3424057	EAST	Friday
D+5	22		14/07/2023	22:00			6.109242308	119.903671		Friday
D+5	23		14/07/2023	23:00			7.098839249	123.6843036		Friday
D+6	0	T1D07090000071500001.grib	15/07/2023	00:00	4.92	-6.42	8.08843619	127.4649363	SOUTH-EAST	Saturday
D+6	1		15/07/2023	01:00			7.98039676	140.0185722		Saturday
D+6	2		15/07/2023	02:00			7.926377045	146.2953901		Saturday
D+6	3		15/07/2023	03:00			7.87235733	152.5722081		Saturday
D+6	4		15/07/2023	04:00			7.7643179	165.125844		Saturday
D+6	5		15/07/2023	05:00			7.710298184	171.4026619		Saturday
D+6	6	T1D07090000071506001.grib	15/07/2023	06:00	7.65	-0.31	7.656278469	177.6794799	SOUTH	Saturday
D+6	7		15/07/2023	07:00			7.724420369	184.230055		Saturday
D+6	8		15/07/2023	08:00			7.75849132	187.5053426		Saturday
D+6	9		15/07/2023	09:00			7.79256227	190.7806301		Saturday
D+6	10		15/07/2023	10:00			7.86070417	197.3312053		Saturday
D+6	11		15/07/2023	11:00			7.89477512	200.6064928		Saturday
D+6	12	T1D07090000071512001.grib	15/07/2023	12:00	7.25	3.21	7.92884607	203.8817804	SOUTH-WEST	Saturday

(b)

D+9	5		18/07/2023	05:00			7.869063572	236.9240005		Tuesday
D+9	6	T1D07090000071806001.grib	18/07/2023	06:00	4.39	6.47	7.818759492	235.8424711	SOUTH-WEST	Tuesday
D+9	7		18/07/2023	07:00			8.826763706	234.613079		Tuesday
D+9	8		18/07/2023	08:00			9.330765812	233.998383		Tuesday
D+9	9		18/07/2023	09:00			9.834767919	233.3836869		Tuesday
D+9	10		18/07/2023	10:00			10.84277213	232.1542949		Tuesday
D+9	11		18/07/2023	11:00			11.34677424	231.5395988		Tuesday
D+9	12	T1D07090000071812001.grib	18/07/2023	12:00	7.47	9.2	11.85077635	230.9249028	SOUTH-WEST	Tuesday
D+9	13		18/07/2023	13:00			11.28708335	236.9492844		Tuesday
D+9	14		18/07/2023	14:00			11.00523686	239.9614752		Tuesday
D+9	15		18/07/2023	15:00			10.72339036	242.973666		Tuesday
D+9	16		18/07/2023	16:00			10.15969737	248.9980477		Tuesday
D+9	17		18/07/2023	17:00			9.877850873	252.0102385		Tuesday
D+9	18	T1D07090000071818001.grib	18/07/2023	18:00	2.48	9.27	9.596004377	255.0224293	WEST	Tuesday
D+9	19		18/07/2023	19:00			9.556041752	251.1404303		Tuesday
D+9	20		18/07/2023	20:00			9.53606044	249.1994308		Tuesday
D+9	21		18/07/2023	21:00			9.516079127	247.2584313		Tuesday
D+9	22		18/07/2023	22:00			9.476116502	243.3764323		Tuesday
D+9	23		18/07/2023	23:00			9.45613519	241.4354328		Tuesday
D+10	0	T1D07090000071900001.grib	19/07/2023	00:00	4.79	8.13	9.436153878	239.4944333	SOUTH-WEST	Wednesday

(c)

Figure C.6: Real-time data XLSX file for the 9^{th} of July 2023.

C.5. Matrix method

Date	Time	Wind speed (m/s)	Wind direction (Â°)	(Predictive) [redacted]-1 Power (kW)	(Predictive) [redacted]-2 Power (kW)	(Predictive) [redacted]-3 Power (k
23/07/2023	00:00	7.5	180	650	660	660
23/07/2023	01:00	7.5	180	650	660	660
23/07/2023	02:00	7	180	560	560	550
23/07/2023	03:00	8.5	210	960	980	1030
23/07/2023	04:00	10	210	1670	1660	1720
23/07/2023	05:00	10	210	1670	1660	1720
23/07/2023	06:00	10.5	210	1760	1790	1840
23/07/2023	07:00	10.5	210	1760	1790	1840
23/07/2023	08:00	11	210	1980	1980	2050
23/07/2023	09:00	11	210	1980	1980	2050
23/07/2023	10:00	10	210	1670	1660	1720
23/07/2023	11:00	13	210	2670	2650	2710
23/07/2023	12:00	11.5	210	2140	2140	2220
23/07/2023	13:00	13	240	2660	2600	2700
23/07/2023	14:00	13	240	2660	2600	2700
23/07/2023	15:00	12	240	2390	2370	2400
23/07/2023	16:00	12	240	2390	2370	2400
23/07/2023	17:00	11	240	1990	1980	2070
23/07/2023	18:00	9	240	1140	1190	1200
23/07/2023	19:00	9	210	1160	1170	1220
23/07/2023	20:00	9	210	1160	1170	1220
23/07/2023	21:00	8	210	770	820	870
23/07/2023	22:00	8	240	800	820	890
23/07/2023	23:00	7.5	240	620	650	690

(a)

26/07/2023	02:00	5.5	240	230	230	240
26/07/2023	03:00	6	240	300	330	320
26/07/2023	04:00	6.5	240	400	410	440
26/07/2023	05:00	6	270	310	300	320
26/07/2023	06:00	6	270	310	300	320
26/07/2023	07:00	5	270	160	160	170
26/07/2023	08:00	5	270	160	160	170
26/07/2023	09:00	5.5	270	220	220	240
26/07/2023	10:00	5.5	270	220	220	240
26/07/2023	11:00	7	270	540	540	540
26/07/2023	12:00	7	270	540	540	540
26/07/2023	13:00	7.5	300	680	640	670
26/07/2023	14:00	7	270	540	540	540
26/07/2023	15:00	7.5	270	660	640	690
26/07/2023	16:00	7	270	540	540	540
26/07/2023	17:00	6	270	310	300	320
26/07/2023	18:00	5.5	270	220	220	240
26/07/2023	19:00	6	240	300	330	320
26/07/2023	20:00	6.5	240	400	410	440
26/07/2023	21:00	6.5	210	410	430	430
26/07/2023	22:00	7	210	500	530	570
26/07/2023	23:00	7.5	210	630	660	690
27/07/2023	00:00	7.5	210	630	660	690
27/07/2023	01:00	8	210	770	820	870
27/07/2023	02:00	8.5	210	960	980	1030
27/07/2023	03:00	8.5	210	960	980	1030
27/07/2023	04:00	9	210	1160	1170	1220
27/07/2023	05:00	9.5	210	1470	1480	1550
27/07/2023	06:00	10	210	1670	1660	1720
27/07/2023	07:00	9.5	210	1470	1480	1550

(b)

Figure C.7: Predictive turbine output forecast for all the 3 chosen turbines in the file "Matrix Method.xlsx" created for the 23^{rd} of July 2023.

31/07/2023	14:00	4	270	50	60	70
31/07/2023	15:00	3.5	270	10	0	0
31/07/2023	16:00	2.5	300	0	0	0
31/07/2023	17:00	2	300	0	0	0
31/07/2023	18:00	1.5	300	0	0	0
31/07/2023	19:00	3	270	0	0	0
31/07/2023	20:00	3.5	270	10	0	0
31/07/2023	21:00	4	270	50	60	70
31/07/2023	22:00	5	240	160	180	170
31/07/2023	23:00	5.5	240	230	230	240
01/08/2023	00:00	6	240	300	330	320
01/08/2023	01:00	6	240	300	330	320
01/08/2023	02:00	6	240	300	330	320
01/08/2023	03:00	6	240	300	330	320
01/08/2023	04:00	6	240	300	330	320
01/08/2023	05:00	6	270	310	300	320
01/08/2023	06:00	6	270	310	300	320
01/08/2023	07:00	6	270	310	300	320
01/08/2023	08:00	6	270	310	300	320
01/08/2023	09:00	6	270	310	300	320
01/08/2023	10:00	6	270	310	300	320
01/08/2023	11:00	6	270	310	300	320
01/08/2023	12:00	6	270	310	300	320
01/08/2023	13:00	5	270	160	160	170
01/08/2023	14:00	5	270	160	160	170
01/08/2023	15:00	4.5	270	100	100	110
01/08/2023	16:00	3.5	270	10	0	0
01/08/2023	17:00	3	300	0	0	0
01/08/2023	18:00	3	300	0	0	0
01/08/2023	19:00	3	270	0	0	0
01/08/2023	20:00	3	270	0	0	0
01/08/2023	21:00	3.5	270	10	0	0
01/08/2023	22:00	3.5	270	10	0	0
01/08/2023	23:00	3.5	240	0	0	0
02/08/2023	00:00	3.5	240	0	0	0

(c)

Figure C.7: Predictive turbine output forecast for all the 3 chosen turbines in the file "Matrix Method.xlsx" created for the 23^{rd} of July 2023.

MTU (CET/CEST)	Hour (From)	Hour (To)	Day of the week	Previous Year Average (EUR/MWh)	Recent 3-Week Average (EUR/MWh)	Forecasted Electricity Price (EUR/MWh)
23/07/2023	00:00	01:00	Sunday	87.93	60.98	5.23
23/07/2023	01:00	02:00	Sunday	81.78	41.53	4.86
23/07/2023	02:00	03:00	Sunday	73.71	34.43	4.38
23/07/2023	03:00	04:00	Sunday	69.23	31.80	4.12
23/07/2023	04:00	05:00	Sunday	67.34	31.95	4.00
23/07/2023	05:00	06:00	Sunday	65.34	32.16	3.88
23/07/2023	06:00	07:00	Sunday	60.20	30.18	3.58
23/07/2023	07:00	08:00	Sunday	61.49	26.90	3.66
23/07/2023	08:00	09:00	Sunday	57.21	24.42	3.40
23/07/2023	09:00	10:00	Sunday	52.41	15.20	3.12
23/07/2023	10:00	11:00	Sunday	48.46	-6.63	2.88
23/07/2023	11:00	12:00	Sunday	38.72	-76.61	2.30
23/07/2023	12:00	13:00	Sunday	36.19	-152.54	2.15
23/07/2023	13:00	14:00	Sunday	14.29	-176.15	0.85
23/07/2023	14:00	15:00	Sunday	18.04	-176.30	1.07
23/07/2023	15:00	16:00	Sunday	21.83	-165.30	1.30
23/07/2023	16:00	17:00	Sunday	38.50	-43.16	2.29
23/07/2023	17:00	18:00	Sunday	60.19	12.93	3.58
23/07/2023	18:00	19:00	Sunday	78.43	42.12	4.66
23/07/2023	19:00	20:00	Sunday	85.54	72.37	5.09
23/07/2023	20:00	21:00	Sunday	88.70	100.11	5.27
23/07/2023	21:00	22:00	Sunday	92.87	109.23	5.52
23/07/2023	22:00	23:00	Sunday	91.64	113.62	5.45
23/07/2023	23:00	00:00	Sunday	84.12	104.41	5.00
24/07/2023	00:00	01:00	Monday	85.69	88.30	82.27
24/07/2023	01:00	02:00	Monday	68.72	70.33	65.98
24/07/2023	02:00	03:00	Monday	65.21	57.22	62.61
24/07/2023	03:00	04:00	Monday	64.19	50.73	61.62
24/07/2023	04:00	05:00	Monday	63.59	53.69	61.05
24/07/2023	05:00	06:00	Monday	69.10	70.77	66.34
24/07/2023	06:00	07:00	Monday	86.94	97.71	83.47
24/07/2023	07:00	08:00	Monday	97.04	106.20	93.17
24/07/2023	08:00	09:00	Monday	97.88	115.56	93.97
24/07/2023	09:00	10:00	Monday	88.42	91.57	84.89
24/07/2023	10:00	11:00	Monday	81.56	52.77	78.30
24/07/2023	11:00	12:00	Monday	75.51	42.10	72.50
24/07/2023	12:00	13:00	Monday	68.66	8.26	65.92
24/07/2023	13:00	14:00	Monday	65.78	18.22	63.15

(a)

Figure C.8: Predictive electricity price forecast initiated on the 23^{rd} of July 2023.

27/07/2023	01:00	02:00	Thursday	82.18	88.04	86.64
27/07/2023	02:00	03:00	Thursday	79.46	81.43	83.78
27/07/2023	03:00	04:00	Thursday	78.21	79.51	82.45
27/07/2023	04:00	05:00	Thursday	78.71	81.00	82.99
27/07/2023	05:00	06:00	Thursday	81.38	88.92	85.80
27/07/2023	06:00	07:00	Thursday	95.91	103.94	101.11
27/07/2023	07:00	08:00	Thursday	95.64	114.36	100.83
27/07/2023	08:00	09:00	Thursday	92.33	118.47	97.34
27/07/2023	09:00	10:00	Thursday	97.08	99.94	102.35
27/07/2023	10:00	11:00	Thursday	87.43	89.61	92.17
27/07/2023	11:00	12:00	Thursday	81.16	80.68	85.56
27/07/2023	12:00	13:00	Thursday	76.50	66.78	80.65
27/07/2023	13:00	14:00	Thursday	67.53	58.28	71.20
27/07/2023	14:00	15:00	Thursday	71.84	59.31	75.74
27/07/2023	15:00	16:00	Thursday	74.07	68.36	78.09
27/07/2023	16:00	17:00	Thursday	83.85	79.08	88.40
27/07/2023	17:00	18:00	Thursday	104.84	89.77	110.53
27/07/2023	18:00	19:00	Thursday	113.59	97.98	119.75
27/07/2023	19:00	20:00	Thursday	122.89	120.82	129.57
27/07/2023	20:00	21:00	Thursday	120.95	150.01	127.51
27/07/2023	21:00	22:00	Thursday	114.71	149.84	120.94
27/07/2023	22:00	23:00	Thursday	111.81	129.53	117.88
27/07/2023	23:00	00:00	Thursday	89.61	115.45	94.47
28/07/2023	00:00	01:00	Friday	79.93	104.97	80.43
28/07/2023	01:00	02:00	Friday	78.15	98.25	78.64
28/07/2023	02:00	03:00	Friday	80.61	92.12	81.11
28/07/2023	03:00	04:00	Friday	84.05	86.20	84.57
28/07/2023	04:00	05:00	Friday	83.00	86.34	83.51
28/07/2023	05:00	06:00	Friday	84.79	87.66	85.32
28/07/2023	06:00	07:00	Friday	99.34	87.67	99.96
28/07/2023	07:00	08:00	Friday	111.27	97.87	111.96
28/07/2023	08:00	09:00	Friday	112.69	100.96	113.39
28/07/2023	09:00	10:00	Friday	111.31	93.32	112.00
28/07/2023	10:00	11:00	Friday	103.41	83.90	104.06

(b)

28/07/2023	17:00	18:00	Friday	99.19	84.77	99.80
28/07/2023	18:00	19:00	Friday	103.86	87.96	104.51
28/07/2023	19:00	20:00	Friday	106.49	123.15	107.15
28/07/2023	20:00	21:00	Friday	116.30	135.52	117.02
28/07/2023	21:00	22:00	Friday	105.14	123.12	105.79
28/07/2023	22:00	23:00	Friday	103.35	106.83	103.99
28/07/2023	23:00	00:00	Friday	86.53	92.30	87.07
29/07/2023	00:00	01:00	Saturday	91.13	89.62	75.21
29/07/2023	01:00	02:00	Saturday	82.26	80.77	67.90
29/07/2023	02:00	03:00	Saturday	77.67	70.71	64.10
29/07/2023	03:00	04:00	Saturday	74.26	66.97	61.29
29/07/2023	04:00	05:00	Saturday	70.76	64.70	58.40
29/07/2023	05:00	06:00	Saturday	71.50	62.99	59.01
29/07/2023	06:00	07:00	Saturday	76.02	64.37	62.74
29/07/2023	07:00	08:00	Saturday	80.08	64.67	66.09
29/07/2023	08:00	09:00	Saturday	79.47	65.55	65.59
29/07/2023	09:00	10:00	Saturday	78.78	61.38	65.03
29/07/2023	10:00	11:00	Saturday	71.48	46.70	59.00
29/07/2023	11:00	12:00	Saturday	67.32	30.96	55.56
29/07/2023	12:00	13:00	Saturday	53.40	24.94	44.07
29/07/2023	13:00	14:00	Saturday	46.35	5.39	38.25
29/07/2023	14:00	15:00	Saturday	49.98	7.50	41.25
29/07/2023	15:00	16:00	Saturday	61.33	22.98	50.62
29/07/2023	16:00	17:00	Saturday	65.51	35.93	54.07
29/07/2023	17:00	18:00	Saturday	76.42	53.09	63.07
29/07/2023	18:00	19:00	Saturday	86.89	86.96	71.71
29/07/2023	19:00	20:00	Saturday	95.07	100.01	78.47
29/07/2023	20:00	21:00	Saturday	99.17	107.07	81.85
29/07/2023	21:00	22:00	Saturday	96.90	110.94	79.98
29/07/2023	22:00	23:00	Saturday	100.67	105.12	83.09
29/07/2023	23:00	00:00	Saturday	94.46	95.02	77.96

(c)

Figure C.8: Predictive electricity price forecast initiated on the 23^{rd} of July 2023.

C.6. Calendar

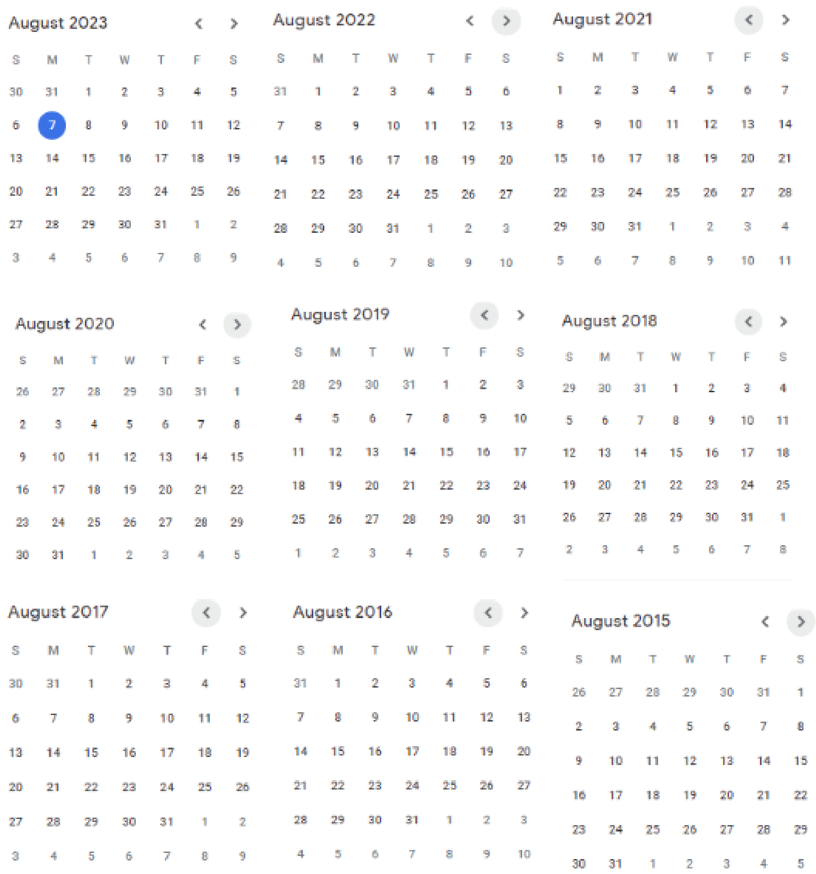

Figure C.9: The calendar month of August from 2018-2023

D
Supplementary graphs

D.1. Literature review

Figure D.1 and Figure D.2 are cited from the research study conducted by Reder et al., 2016.

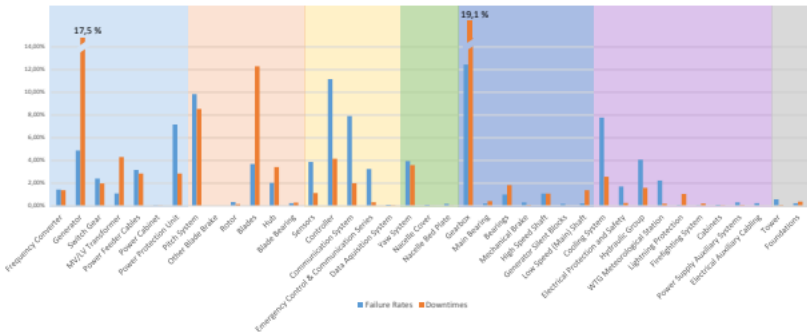

Figure D.1: Normalised failure rates and downtimes for Geared G ≥ 1MW turbines

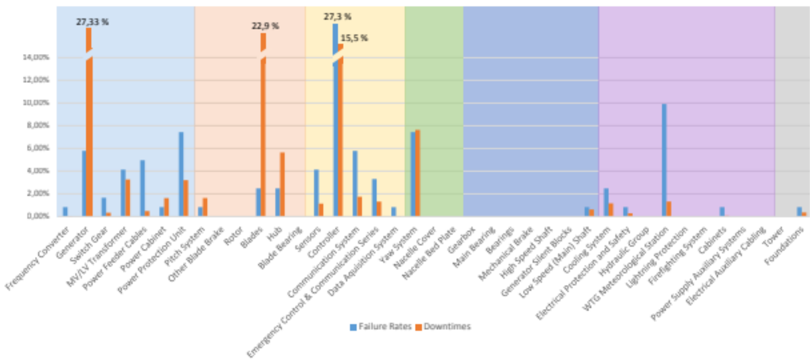

Figure D.2: Normalised failure rates and downtimes for Direct Drive turbines

D.2. FMWTP

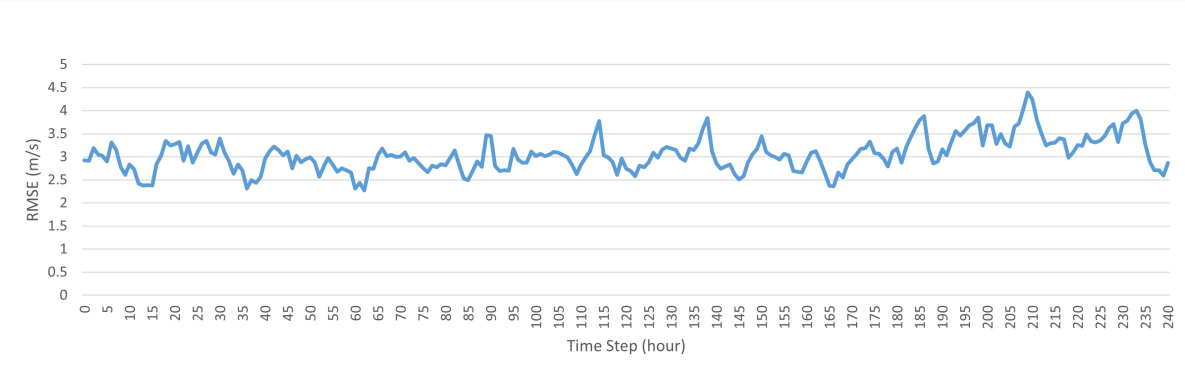

Figure D.3: Wind speed accuracy

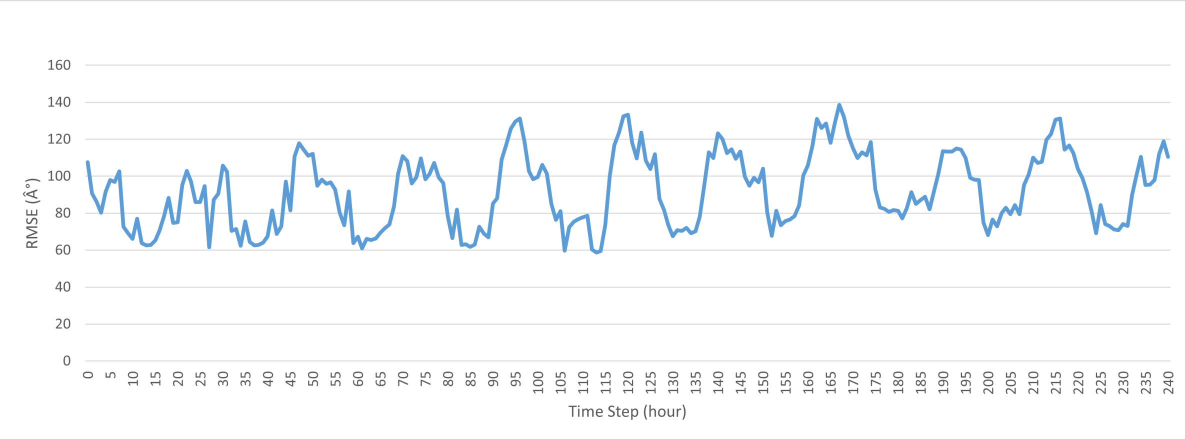

Figure D.4: Wind direction accuracy

D.3. Limitations

21/08/2023	18:00	5	4.38	90
21/08/2023	19:00	4.5	4.47	91
21/08/2023	20:00	4.5	4.42	92
21/08/2023	21:00	4	3.10	93
21/08/2023	22:00	4	2.13	94
21/08/2023	23:00	3.5	1.82	95
22/08/2023	00:00	3.5	2.42	96
22/08/2023	01:00	3	1.67	97
22/08/2023	02:00	3	1.98	98
22/08/2023	03:00	3	2.87	99
22/08/2023	04:00	3.5	4.15	100
22/08/2023	05:00	4	5.05	101
22/08/2023	06:00	4.5	5.95	102
22/08/2023	07:00	3	6.43	103
22/08/2023	08:00	2	5.97	104
22/08/2023	09:00	1.5	5.02	105
22/08/2023	10:00	1	4.75	106
22/08/2023	11:00	1	4.13	107
22/08/2023	12:00	0.5	4.95	108
22/08/2023	13:00	1.5	5.50	109
22/08/2023	14:00	1.5	5.82	110
22/08/2023	15:00	2	5.73	111
22/08/2023	16:00	3.5	5.02	112
22/08/2023	17:00	4	5.67	113
22/08/2023	18:00	5	5.48	114
22/08/2023	19:00	4.5	4.65	115
22/08/2023	20:00	4	4.25	116
22/08/2023	21:00	3.5	3.92	117
22/08/2023	22:00	3.5	3.07	118
22/08/2023	23:00	3	3.55	119
23/08/2023	00:00	3	3.62	120

Figure D.5: FMWTP per 3-hour data comparison with turbine data.

24/08/2023	01:00	2	8.67	145
24/08/2023	02:00	2.5	8.35	146
24/08/2023	03:00	2.5	8.57	147
24/08/2023	04:00	2.5	9.10	148
24/08/2023	05:00	2.5	7.25	149
24/08/2023	06:00	2.5	8.08	150
24/08/2023	07:00	2.5	7.43	151
24/08/2023	08:00	2.5	5.67	152
24/08/2023	09:00	2	3.75	153
24/08/2023	10:00	2	3.58	154
24/08/2023	11:00	2	2.55	155
24/08/2023	12:00	1.5	4.40	156
24/08/2023	13:00	3	4.73	157
24/08/2023	14:00	4	6.02	158
24/08/2023	15:00	4.5	6.18	159
24/08/2023	16:00	6	6.25	160
24/08/2023	17:00	6.5	6.00	161
24/08/2023	18:00	7.5	5.32	162
24/08/2023	19:00	7	5.30	163
24/08/2023	20:00	6.5	5.07	164
24/08/2023	21:00	6.5	3.68	165
24/08/2023	22:00	6	7.72	166
24/08/2023	23:00	5.5	7.55	167
25/08/2023	00:00	5.5	5.42	168
25/08/2023	01:00	5	3.98	169
25/08/2023	02:00	4.5	3.93	170
25/08/2023	03:00	4.5	3.05	171
25/08/2023	04:00	3.5	2.80	172
25/08/2023	05:00	3.5	1.43	173

Figure D.6: FMWTP per 6-hour data comparison with turbine data.